Dissertation zur Erlangung des Doktorgrades
der Fakultät für Chemie und Pharmazie
der Ludwig-Maximilians-Universität München

Characterisation of CHRAC14 and CHRAC16, the two Histone Fold Subunits of the Chromatin Accessibility Complex

Klaus Felix Hartlepp
aus
Augsburg

2006

Erklärung

Diese Dissertation wurde im Sinne von § 13 Abs. 3 bzw. 4 der Promotionsordnung vom 29. Januar 1998 von Herrn Prof. Dr. Peter Becker betreut und von Herrn Prof. Dr. Patrick Cramer vor der Fakultät für Chemie und Pharmazie vertreten.

Ehrenwörtliche Versicherung

Diese Dissertation wurde selbständig, ohne unerlaubte Hilfe erarbeitet.

München, am 23. Januar 2006

K. Felix Hartlepp

....

K. Felix Hartlepp

Dissertation eingereicht am	27.01.2006
1. Gutachter	Prof. Dr. Peter Becker
2. Gutachter	Prof. Dr. Patrick Cramer
Mündliche Prüfung am	22.03.2006

To make them run easily and swiftly, the axles of carriages are anointed; and for much the same purpose, some whalers perform an analogous operation upon their boat; they grease the bottom. Nor is it to be doubted that as such a procedure can do no harm, it may possibly be of no contemptible advantage; considering that oil and water are hostile; that oil is a sliding thing, and that the object in view is to make the boat slide bravely.

Herman Melville – Moby Dick, 1851

Acknowledgements

Here, I would like to express my gratitude to everybody who supported me during my PhD thesis.

First of all, I would like to thank my supervisor Prof. Peter Becker for giving me the opportunity to work on an exciting project in an excellent environment. Peter's constant support, his encouragement and expertise have been very inspiring and motivating and were especially helpful to me in the most challenging situations.

I am also deeply grateful to Dr. Anton Eberharter for teaching me several techniques that have been crucial for this work, discussing my results and giving me valuable advise throughout my thesis, providing me with nucleosomes, baculoviruses, and other materials, proof-reading of this manuscript and his Austrian humor.

I am much obliged to the fruitful collaboration with Drs. Christoph Müller, Carlos Fernández-Tornero and Tim Grüne (EMBL Grenoble Outstation), who did not only perform the crystal structure analysis in this work, but also instructed me in protein crystallisation and introduced me to the basics of structure determination.

Moreover, I thank Dr. Elisabeth Kremmer and her colleagues (GSF, Munich) for producing and screening the α-CHRAC14/α-CHRAC16 rat monoclonal antibodies, Norbert Mücke and Prof. Jörg Langowski (DKFZ, Heidelberg) for performing analytical ultracentrifugation studies, and Dr. Axel Imhof, Dr. Lars Israel and Tilman Schlunck (Zentrallabor für Proteinanalytik, ABI, Munich) for mass spectrometry analysis.

I would also like to thank all the people working at the ABI department of molecular biology for permanent help and advise in daily lab life and for creating a great atmosphere. It is a pleasure to work with you!

Special thanks go to my parents Ingrid and Werner Hartlepp, who strongly supported me both financially and by constant motivation during the past decade of my studies and thereby contributed fundamentally to this work.

Finally, I thank Hubert Kettenberger, not only for endless discussions about my work, for sharing his knowledge of structural biology, chemistry and transcription, for proof-reading of this manuscript and for his formatting skills, but also for being there.

Table of contents

1 Summary 1

2 Introduction 2
2.1 Chromatin structure 2
2.1.1 The nucleosome 2
2.1.2 Higher order structures of chromatin 3
2.2 The histone fold 5
2.2.1 Structure of the core histones 5
2.2.2 Histone fold proteins 6
2.2.2.1 Archeal histone fold proteins 6
2.2.2.2 TATA box-binding protein-associated factors (TAFs) 7
2.2.2.3 Negative Cofactor 2 (NC-2) 9
2.2.2.4 Nuclear Factor Y (NF-Y) 9
2.2.2.5 Subunits of DNA Polymerase epsilon 10
2.2.2.6 Subunits of the Chromatin Accessibility Complex (CHRAC) 10
2.3 Chromatin dynamics and regulation 11
2.3.1 Histone modifications 11
2.3.2 Histone variants 12
2.3.3 Histone chaperones 13
2.3.4 HMG box proteins 14
2.3.5 ATP-dependent chromatin remodelling complexes 15
2.3.5.1 SWI/SNF complexes 17
2.3.5.2 ISWI complexes 17
2.3.5.3 CHD1/Mi-2 complexes 22
2.3.5.4 INO80/SWR1 complexes 22
2.4 Insights into structure and mechanism of ATP-dependent chromatin remodelling 23
2.4.1 A variety of remodelling scenarios 23
2.4.2 Mechanisms of chromatin remodelling: DNA-twisting or DNA-bulging? 24
2.4.3 The Rad54 ATPase domain 26
2.4.4 SWI/SNF complexes 28
2.4.5 ISWI-containing complexes 29
2.4.5.1 ISWI complexes in Drosophila 29
2.4.5.2 ISW2 31
2.5 The Chromatin Accessibility Complex (CHRAC) 33

3 Materials and methods 35
3.1 Materials 35
3.1.1 Solutions, buffers and media 35
3.1.2 Organisms, cells and strains 37
3.1.2.1 E. coli strains 37
3.1.2.2 Insect cells and fly lines 37
3.1.2.3 Baculoviral expression vectors 37
3.1.3 Vectors, plasmids and oligonucleotides 38
3.1.3.1 Vectors and plasmids 38
3.1.3.2 Oligonucleotides 40
3.1.3.3 Antibodies 45
3.2 Methods 47
3.2.1 Cloning of expression vectors 47
3.2.1.1 Recombinant CHRAC14-CHRAC16 in E. coli 47
3.2.1.2 In vitro translation of ACF1 deletion constructs 47
3.2.2 Site-directed mutagenesis of expression vectors 47
3.2.3 Expression and purification of recombinant CHRAC subunits from *E. coli* 48
3.2.4 Expression and purification of recombinant CHRAC subunits from Sf9-cells ... 49
3.2.5 *in vitro*-translation 49
3.2.6 SDS-PAGE and Western blotting 50
3.2.7 GST-pull-down assays 50
3.2.8 FLAG-co-immunoprecipitations from Sf9 cell extracts 50
3.2.9 Production of monoclonal antibodies 51
3.2.10 Immunoprecipitation 51
3.2.11 Immunofluorescence on S2 cells 52
3.2.12 Immunofluorescence on polytene chromosomes 52
3.2.13 Immunofluorescence on *Drosophila* embryos 53
3.2.14 Crystallisation of recombinant CHRAC14-CHRAC16 53
3.2.15 Structure determination of recombinant CHRAC14-CHRAC16 54
3.2.16 RT-PCR 55
3.2.17 Production of four way junction DNA 55
3.2.18 Electrophoretic mobility shift assay (EMSA) 55
3.2.19 DNA pull-down assay 56
3.2.20 Nucleosome mobilisation assay 56
3.2.21 ATPase assay 56
3.2.22 HAT-assay 57
3.2.23 Standard molecular biology techniques 57

4 Results 58
4.1 Expression of recombinant CHRAC14-CHRAC16 58
4.1.1 Establishment of a bicistronic expression system for CHRAC14-CHRAC16 in *E. coli* 58
4.1.2 Expression of CHRAC14-CHRAC16 in a eukaryotic system (Sf9-cells) 61
4.1.2.1 Post-translational modification 61
4.1.2.2 Co-purification of an ATP-dependent remodelling activity from Sf9-cells with recombinant CHRAC14-CHRAC16 63
4.2 Characterisation of monoclonal antibodies directed against CHRAC14 and CHRAC16 64
4.2.1 Western blotting 64
4.2.2 Immunoprecipitation 67
4.2.3 Immunofluorescence 67
4.2.3.1 S2-cells and polytene chromosomes 67
4.2.3.2 Drosophila embryos 69
4.2.4 RT-PCR 71
4.3 Protein-protein interactions of CHRAC14-CHRAC16 with ACF1 72
4.3.1 Mapping of the interaction domain with ACF1 72
4.3.1.1 Co-expression studies in Sf9 cells 72
4.3.1.2 Interaction studies with in vitro-translated ACF1 constructs 73
4.3.2 Interaction of ACF1 with CHRAC14-CHRAC16 deletion variants 74
4.4 Composition and structure of the CHRAC14-CHRAC16 heterodimer 75
4.4.1 Sequence homology with different histone fold proteins 75
4.4.2 Crystal structure of CHRAC14-CHRAC16 78
4.5 DNA-binding properties of CHRAC14-CHRAC16 81
4.5.1 Structural considerations 81
4.5.2 Influence of the CHRAC14-CHRAC16 C-terminal tails on DNA binding 83
4.5.3 Dependence of the CHRAC14-CHRAC16-DNA interaction on DNA fragment length 84
4.5.4 Interaction with four-way junction DNA 88
4.6 Influence of CHRAC14-CHRAC16 on ACF-driven nucleosome mobilisation 89
4.6.1 Enhancement of the ACF-mediated nucleosome sliding activity by CHRAC14-CHRAC16 89
4.6.2 Dependence of the nucleosome sliding enhancement on the ACF1 WAC motif 91
4.6.3 Behaviour of C- and N-terminal deletion mutants of CHRAC14 and CHRAC16 in nucleosome mobilisation 92

5 Discussion 95
5.1 How do CHRAC14 and CHRAC16 interact? 95
5.1.1 Conclusions based on co-expression in *E. coli* 95
5.1.2 Heterodimer formation by CHRAC14-CHRAC16 96
5.2 How do the histone fold subunits function within CHRAC? 97
5.2.1 Functional similarities of histone-fold CHRAC subunits to other histone-like proteins and HMGB1 97
5.2.2 CHRAC histone fold subunits and nucleosome remodelling 100
5.2.3 A potential mechanism of CHRAC histone fold subunits 103
5.3 What is the role of CHRAC histone fold subunits *in vivo*? 105
5.3.1 Are ACF and CHRAC distinct complexes? 105
5.3.2 Potential roles of CHRAC histone fold subunits 106
5.3.2.1 Regulation of chromatin structure and transcription 106
5.3.2.2 Crosstalk between CHRAC and DNA polymerase epsilon 107
5.3.2.3 Potential regulatory roles 109
5.4 Open questions and future experiments 110

Appendix 114
Plasmid maps 114
List of abbreviations and acronyms 115

References 119

Curriculum Vitae 135

1 Summary

In eukaryotic nuclei, the DNA double helix is wound up and condensed into chromatin through the interaction with histones and further proteins. Several factors regulate the chromatin structure, allow unfolding or condensation of the chromatin fibre and permit or restrict access to DNA. One prominent class of chromosomal regulators is represented by ATP-dependent chromatin remodelling complexes, which use the energy derived from ATP-hydrolysis to break or alter histone-DNA contacts.

The ATP-utilising Chromatin Assembly and Remodelling Factor (ACF) and the Chromatin Accessibility Complex (CHRAC) are two closely related ATP-dependent chromatin remodelling factors. ACF consists of the ATPase ISWI and ACF1, a large protein that influences both the quality and efficiency of ISWI activity. CHRAC contains ISWI and ACF1 as well, but in addition the two small histone fold proteins CHRAC14 and CHRAC16. In this work, the CHRAC14 and CHRAC16 subunits are characterised both structurally and functionally.

The generation of a bicistronic expression plasmid allowed the expression and purification of highly pure recombinant CHRAC14-CHRAC16 in stoichiometric amounts. The crystal structure of the CHRAC14-CHRAC16 complex was solved at a resolution of 2.4 Å and demonstrates that the two proteins interact with each other via their histone fold motifs, thereby closely resembling the structure of histones H2A-H2B and NFYB-NFYC, the histone fold subunits of nuclear factor Y (NF-Y). Rat monoclonal antibodies against CHRAC14 and CHRAC16 were raised and characterised, but due to their poor affinity, they turned out to be only of limited use for the analysis of the two proteins. CHRAC14-CHRAC16 interact with the N-terminus of ACF1, including the conserved WAC motif. They have a weak affinity for DNA, and studies with CHRAC14-CHRAC16 deletion variants revealed that their C-termini play important but distinct roles in DNA binding. Finally, CHRAC14-CHRAC16 facilitate ACF-dependent nucleosome mobilisation, and their ability to enhance ACF activity depends on both the interaction with the ACF1 N-terminus and the dynamic binding to DNA.

In the light of profound similarities to the effects of HMGB1 (high mobility group box protein 1) on nucleosome sliding, these data imply that the CHRAC14-CHRAC16 subcomplex operates as a 'DNA chaperone' and assists ACF1 and ISWI during ATP-dependent nucleosome remodelling by providing a transient DNA binding surface.

This work provides the basis for further experiments to gain more insights into the mechanistic details of CHRAC-dependent nucleosome remodelling and to explore the roles of CHRAC in the living cell.

2 Introduction

2.1 Chromatin structure

2.1.1 The nucleosome

The complex and dynamic arrangement of the eukaryotic genome is represented by chromatin. All DNA-related processes like transcription, replication and repair depend on chromatin structure, and tight regulation of this structure is necessary in order to guarantee the reliable execution of these viable processes. Hence, chromatin is much more than just a smart way of storing DNA within the nucleus.

The 'building block' of chromatin is the nucleosome, which consists of a globular protein moiety that is wrapped in DNA (Figure 2.1). The protein components of the nucleosome are the four core histones, H2A, H2B, H3 and H4. Histones belong to the most conserved proteins in nature, which reflects their universal function and importance. They dimerise via a conserved structural motif, the histone fold (see 2.2), and build up an octamer.

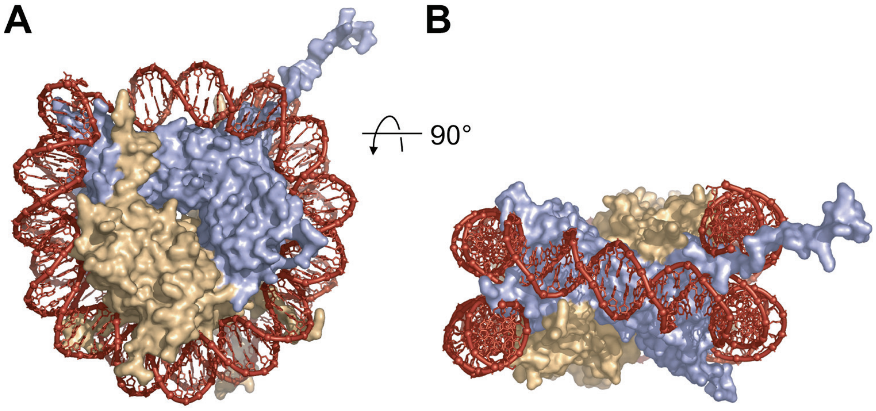

Figure 2.1: Crystal structure of the nucleosome core particle (Luger *et al.*, 1997). A: side view, B: view of nucleosomal dyad. The views in A and B are related by a 90° rotation around a horizontal axis. The surface of histones H3 and H4 is shown in blue and the surface of histones H2A and H2B is shown in orange. The figure was produced with the programme PyMol (DeLano, 2002).

The crystal structure of the core nucleosome particle at 2.8 Å (Luger *et al.*, 1997) shows that a $(H3\text{-}H4)_2$ tetramer builds the centre of the nucleosome. Tetramerisation of two H3-H4 dimers occurs trough a four-helix bundle formed by the H3 histone fold (see Figure 2.3 B). To each side of the tetramer, one H2A-H2B dimer is attached by forming a similar four-helix bundle between H4 and H2B. 147 base pairs of DNA are wrapped around the octamer surface in about 1.7 turns to form the disc-shaped structure of the nucleosome. The N-terminal tails of the histones are largely unstructured. They stick out from the compact core structure and provide a platform for several regulatory mechanisms (see 2.3.1). While the H3 and H2B tails pass between the gyres of the DNA, the tails of H4 and H2A protrude laterally from the nucleosome core particle (Luger *et al.*, 1997).

The nucleosomes are connected by linker DNA, which can be variable in length. Binding of one molecule of linker histone H1 per nucleosome completes the chromatosome. The linker histone organises another 20 base pairs of DNA, restricts its accessibility and is important for chromatin condensation. Condensed chromatin folds into higher order structures.

2.1.2 Higher order structures of chromatin

The second level of DNA condensation following nucleosomal compaction is the so-called 30 nm fibre, a helical array of nucleosomes with a diameter of 30 nm. Beyond the 30 nm fibre, the hierarchical packaging of chromatin into higher order structures is only poorly understood, although several studies have addressed the organisation of chromatin 'domains' or 'loops' from early on (Filipski *et al.*, 1990; Igo-Kemenes and Zachau, 1978). Chromatin condensation culminates in the highly compacted structure of mitotic chromosomes. The N-terminal histone termini, phosphorylation of histone H3 serine 10 (H3S10, see also 2.3.1) as well as architectural proteins such as the condensin complex are required for mitotic chromatin compaction (Woodcock and Dimitrov, 2001).

The most favoured models of 30 nm fibre organisation are the so-called solenoid or one-start helix and the two-start helix. The one-start model suggests that the nucleosomes follow one after another on the same helical path, connected by bent linker DNA (Finch and Klug, 1976). In the two-start helix, two consecutive nucleosomes are placed in two different levels of the helix and are connected by straight linker DNA (Woodcock and Dimitrov, 2001). Two different arrays are conceivable for the two-start helix: In the supercoiled or helical ribbon model, the nucleosomes are arranged in a zigzag fashion, and the resulting ribbon is wound into a helix. In the twisted or crossed linker model, two consecutive nucleosomes are placed on opposite sides of the helical axis, with the linker DNA sections crossing each other in the helix centre.

Recently, Richmond and colleagues showed by crosslinking of nucleosomal arrays followed by cleavage of the linker DNA, that the 30 nm fibre is likely to be organised in a two start fashion (Dorigo *et al.*, 2004). The biochemical analysis was confirmed by the crystal structure of a tetranucleosome at 9 Å resolution (Schalch *et al.*, 2005, see Figure 2.2). The structure shows that the linker DNA connects two stacks of nucleosomes in a fashion that closely resembles the two start crossed linker model of the 30 nm fibre. The fact that the linker DNA exists in a straight and a bent conformation in the crystal structure of the tetranucleosome argues for a dinucleosome to be the building unit of higher order chromatin (Schalch *et al.*, 2005).

However, despite the solved crystal structure of the tetranucleosome, the discussion about the 30 nm fibre organisation continues. Rhodes and colleagues address this question by *in vitro*-reconstitution of nucleosomal arrays that contain linker histones. Their electron microscopy studies of their reconstituted 30 nm fibres argue for a solenoidal one-start organisation, in which nucleosome number seven interdigitates between nucleosomes number one and two (Huynh *et al.*, 2005) and unpublished results.

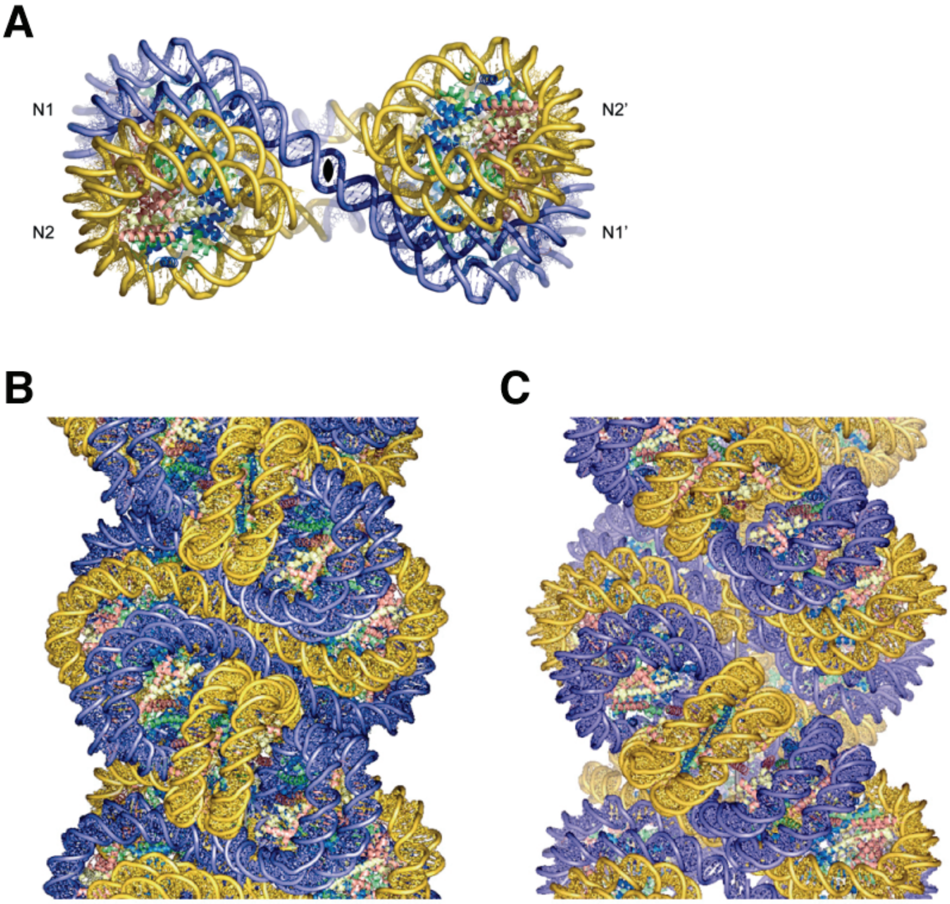

Figure 2.2: A: Crystal structure of the tetranucleosome. B: Idealised model of the 30 nm chromatin fibre based on the structure of nucleosome N2 in the tetranucleosome (see panel A). C: 'Direct' model based on the parameters of nucleosomes N1 and N2 of the tetranucleosome structure (panel A). Both models shown in panels B and C are two start models of the crossed linker type. Adapted from (Schalch *et al.*, 2005).

2.2 The histone fold

2.2.1 Structure of the core histones

The core histones H2A, H2B, H3 and H4 are built of three structural elements: The so-called histone fold motif, structured regions adjacent to the histone fold that are specific for the different histone types and the flexible and unstructured N- and C-terminal tails. These components are also present in the crystal structure of histones H3 and H4 shown in Figure 2.3 (Luger *et al.*, 1997). The histone fold is a short and rather simple structural motif consisting of three α-helices connected by two flexible loops. The first and the third helix are rather short and consist of approximately eleven residues, whereas the second (central) helix is longer and contains approximately 27 residues. The lengths of these helices vary from histone to histone by one or two residues (Arents and Moudrianakis, 1995). This characteristic structural composition seems to be the result of a tandem duplication of a short helix-loop-helix motif. It should be pointed out that in contrast to the core histones, the linker histones have evolved from a different structural ancestor (Arents and Moudrianakis, 1993; Arents and Moudrianakis, 1995).

The histone fold motif is a potent protein dimerisation module, and indeed, no folded histone monomers have been observed under physiological conditions. The dimerisation occurs head-to-tail in a so-called 'handshake' manner, with the two central α-helices packing against each other (Figure 2.3 A). The conserved residues that form the interaction surface are predominantly hydrophobic. Furthermore, conserved residues that are responsible for DNA contacts are located within the first helix and the interhelical loops of the histone fold (Arents *et al.*, 1991; Arents and Moudrianakis, 1995). Apart from the 'classical' core histones, the histone fold motif is also found in a variety of other proteins, including general transcription factors, transcriptional activators and subunits of HAT[1] (histone acetyltransferase) and DNA Polymerase complexes (see 2.2.2).

---

[1] A list of abbreviations and acronyms used in this work is given in the appendix.

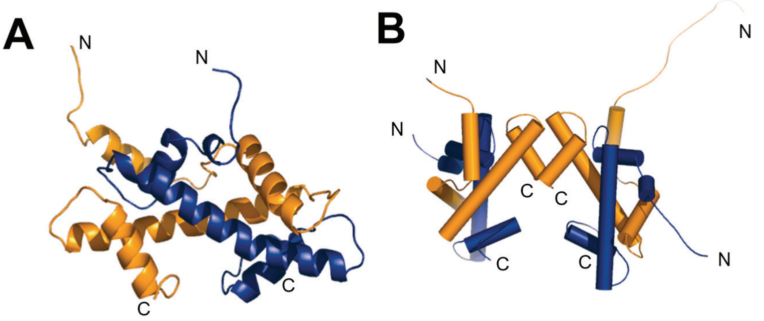

Figure 2.3: Crystal structure of the histones H3 (orange) and H4 (blue) in the nucleosome core particle (Luger *et al.*, 1997). A: H3-H4 dimer showing the 'handshake' histone fold. B: $(H3\text{-}H4)_2$ tetramer. Two heterodimers dimerise via a four-helix bundle formed by the two histone H3 molecules. The figures were produced with the programme PyMol (DeLano, 2002). Note that panels A and B are not shown in the same scale.

2.2.2 Histone fold proteins

2.2.2.1 Archeal histone fold proteins

The histone fold motif is not exclusively restricted to the eukaryotic kingdom, because histone fold proteins have also been found in archea, but not in bacteria. The amino acid sequence of archeal histones is most similar to that of the eukaryotic histones H3 and H4, which hints at a common ancestor. Usually, the archeal histones have only 66 to 69 residues and – apart from few exceptions – lack any N- and C-terminal tail extensions. Only few archeal histones have C-terminal histone tails of about 30 amino acid residues, but these extensions are not related to eukaryotic histone tails, and some archeal species possess polypeptide chains including two tandemly arranged histone fold motifs that have been shown to fold into an intramolecular histone fold dimer (reviewed in Reeve *et al.*, 2004). The eukaryotic C- and N-terminal extensions that are crucial for histone modifications and other kinds of regulatory mechanisms must have evolved at a later point in time. Besides, archeal histones like HMfA and HMfB (histone from *Methanothermus fervidus*) can form homodimers as well as heterodimers, both *in vitro* and *in vivo* (Grayling *et al.*, 1996; Sandman *et al.*, 1994). This might reflect different biological functions of homo- and heterodimers. By crosslinking experiments, archeal histones have been shown to form tetramers *in vivo*, which are able to protect approximately 60 base pairs of DNA from nuclease digestion (Grayling *et al.*, 1997). Therefore, the archeal histones seem to organise DNA in a similar manner than the histone H3-H4 tetramer in eukaryotes, which organise approximately 80 base pairs of DNA in the absence of histone H2A-H2B dimers (reviewed in Pereira and Reeve, 1998; Reeve *et al.*, 2004).

2.2.2.2 *TATA box-binding protein-associated factors (TAFs)*

Together with the TATA box-binding protein (TBP), the TAFs (TBP-associated factors) make up the general transcription factor TFIID, which is crucial for initiation of transcription by RNA Polymerase II. TBP binds directly to DNA, inducing a sharp bend. Subsequently, other general transcription factors and RNA Polymerase II are recruited to form the preinitiation complex (PIC). Furthermore, TAFs are also subunits of several multi-protein complexes lacking TBP, such as the yeast SAGA histone acetyltransferase complex, the TBP-free TAF-containing complex (TFTC), and the metazoan PCAF/GCN5 and STAGA complexes (reviewed in Müller and Tora, 2004). All these complexes – including TFIID – contain a histone acetyltransferase activity that changes chromatin structure (Brand *et al.*, 1999b; Grant *et al.*, 1998; Mizzen *et al.*, 1996, see also 2.3.1).

The existence of histone-like structural motifs in TAFs was first suggested by sequence homology and their ability to form specific dimers (Kokubo *et al.*, 1994). The crystal structure of *Drosophila* TAF6-TAF9[2] revealed that these TFIID subunits form tetramers reminiscent of histone H3-H4 (Xie *et al.*, 1996), and the presence of histone octamer-like structures within TFIID has been proposed (Hoffmann *et al.*, 1996). Indeed, a striking number of TAFs have histone fold domains. For instance, in yeast, nine out of the fourteen TAFs are histone fold proteins (Gangloff *et al.*, 2001; Gangloff *et al.*, 2000; Reese *et al.*, 2000; Sanders and Weil, 2000). In contrast to the small nucleosomal core histones, the histone fold TAFs show a wide variability in size, ranging in human approximately from 18 kDa (hTAF13) to 140 kDa (hTAF3) (Tora, 2002). Consequently, the histone fold domains of the larger histone fold TAFs make up only a minor proportion of the polypeptide.

In vitro reconstitution studies of yeast TAF9, TAF6, TAF12 and TAF4 revealed that they form an octameric complex similar to the core histone octamer. yTAF9 and yTAF6 are believed to form a H3-H4-like tetramer like their counterparts in *Drosophila* (Xie *et al.*, 1996), whereas yTAF12 and yTAF4 dimerise in a histone H2A-H2B-like fashion. Presumably, these dimers flank each side of the $(\text{yTAF9-yTAF6})_2$ tetramer to complete the octamer structure (Selleck *et al.*, 2001). Moreover, temperature-sensitive phenotypes of mutations within these histone fold TAFs can be compensated by overexpressing the putative octamer interaction partners, but not by overexpressing other TAFs (Selleck *et al.*, 2001).

Electron microscopy-derived structural models of human and yeast TFIID reveal a clamp- or horseshoe-like structure consisting of three prominent lobes. TBP is located close to the central lobe, consistent with the hypothesis that the groove within TFIID serves as DNA binding site (Andel *et al.*, 1999; Brand *et al.*, 1999a; Leurent *et al.*, 2002; Leurent *et al.*, 2004). The histone fold TAFs reside in all three lobes of TFIID, and at least two copies of each histone fold TAF are present in the EM structure. The TAF6-TAF9- and the TAF4-TAF12 histone-like pairs are found both together and apart from each other, suggesting that the predicted octamer (Selleck *et al.*, 2001, see above) could still form within TFIID, but indicating that these TAFs exist also separately (Leurent *et al.*, 2002).

---

[2] For detailed description of the unified, species-independent TAF nomenclature, see Tora, L. (2002) A unified nomenclature for TATA box binding protein (TBP)-associated factors (TAFs) involved in RNA polymerase II transcription. *Genes Dev*, **16**, 673-675.

As mentioned above, histone-like TAFs are also part of multiprotein complexes other than TFIID. In these complexes, they are either found associated with other histone-like TAFs (e. g. TAF6-TAF9) or with different histone fold proteins that are specific for the respective complex and not present in TFIID. For instance, yTAF12 interacts with yTAF4 in TFIID, but with Ada1p in the SAGA complex (Gangloff *et al.*, 2000). Similarly, yTAF10 is believed to dimerise with both yTAF3 and yTAF8 in TFIID and with Spt7p in the SAGA complex (Gangloff *et al.*, 2001). Interestingly, the SAGA component Spt3p contains two histone fold motifs located at the N- and C-terminus that are homologous to the histone fold motifs of human TAF11 and TAF13. Therefore, it has been speculated that these two domains form an intramolecular histone fold (Birck *et al.*, 1998).

The reason for the frequent occurrence of the histone fold structural motif in TFIID, SAGA and related complexes is unknown. The histone fold TAFs are essential, and in some cases, their histone fold domains alone are sufficient to support growth (Gangloff *et al.*, 2001). It has been suggested that the histone fold dimers, tetramers and octamers may bind DNA in a similar way than the histones in the nucleosome. However, several of the conserved basic residues that are responsible for interacting with the DNA backbone within the nucleosome structure (Luger and Richmond, 1998) are not conserved in histone fold TAFs, and the reconstituted yeast histone fold TAF octamer has been found not to interact with DNA (Selleck *et al.*, 2001).

TAFs might have adopted histone fold domains simply because they serve as very efficient protein dimerisation modules. A recent study revealed that hTAF10, a histone fold TAF without intrinsic nuclear localisation signal (NLS), is imported into the nucleus only in complex with one of its three histone fold interaction partners. The resulting histone fold dimers are likely to be imported via different pathways, suggesting tight regulatory mechanisms (Soutoglou *et al.*, 2005).

Certainly, histone fold TAFs have also architectural functions in their respective complexes (Gangloff *et al.*, 2000; Sanders and Weil, 2000; Selleck *et al.*, 2001). Likewise, the recent EM structure of the SAGA complex suggests a central scaffold consisting of TAFs and TAF-like subunits that serves as an assembly platform for proteins responsible for SAGA-specific functions (Wu *et al.*, 2004).

2.2.2.3 Negative Cofactor 2 (NC-2)

Negative Cofactor 2 (NC-2) has originally been found in human cell extracts as an interaction partner of TBP that inhibits transcription by RNA Polymerase II (Meisterernst and Roeder, 1991). It consists of the two subunits Drap1 (NC-2α) and Dr1 (NC-2β), which are both essential for yeast viability, and a knockout of murine Drap1 leads to severe phenotypes in early embryonic development (Iratni *et al.*, 2002; Kim *et al.*, 1997). The NC-2 subunits are histone fold proteins and interact with each other in a histone H2A-H2B-like fashion. It has been reported that the NC-2 heterodimer binds to TBP-promoter complexes via its histone fold (Goppelt *et al.*, 1996). The crystal structure of NC-2 together with TBP bound to DNA has been solved and shows that NC-2 binds to the DNA at the opposite side of TBP, thereby preventing the interaction with the general transcription factors TFIIA and TFIIB (Kamada *et al.*, 2001). Recently, it has been reported that the specificity of TBP for TATA elements is significantly reduced when it is complexed by NC-2 and that NC-2 is able to load TBP onto TATA-less DNA sequences. Therefore, it has been postulated that NC-2 might also function as a recruitment factor, which directs TBP to TATA-less promoters (Gilfillan *et al.*, 2005).

2.2.2.4 Nuclear Factor Y (NF-Y)

Nuclear Factor Y (NF-Y, also termed CBF and HAP complex in *S. cerevisiae*) is a heterotrimeric transcriptional activator that binds with high affinity and specificity to the CCAAT box of promoters, but also to 'unorthodox' CCAAT sites in introns or promoter-distant locations (Maity and de Crombrugghe, 1998; Testa *et al.*, 2005). It interacts with general transcription factors, especially TFIID, as well as with other prominent transcriptional regulators such as c-myc and p53 (Frontini *et al.*, 2002; Imbriano *et al.*, 2005; Izumi *et al.*, 2001). All three subunits, NFYA, NFYB and NFYC, contain highly conserved core regions that are required for CCAAT binding, whereas the sequence extensions that contain the activator domains are less conserved (McNabb *et al.*, 1995; Sinha *et al.*, 1995). Crosslinking experiments revealed that all three subunits interact directly with DNA (Liang and Maity, 1998). The NFYB and NFYC subunits are histone fold proteins. The structure of the NFYB-NFYC heterodimer has been solved and shows high similarity to the histones H2A and H2B and also to NC-2α and NC-2β (Romier *et al.*, 2003). An α-helix that follows directly after the histone fold motif of the NFYC-subunit (αC) is crucial for the interaction with the non-histone fold subunit NFYA and other transcription factors (Romier *et al.*, 2003).

2.2.2.5 *Subunits of DNA Polymerase epsilon*

DNA Polymerase epsilon (DNA Pol ε) is conserved throughout eukaryotes. In yeast, it is essential for replication (Morrison *et al.*, 1990), but plays also a role in DNA repair, since it catalyses DNA synthesis after UV-irradiation (Budd and Campbell, 1995). It has been proposed that DNA Pol ε functions as a sensor of the S phase checkpoint in cell cycle control by recognising DNA damage and blocked DNA replication (Araki *et al.*, 1995; Navas *et al.*, 1995). Recent findings suggest that DNA Pol ε functions in concert with DNA Pol α and DNA Pol δ at multiple replication forks during S phase (Hiraga *et al.*, 2005).

Yeast DNA Pol ε consists of four subunits. The catalytic subunit, Pol2p, is associated with Dpb2p (for DNA Polymerase B), and both subunits are essential for viability (Hamatake *et al.*, 1990; Sugino, 1995). In contrast, the two small histone fold subunits Dpb3p and Dpb4p are non-essential, and their function is poorly understood (Araki *et al.*, 1991; Ohya *et al.*, 2000). The human DNA Pol ε complex contains four polypeptides as well, which are all orthologues of the yeast subunits (Li *et al.*, 2000).

2.2.2.6 *Subunits of the Chromatin Accessibility Complex (CHRAC)*

To date, the Chromatin Accessibility Complex (CHRAC, for more detailed descriptions, see 2.3.5.2 and 2.5), is the only ATP-dependent remodelling factor that is known to contain histone fold subunits. CHRAC was originally discovered in *Drosophila* (Varga-Weisz *et al.*, 1997), and its four-subunit composition is conserved throughout eukaryotes (see 2.5).

Interestingly, yeast CHRAC shares its histone fold subunit Dpb4p with DNA Pol ε (see 2.2.2.5). Whereas Dpb4p interacts with Dpb3p in DNA Pol ε, its interaction partner in yCHRAC is another histone fold protein termed Dls1p (Dpb3-like subunit 1) (Iida and Araki, 2004). Likewise, the p17 subunit of human CHRAC is also a member of human DNA Pol ε (Li *et al.*, 2000; Poot *et al.*, 2000). It has been proposed that DNA Pol ε and CHRAC might have counteracting functions at telomeres (Iida and Araki, 2004), but this connection between DNA replication and chromatin remodelling and its functional implications need to be further investigated.

In *Drosophila*, no histone fold subunits have been described for DNA Pol ε, which might just be due to their small size (Aoyagi *et al.*, 1997; Oshige *et al.*, 2000). Therefore, it remains to be clarified if the *Drosophila* histone fold subunit CHRAC14, which is the corresponding orthologue of yeast Dpb4p and human CHRAC17, is shared between CHRAC and DNA Pol ε.

2.3 Chromatin dynamics and regulation

2.3.1 Histone modifications

The N-terminal core histone tails are flexible, intrinsically unstructured and protrude from the nucleosome core particle (Luger *et al.*, 1997), see 2.1.1). They are the target of a complicated network of factors regulating chromatin structure. Histone modifying enzymes usually reside in large protein complexes and set covalent marks at distinct residues of the histone tails, but also at certain residues within the nucleosome core structure. These covalent modifications alter the chromatin structure and serve as labels that are recognised by a variety of chromatin binding proteins, transcriptional activators or repressors and ATP-dependent chromatin remodelling factors (Fischle *et al.*, 2003). The entirety of the different histone modifications has been termed 'histone code', because its potentially combinatorial character extends the information laid down in the genetic code and adds another level of complexity to chromatin regulation (Jenuwein and Allis, 2001; Turner, 2002).

Histone modifications include phosphorylation, acetylation, methylation, ubiquitinylation, SUMOylation, and poly-ADP-ribosylation (reviewed in Turner, 2005). A short summary of the most important modifications shall be given in the following paragraph.

Histone acetyltransferases (HATs) acetylate the side chains of lysine residues and can be divided into five different classes (Carrozza *et al.*, 2003). Acetylation of histones is highly reversible, and there are three classes of histone deacetylases (HDACs) in yeast and four classes in mammals, respectively (Yang and Gregoire, 2005). Generally, acetylation unfolds the chromatin structure and makes it competent for transcription (Eberharter and Becker, 2002). Prominent examples for this transcriptional activation are the acetylation of promoter proximal regions by the yeast SAGA complex (which contains the HAT Gcn5p) (Vignali *et al.*, 2000b) or the hyperacetylation of the male X chromosome at histone H4 lysine 16 in *Drosophila* through MOF (males absent on the first), a component of the dosage compensation complex (Smith *et al.*, 2000). However, some HATs of the MYST family (MOZ, Ybf2/Sas3, Sas2, Tip60), e. g. Sas2p and Sas3p in yeast, cause transcriptional silencing at certain loci. Furthermore, histone acetylation is also implicated in DNA repair, DNA replication and cell cycle progression(Carrozza *et al.*, 2003).

Methylation marks are set by histone methyltransferases (HMTs). Compared to acetylation, the nature of this modification is more complex, because not only the amino groups of lysine residues but also the guanidino groups of arginine residues can be methylated. Furthermore, lysines can be mono-, di- and trimethylated and arginines mono- or dimethylated. Methyl marks are considered to be rather stable modifications, however, specific demethylase enzymes have been discovered recently (Cuthbert *et al.*, 2004; Shi *et al.*, 2004; Tsukada *et al.*, 2005).

The readout of the histone methylations strongly depends on the methylated residue. While methylation of the lysine residue 4 of the histone H3 tail (H3K4) is associated with actively transcribed genes (Santos-Rosa *et al.*, 2002), methylation of the lysine residue 9 (H3K9) creates a binding site for HP1 (heterochromatin protein 1), which is a landmark of silent chromatin (Greil *et al.*, 2003; Lachner *et al.*, 2001).

Phosphorylation of histone H3 serine 10 (H3S10) during mitosis is crucial for chromosome condensation and cell-cycle progression. Besides, histone phosphorylation is also implicated in transcriptional activation during interphase (Nowak and Corces, 2004). The vicinity of H3S10 to the lysine residues H3K9 and H3K14, which are known to be modified by acetylation and/or methylation has led to speculations about a cross-talk between phosphorylation and acetylation at the H3 tail (Clayton and Mahadevan, 2003; Mateescu *et al.*, 2004; Nowak and Corces, 2004). Furthermore, phosphorylation of specific serine residues in the histone variants H2A.X in mammals and H2Av in *Drosophila* is linked to DNA double strand break repair (see 2.3.2, Peterson and Cote, 2004; Redon *et al.*, 2002).

Recently, an increasing number of studies report functional connections between different histone modifications, providing more and more evidence for the histone code hypothesis. For example, interactions exist between acetylation and phosphorylation at the histone H3 tail (see above). Other correlations have been described, such as the relationship between histone H2B mono-ubiquitinylation and histone H3 methylation at lysine residues 4 and 79 (Shahbazian *et al.*, 2005) or links between histone methylation and deacetylation (Carrozza *et al.*, 2005; Keogh *et al.*, 2005).

2.3.2 Histone variants

In contrast to the regular core histones, histone variants are incorporated into chromatin independently of DNA replication. For many variant histones, the understanding of the specific functions, their deposition and the targeting of interacting factors is not very extensive yet, but constantly growing (Jin *et al.*, 2005a; Sarma and Reinberg, 2005).

There are two major variants of histone H3. The histone variant H3.3 differs only in four residues from canonical H3, and is closely linked to actively transcribed chromatin (Ahmad and Henikoff, 2002). Interestingly, the canonical yeast histone H3 is identical to the H3.3 variant of higher eukaryotes, which is consistent with the rather open and actively transcribed state of the yeast genome. In agreement with the presence of H3.3 in transcriptionally active regions, it is enriched in post-translational modifications that are characteristic for active chromatin, such as lysine 4-methylation and acetylation of several lysine residues (see 2.3.1).

The second prominent histone H3 variant, centromere protein A (CENP-A), is specifically incorporated into centromeric regions. During mitosis, CENP-A-phosphorylation at the kinetochores is thought to be a crucial step in chromosome segregation (Zeitlin *et al.*, 2001).

The yeast histone variant Htz1p (an orthologue of the mammalian variant H2A.Z) is required for transcription of certain genes and serves as a barrier for spreading of heterochromatic modifications into euchromatin (Kamakaka and Biggins, 2005). Htz1p-containing nucleosomes are less stable, which could play a role in activating repressed promoters (Zhang *et al.*, 2005). In contrast to yeast Htz1p, the variant H2A.Z co-localises with heterochromatin protein 1 (HP-1) in heterochromatic foci of higher eukaryotes (Rangasamy *et al.*, 2003), and a knockdown of this H2A variant leads to genomic instability (Rangasamy *et al.*, 2004).

Whereas H2A.Z is concentrated in distinct chromosomal domains, the H2A.X variant appears to be widely and randomly incorporated into the genome. The C-terminal part of H2A.X contains a serine residue that gets specifically phosphorylated in the vicinity of DNA double strand lesions. Therefore, phosphorylated H2A.X serves as a marker for DNA damage and is thought to recruit components of the repair machinery. The only H2A variant in *Drosophila*, H2Av, combines properties of both H2A.Z and H2A.X, but the functional consequences are not clear.

Vertebrates have two more H2A variants. H2A.Bbd (for Barr body deficient) alters the nucleosome structure significantly, resulting in more accessible nucleosomal core particles. Consistently, it is mainly present in actively transcribed chromatin, whereas it is absent on the inactivated X chromosome in females, the Barr body (Bao *et al.*, 2004). By contrast, the variant histone macroH2A is specifically enriched in the Barr body. With its 20 kDa C-terminal domain, it is thought to recruit HDACs and other factors involved in silencing.

2.3.3 Histone chaperones

The concentration of histone proteins has to be tightly regulated, because the exact stoichiometry of the core histones is crucial for the eukaryotic cell. In fact, overexpression of either of the two histone pairs H2A/H2B or H3/H4 can lead to chromosome loss in yeast (Meeks-Wagner and Hartwell, 1986). Besides other regulatory mechanisms, the histone levels are managed by histone chaperones. These factors associate with histones outside of chromatin, keep them soluble and communicate with other histone-interacting partners.

Several classes of histone chaperones have been described, and distinct functions can be assigned to each class. Some prominent examples for histone chaperones shall be mentioned here: Nucleoplasmin is a H2A/H2B-specific factor that can serve as a 'histone sink' and is able to maintain a pool of histones ready for transfer to other chaperones. The function of CAF-1 (chromatin assembly factor 1), a histone H3/H4-specific chaperone, is tightly linked to the DNA replication- and repair-dependent histone deposition. The yeast Hir (histone regulation) proteins and their vertebrate counterpart Hira assist in chromatin assembly pathways independent of DNA replication, and Nap-1 (nucleosome assembly protein 1) is thought to be involved in histone transfer between the cytosol and the nucleus and in cell cycle regulation. Furthermore, some histone binding factors, such as the retinoblastoma-associated proteins 46 and 48 (RbAP46/48) and actin-related proteins (ARPs) are *bona fide* subunits of several chromatin-modifying complexes like histone acetyltransferase or chromatin remodelling complexes (see 2.3.5, reviewed in Loyola and Almouzni, 2004).

2.3.4 HMG box proteins

The High Mobility Group (HMG) box, an amino acid motif of approximately 80 residues, is the common feature of HMG box proteins. The structure of this motif consists of three α-helices, which adopt an L-like shape. HMG boxes have either a strong preference for structured or distorted DNA over B-form DNA, or they bend linear DNA tightly upon binding.

HMG proteins are divided into the three classes HMGB, HMGA and HMGN, which have distinct properties (Bustin, 2001). Amongst other features, the three classes differ in the DNA sequence specificity, ranging from none to very high. However, all classes share a sequence-independent affinity for four-way junction DNA.

The HMGB (b for box) class with its most prominent members HMGB1 and HMGB2 in vertebrates and HMG-D in *Drosophila* contains one or two HMG boxes and an acidic C-terminal tail. These proteins display no DNA sequence specificity and bind only weakly to linear DNA. They are very abundant in the nucleus, with an average of one molecule per every ten to fifteen nucleosomes, and have been described as 'architectural facilitators' of chromosomal structure (Thomas and Travers, 2001). Apart from this global role on chromatin, these proteins have a variety of more distinct functions. For example, they assist in the assembly of certain transcriptional regulators on DNA, especially if the resulting complex contains tightly bent DNA. This chaperone role has been shown e. g. for steroid hormone receptors, p53 or in V(D)J recombination (Agresti *et al.*, 2005; Boonyaratanakornkit *et al.*, 1998; Fugmann *et al.*, 2000; Jayaraman *et al.*, 1998). Furthermore, HMGB1 is able to interact with TBP bound to the TATA box and interferes with the general transcription factor TFIIB, thereby repressing transcription initiation. In contrast, HMGB2 has an activating function on transcription initiation (Thomas and Travers, 2001).

HMGB1 and the *Drosophila* orthologue HMG-D are able to bind to the DNA entry/exit site of the nucleosome core particle, in analogy to the linker histone H1 (Nightingale *et al.*, 1996; Ragab and Travers, 2003). In the pre-blastoderm stage of early *Drosophila* development, HMG-D functions as a specialised linker protein prior to the incorporation of histone H1. In later developmental stages, HMG-D is substituted by H1 (Ner *et al.*, 2001; Ner and Travers, 1994). However, clear differences in linker DNA binding exist between HMG-D and linker histones: Both linker histone binding and HMG-D binding induce changes in the DNA accessibility, but the observed patterns are distinct. In general, the DNA accessibility is reduced at most locations by the linker histones, while HMG-D increases DNA accessibility at several sites (Ragab and Travers, 2003).

Moreover, several indications imply a role of HMG-motif proteins in ATP-dependent chromatin remodelling. The SWI/SNF-type chromatin remodelling complexes BAF and BRM (see 2.3.5.1 and Table 2.I) contain HMG-box subunits (Papoulas *et al.*, 2001; Wang *et al.*, 1998), and HMGB1 facilitates nucleosome mobilisation by ACF (see 2.3.5.2 and Table 2.II, Bonaldi *et al.*, 2002). These and other lines of evidence have led to the hypothesis that HMGB proteins play an essential role in changing the nucleosome structure in a way that it is primed for nucleosome remodelling (Travers, 2003).

2.3.5 ATP-dependent chromatin remodelling complexes

Chromatin Remodelling complexes disrupt or modulate nucleosomal histone-DNA contacts in an ATP-dependent manner. They take part in the regulation of chromatin-related processes such as transcription, DNA replication and DNA repair (Becker and Hörz, 2002, see 2.4.1). All of these complexes contain a superfamily 2 (SF2)-class ATPase subunit (Eisen *et al.*, 1995, see 2.4.3). The remodelling ATPases can be divided into different subcategories, according to the presence of characteristic functional domains. So far, seven of these SF2-type ATPase subcategories have been implicated in chromatin remodelling. The ATPases of the Swi2p/Snf2p, ISWI, CHD1/Mi-2 and Swr1p/Ino80p type are the best understood (Eberharter and Becker, 2004).

Table 2.I: Chromatin remodelling ATPases and their complexes in different species. See text for details.

ATPase subclass	*S. cerevisiae*	*D. melanogaster*	*H. sapiens*
Swi2p/Snf2p	SWI/SNF[a] RSC[b]	BRM/BAP[c] PBAP[d]	BAF[e] hBRM/hBRG1[e] PBAF[e] WINAC[f] NUMAC[g]
ISWI[h]	ISW1a ISW1b ISW2 yCHRAC	NURF ACF CHRAC	hNURF hACF hCHRAC hWICH hRSF
CHD1/Mi-2	Chd1p[i]	dMi-2[j]	NuRD[k] CHD1[l] MeCP1[m]
Swr1p/Ino80p	INO80[n] SWR1[o]	dTIP60[p]	hINO80[q] SRCAP[r] TRRAP/TIP60[s]

[a] (Cairns *et al.*, 1994; Neigeborn and Carlson, 1984; Peterson *et al.*, 1994; Stern *et al.*, 1984)
[b] (Cairns *et al.*, 1996)
[c] (Dingwall *et al.*, 1995; Papoulas *et al.*, 1998; Tamkun *et al.*, 1992)
[d] (Mohrmann *et al.*, 2004)
[e] (Becker and Hörz, 2002; Eberharter and Becker, 2004; Phelan *et al.*, 1999; Vignali *et al.*, 2000a) and references therein
[f] (Kitagawa *et al.*, 2003)
[g] (Xu *et al.*, 2004)
[h] for references of ISWI-containing complexes, see Table 2.II
[i] (Tran *et al.*, 2000)
[j] (Brehm *et al.*, 2000)
[k] (Tong *et al.*, 1998; Xue *et al.*, 1998; Zhang *et al.*, 1998)
[l] (Kelley *et al.*, 1999; Stokes and Perry, 1995)
[m] (Feng and Zhang, 2001)
[n] (Shen *et al.*, 2000)
[o] (Kobor *et al.*, 2004; Krogan *et al.*, 2003; Mizuguchi *et al.*, 2004)
[p] (Kusch *et al.*, 2004)
[q] (Jin *et al.*, 2005b)
[r] (Cai *et al.*, 2005)
[s] (Cai *et al.*, 2005; Cai *et al.*, 2003; Jin *et al.*, 2005a)and references therein

2.3.5.1 *SWI/SNF complexes*

Swi2p/Snf2p-type ATPases reside in large multi-subunit complexes containing actin and/or actin-related proteins (ARPs). The eleven-subunit SWI/SNF complex from *S. cerevisiae* improves the efficiency of DNA replication and plays an important role in both repression and activation of distinct sets of genes (Becker and Hörz, 2002). There is a functional interplay between SWI/SNF-dependent chromatin remodelling and histone acetylation (reviewed in Eberharter *et al.*, 2005). For instance, Swi2p/Snf2p-type ATPases contain a bromodomain (brd), a protein motif which has been shown to bind to acetylated lysine residues (Zeng and Zhou, 2002), and the SWI/SNF complex recruits the histone acetyl-transferase Gcn5p to certain promoters. It has also been proposed that tight repression of yeast promoters correlates with SWI/SNF-dependent activation (Krebs *et al.*, 2000).

RSC (remodels the structure of chromatin) is another remodelling complex in yeast that is closely related to SWI/SNF. Most of its 15 different subunits, including the ATPase subunit Sth1p (Snf two homologous), are either homologous or identical to SWI/SNF subunits. However, RSC is more abundant than the SWI/SNF complex and, in contrast to SWI/SNF, essential for yeast viability. This is probably due to the regulation of ribosomal and cell wall-specific genes (Becker and Hörz, 2002; Mohrmann and Verrijzer, 2005).

Orthologous complexes for both SWI/SNF and RSC have been purified from *Drosophila* and human cells (Eberharter and Becker, 2004; Mohrmann and Verrijzer, 2005, see also Table 2.I). The SWI/SNF complex corresponds to the human BAF and the *Drosophila* brahma (BRM) complex, while the complexes orthologous to the RSC complex are PBAF in humans and BAP in *Drosophila.* A number of additional SWI/SNF-like complexes have been described in higher eukaryotes, but their functions and subunit compositions are less well defined and depend largely on the isolation conditions. BRG1, the ATPase subunit of several human SWI/SNF-related complexes, is an essential cell cycle regulator and tumor suppressor (Mohrmann and Verrijzer, 2005; Smith and Peterson, 2005).

2.3.5.2 *ISWI complexes*

ISWI (imitation *SWI*) was found in a screen for genes related to the *Drosophila* Swi2p/Snf2p orthologue brahma (brm) (Elfring *et al.*, 1994). ATPases of the ISWI type contain SANT-like domains (for SWI3, ADA2, N-CoR, TFIIIB) that are related to the Myb DNA binding domain (Aasland *et al.*, 1996; Grüne *et al.*, 2003, see 2.4.5.1). ISWI shows nucleosome-stimulated ATPase activity and is able to remodel chromatin *in vitro* (Corona *et al.*, 1999). In *Drosophila*, an ISWI null mutation is lethal, although the development progresses until the larval stages due to maternal deposition of ISWI in the embryo. A dominant negative form of ISWI causes a severe disorder of the male X chromosome, but not the female X chromosome (see Figure 2.4, Deuring *et al.*, 2000). Due to the sex-specific phenotype, a link between ISWI-dependent chromatin remodelling and dosage compensation seems to be likely.

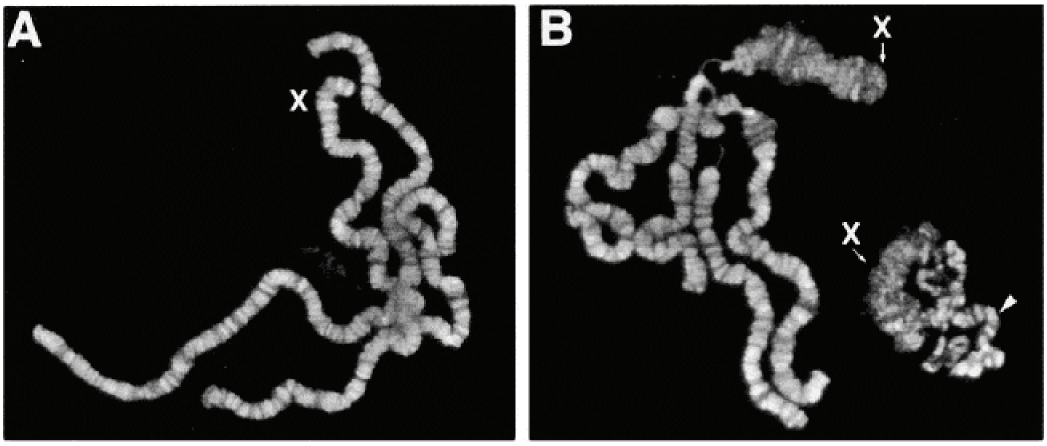

Figure 2.4: C-terminally truncated forms of ISWI lead to a severe derangement of the male X chromosome in *Drosophila*. (A) Polytene chromosomes from a female $ISWI^{1}/ISWI^{2}$ mutant larva, (B) Polytene chromosomes from a male $ISWI^{1}/ISWI^{2}$ mutant larva. The X chromosome is marked, and the arrowhead indicates an autosome. From (Deuring *et al.*, 2000).

In contrast to the multi-subunit SWI/SNF complexes, ISWI complexes contain only two to four different polypeptides.

With exception of the human RSF complex and the yeast ISW complexes (see Table 2.II), ISWI is generally associated with proteins of the BAZ/WAL family (bromodomain adjacent to zinc finger/WSTF-ACF1-like) (Eberharter and Becker, 2004). These large polypeptides carry conserved motifs such as the zinc finger-containing plant homeo domains (PHD) (Aasland *et al.*, 1995) and a bromodomain. In *Drosophila*, three distinct ISWI-containing complexes have been described: Nucleosome Remodelling Factor (NURF), ATP-utilising Chromatin Assembly and Remodelling Factor (ACF) and the Chromatin Accessibility Complex (CHRAC) (reviewed in Längst and Becker, 2001b). A summary of the different types of ISWI-complexes, their subunits and orthologues in different species is given in Table 2.II.

The *Drosophila* NURF complex comprises ISWI, the ACF1-related protein NURF301, the WD40 repeat protein p55 and the pyrophosphatase p38 (Table 2.II, Gdula *et al.*, 1998; Martinez-Balbas *et al.*, 1998; Tsukiyama and Wu, 1995). *nurf301* null mutations are lethal, and truncated versions of NURF301 impair the expression of the homeotic *ultrabithorax* and *engrailed* genes, cause the formation of melanotic tumors in 3rd instar larvae and phenocopy the highly aberrant X chromosome structure in male $ISWI^{1}/ISWI^{2}$ mutants (see above, Badenhorst *et al.*, 2002). NURF is also a coactivator of the *Drosophila* ecdysone receptor (EcR) and interacts physically with EcR in an ecdysone-dependent manner (Badenhorst *et al.*, 2005).

ACF and CHRAC (see also 2.5) are two very closely related chromatin remodelling factors, which both share the ATPase ISWI and the large subunit ACF1 (Table 2.II). They differ only by the presence of the two predicted histone fold proteins p14 and p16 in CHRAC (Eberharter *et al.*, 2001; Ito *et al.*, 1997). Whereas deletion of the large NURF subunit (NURF301) causes lethality in larval stages (Badenhorst *et al.*, 2002), ACF1, the large subunit of ACF and CHRAC, is not essential for viability. However, a homozygous *acf* $^{-/-}$ mutation causes approximately 65% embryonic lethality in flies. Presumably, the surviving embryos escape because of redundant chromatin remodelling and assembly factors and show a developmental delay until the third instar larval stage. Adult *acf* $^{-/-}$ flies display phenotypes affecting position effect variegation (Fyodorov *et al.*, 2004).

The two mammalian isoforms of ISWI, SNF2H and SNF2L, reside in various remodelling complexes. To date, human NURF is the only remodelling factor that contains the SNF2L isoform of ISWI. Mutations in BPTF, the human orthologue of NURF301, cause defects in the expression of the human engrailed-1 and engrailed-2 genes, similar to the effects described for the *Drosophila engrailed* and *ultrabithorax* genes (see above). This suggests a role for hNURF in neural development (Barak *et al.*, 2003). Apart from the orthologues of the *Drosophila* ISWI complexes NURF, ACF and CHRAC, a number of additional ISWI-containing remodelling machines have been described in vertebrates (Eberharter and Becker, 2004). For example, the murine NoRC (Nucleolar Remodelling Complex, see Table 2.II) specifically regulates RNA Polymerase I transcription (Strohner *et al.*, 2001). The WICH complex (WSTF-ISWI Chromatin Remodelling Complex, see Table 2.II) contains SNF2H and the Williams Syndrome transcription factor (WSTF) and has been shown to be involved in the replication of pericentric heterochromatin (Bozhenok *et al.*, 2002).

Biochemical fractionation suggested the presence of at least four distinct ISWI-containing chromatin remodelling complexes in *Xenopus* egg extracts (Guschin *et al.*, 2000a). Hirano and colleagues showed that one of the two major ISWI complexes in *Xenopus* egg extracts corresponds to *Xenopus* CHRAC (xCHRAC), consisting of xISWI, xACF1 and two small polypeptides of 20 and 18 kDa, respectively. The second major complex corresponds to the *Xenopus* orthologue of WICH (MacCallum *et al.*, 2002, see Table 2.II). According to this study, the association of ISWI with chromatin is cell-cycle regulated and depends on the INCENP-aurora B kinase complex, which is also responsible for histone H3 serine 10 phosphorylation during mitosis (MacCallum *et al.*, 2002).

Two ISWI-related ATPases, Isw1p and Isw2p, exist in *S. cerevisiae*. The two proteins are present in distinct complexes (see Table 2.II). Isw1p forms the ISW1a complex with Ioc3p and the ISW1b complex with Ioc2p and Ioc4p, respectively. Isw2p resides in ISW2, a complex reminiscent of *Drosophila* ACF, and in yCHRAC (Corona and Tamkun, 2004; Mellor and Morillon, 2004). However, the amino acid sequence of the largest polypeptide in ISW2 and yCHRAC, Itc1p, is not conserved in higher eukaryotes, only the N-terminus shows similarity to the N-terminal WAC motif of ACF1. A yeast orthologue to the *Drosophila* NURF complex has not been described yet. The yeast ISW complexes are involved in diverse processes like DNA replication, chromatin assembly and transcriptional regulation of RNA Polymerases I and II (Eberharter and Becker, 2004).

Table 2.II: ISWI-containing chromatin remodelling complexes and their conservation in different species. ISWI-type ATPase subunits are printed in red, BAZ/WAL family proteins are printed in blue, and histone fold proteins are printed in green. See text for details.

	NURF	**ACF**	**CHRAC**	**WICH**	**further complexes**	
Saccharomyces cerevisiae		**ISW2**[a] **Isw2p** Itc1p	**yCHRAC**[b] **Isw2p** Itc1p **Dpb4p** **Dls1p**		**ISW1a**[c] **Isw1p** Ioc3p	**ISW1b**[c] **Isw1p** Ioc2p Ioc4p
Drosophila melanogaster	**NURF**[d] **ISWI** **NURF301** p55 p38	**ACF**[e] **ISWI** **ACF1**	**CHRAC**[f] **ISWI** **ACF1** **CHRAC14** **CHRAC16**			
Xenopus laevis			**xCHRAC**[g] **xISWI** **xACF1** **p20** **p18**	**xWICH**[g] **xISWI** **xWSTF**	**additional complexes**[h] subunit composition not specified	
Mus musculus		**mACF**[i] **mSNF2H** **mACF1**	**mCHRAC**[j] **mSNF2H** **mACF1** **YBL1** **YCL1**	**mWICH**[k] **mSNF2H** **mWSTF**	**NoRC**[l] **mSNF2H** **TIP5**	
Homo sapiens	**hNURF**[m] **hSNF2L** **BPTF** RbAP48 RbAP46	**hACF**[n] **hSNF2H** **hACF1**	**hCHRAC**[o] **hSNF2H** **hACF1** **hCHRAC17** **hCHRAC15**	**hWICH**[k] **hSNF2H** **WSTF**	**RSF**[p] **hSNF2H** RSF-1	

[a] (Goldmark *et al.*, 2000; Tsukiyama *et al.*, 1999)
[b] (Iida and Araki, 2004)
[c] (Vary *et al.*, 2003)
[d] (Tsukiyama *et al.*, 1995; Tsukiyama and Wu, 1995)
[e] (Ito *et al.*, 1997; Ito *et al.*, 1999)
[f] (Corona *et al.*, 2000; Eberharter *et al.*, 2001; Varga-Weisz *et al.*, 1997)
[g] (MacCallum *et al.*, 2002)
[h] (Guschin *et al.*, 2000a)
[i] (Collins *et al.*, 2002)
[j] (Bolognese *et al.*, 2000), inferred from sequence homology of YBL1-YCL1 to CHRAC14-CHRAC16
[k] (Bozhenok *et al.*, 2002)
[l] (Strohner *et al.*, 2001)
[m] (Barak *et al.*, 2003)
[n] (Bochar *et al.*, 2000; Jones *et al.*, 2000; LeRoy *et al.*, 2000)
[o] (Poot *et al.*, 2000)
[p] (LeRoy *et al.*, 1998; Loyola *et al.*, 2003)

2.3.5.3 *CHD1/Mi-2 complexes*

CHD-type ATPases are characterised by the presence of two tandemly arranged chromodomains, which have been reported to bind to methylated histone tails, RNA and DNA (Aasland and Stewart, 1995; Akhtar *et al.*, 2000; Bouazoune *et al.*, 2002). The Mi-2α (CHD3) and Mi-2β (CHD4) family members contain a pair of PHD fingers in addition. While yeast Chd1p and *Drosophila* CHD1 appear to act as monomers (Lusser *et al.*, 2005; Tran *et al.*, 2000), the Mi-2 proteins are the ATPase subunits of the multi-subunit NuRD complexes (Nucleosome Remodelling and Deacetylation, also referred to as Mi-2, Mi-2/NuRD, MeCP1 and NRD complexes (Bowen *et al.*, 2004)) in higher eukaryotes. NuRD slides nucleosomes *in vitro* (Brehm *et al.*, 2000; Guschin *et al.*, 2000b). This complex also displays histone deacetylase activity through the HDAC1 and 2 subunits in mammals and Rpd3 in *Xenopus* and *Drosophila*. Hence, NuRD complexes combine ATP-dependent chromatin remodelling with histone-modification. Furthermore, Mi-2 has been reported to be associated with methylated-DNA-binding (MBD) proteins (Bowen *et al.*, 2004). Since DNA methylation and histone deacetylation are known to play a role in gene silencing, the NuRD complex is thought to be recruited to methylated DNA and to effect transcriptional repression through chromatin compaction (Bowen *et al.*, 2004; Xue *et al.*, 1998).

The subunit composition of NuRD complexes is heterogeneous. For instance, the MTA (metastasis associated) proteins that stimulate the HDAC activity in NuRD (Zhang *et al.*, 1999) represent one class of subunits that vary due to differential expression of different paralogues in different cell types. Therefore, a functional specialisation resulting from incorporation of unique gene products into the NuRD complex has been postulated (Bowen *et al.*, 2004).

2.3.5.4 *INO80/SWR1 complexes*

ATPases of the Ino80p and Swr1p type contain a split ATPase domain that is divided by an insertion into two parts. In addition, most of these ATPases contain a SANT domain (see 2.3.5.2 and 2.4.5.1).

Like SWI/SNF complexes, this class of remodelling complexes contains actin-related proteins (ARPs). Besides, both complexes contain the two AAA$^+$-ATPases Rvb1p and Rvb2p (mammalian orthologues: Tip49a and Tip49b), which are related to the bacterial RuvB helicase, being involved in DNA repair.

SWR1 catalyses the ATP-dependent replacement of histones H2A/H2B by histone dimers carrying the variant H2A.Z (Krogan *et al.*, 2003; Mizuguchi *et al.*, 2004), whereas INO80 induces ATP-dependent nucleosome sliding and may be involved in DNA repair and transcriptional regulation. The human complexes have been described recently (Cai *et al.*, 2005; Jin *et al.*, 2005b).

DOMINO is yet another remodelling ATPase with a split catalytic domain of the Ino80p type. It resides in the *Drosophila* Tip60 HAT complex, which is required to remove phosphorylated histone H2Av variants from the sites of double strand break repair. The remodelling complex catalyses the acetylation of the phosphorylated H2Av via its histone acetyltransferase subunit Tip60, and the INO80-type remodelling ATPase DOMINO is obligatory for the exchange of the marked histone with an unmodified H2Av (Kusch *et al.*, 2004).

2.4 Insights into structure and mechanism of ATP-dependent chromatin remodelling

Potential mechanisms of ATP-dependent chromatin remodelling have been subject of investigation for a long time, and several different models are currently discussed. Some recent studies shed light on the structural organisation of several remodelling complexes and thereby provide new insights into the way remodelling machines work.

2.4.1 A variety of remodelling scenarios

Nucleosome remodelling alters the regular interactions between DNA and histones in an ATP-dependent manner, so that the accessibility to DNA is increased. This can be achieved by different means, depending on the type of remodelling complex and the specific reaction conditions. Different strategies for nucleosome remodelling include the removal of histone dimers or the entire histone octamer, the exchange of histones by histone variants, the creation of an altered path of the DNA along the histone octamer surface, partial DNA unwrapping at the nucleosomal DNA entry/exit site and the movement of nucleosomes along the DNA double helix (Flaus and Owen-Hughes, 2004; Längst and Becker, 2004). All of these different phenomena require the energy-consuming disruption of non-covalent interactions between histones and DNA. The presumed global ATP-dependent rearrangement of nucleosomes within native chromatin has been described as ‘chromatin fluidity’ (Kingston and Narlikar, 1999).

Some remodelling complexes catalyse very specific reactions such as the exchange of histone H2A/H2B dimers by the variant H2A.Z/H2B dimers by the SWR1 complex (Mizuguchi *et al.*, 2004). However, other remodelling events are performed by several complexes, which explains functional redundancy in some cases. For instance, remodelling ATPases of all four classes have been shown to induce nucleosome sliding *in vitro*, i.e. the change of the histone octamer position by movement along the DNA sequence (Brehm *et al.*, 2000; Jin *et al.*, 2005b; Längst *et al.*, 1999; Whitehouse *et al.*, 1999). Nevertheless, striking qualitative and quantitative differences between the various remodelling complexes have been reported.

2.4.2 Mechanisms of chromatin remodelling: DNA-twisting or DNA-bulging?

Different mechanistic models can explain the phenomena described in 2.4.1. Some of them appear more feasible than others. Although breaking all histone-DNA contacts at once seems to be an unlikely event due to the high energy cost involved, large segments of nucleosomal DNA are able to unwrap and rewrap spontaneously in a millisecond time scale (Li *et al.*, 2005). Nevertheless, these stochastic occurrences do not seem to be responsible for the remodelling event itself, but are rather thought to allow 'pioneer regulators' such as nucleosome remodelling complexes access to nucleosomal DNA.

The so-called 'twist diffusion' model suggests that nucleosome mobilisation is achieved by twists in the DNA created by rotational force around the axis of the DNA double helix without lifting the DNA off the histone octamer surface. The created torsion would disrupt the histone-DNA contacts within the nucleosome core particle, and new contacts with the backbone of adjacent DNA bases would be reinstated instead. The propagation of these twist defects around the histone octamer surface would eventually lead to the change of the nucleosome position (Van Holde and Yager, 1985; Varga-Weisz and Becker, 1998). High resolution structures of the nucleosome core particle at 1.9 Å resolution demonstrated that twist defects can indeed be accommodated by the nucleosome (Richmond and Davey, 2003). The DNA double helix is not bent uniformly around the histone octamer surface, but contains various distortions and kinks, which are due to the anisotropic flexibility of the DNA, its sequence and irregularities of the histone octamer. The comparison of the crystal structures of a nucleosome core particle containing 147 DNA base pairs with two different 146 base pair structures revealed that in the latter structures, the DNA is stretched at regions distant from the DNA termini to compensate for the lack of one base pair, which introduces a one base pair twist defect (Figure 2.5 A). The crystal structures can be interpreted as trapped intermediate states of the twist diffusion model (Richmond and Davey, 2003).

DNA twisting might also be utilised by ATP-dependent chromatin remodelling complexes. Swi2p/Snf2p-type ATPases belong to the ATPase superfamily 2 (SF2), which also includes helicases that are able to translocate along the DNA backbone (see also 2.4.3). Numerous studies suggested that remodelling ATPases are DNA translocases (Flaus and Owen-Hughes, 2004; Saha *et al.*, 2005; Whitehouse *et al.*, 2003), and translocation might distort or twist the DNA double strand along its helical axis. In fact, several remodelling ATPases, including Swi2p/Snf2p, ISWI and Mi-2, have been shown to introduce such negative superhelical torsion in circular DNA, which could be used for disruption of the interactions between histones and DNA (Havas *et al.*, 2000, see Figure 2.5 B and 2.4.3).

However, several lines of evidence argue against an exclusive twist diffusion mechanism in ATP-dependent nucleosome remodelling. DNA single strand breaks (nicks) or gaps should abrogate nucleosome remodelling, since they cause the dissipation of torsional energy, and the force created by DNA twisting is not able to propagate beyond the strand break. Yet, it has been demonstrated for several remodelling factors including ISWI, RSC, hSWI/SNF and xMi-2 that nicked DNA does not restrain nucleosome remodelling (Aoyagi and Hayes, 2002; Aoyagi *et al.*, 2003; Längst and Becker, 2001a; Lorch *et al.*, 2005). Moreover, bulky DNA modifications should sterically hinder the rotation of nucleosomal DNA around its helical axis, but they do not block nucleosome sliding, either (Aoyagi and Hayes, 2002; Aoyagi *et al.*, 2003; Strohner *et al.*, 2005).

These findings argue for an alternative mechanism of nucleosome remodelling. Remodelling factors such as SWI/SNF or ACF move the nucleosome along the DNA sequence in discrete step sizes (Kassabov *et al.*, 2003; Strohner *et al.*, 2005). These observations suggest that nucleosome mobilisation occurs by the creation of DNA loops rather than by the creation of torsional stress. According to the so-called loop recapture model, the remodelling complex contacts and translocates on the linker DNA, while it remains anchored on the nucleosome particle, thereby creating a DNA bulge on the histone octamer surface (Becker, 2005; Längst and Becker, 2004), see Figure 2.5 C). This way of 'anchored translocation' has been demonstrated for various remodelling factors (Eberharter *et al.*, 2004b; Saha *et al.*, 2005), see 2.4.4 and 2.4.5.1) Once created, the DNA loop could be propagated around the nucleosome without any further energy input, since for every histone-DNA contact that is broken at one end of the loop, a new one is created at the other end (Figure 2.5 C, Becker, 2002). This mechanism also explains nucleosome remodelling in the presence of DNA nicks, gaps or bulky barriers (see above).

Nevertheless, it is possible that both effects – DNA torsion and DNA bulging – contribute to nucleosome remodelling and mobilisation *in vivo*.

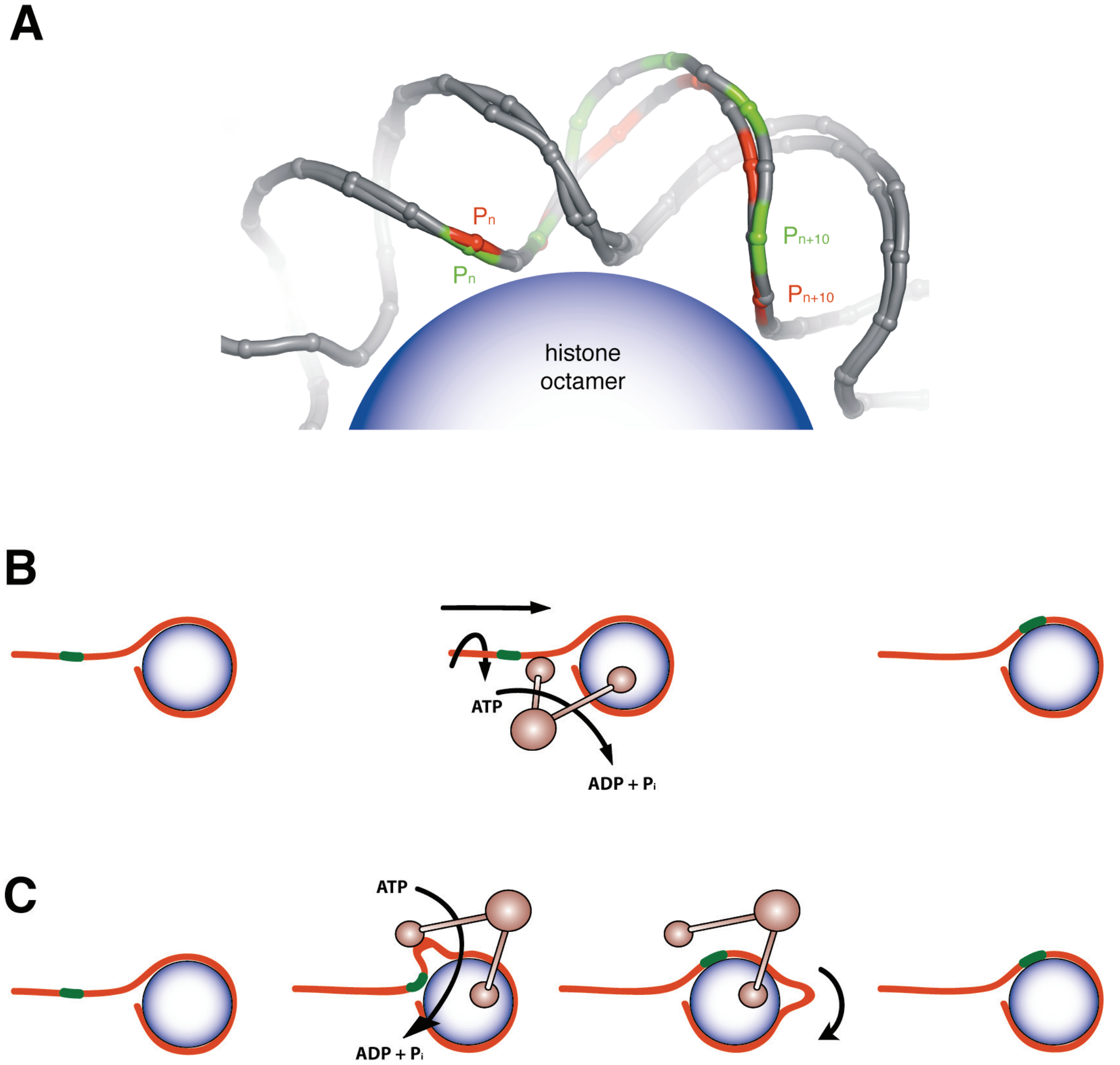

Figure 2.5: Potential mechanisms of nucleosome repositioning. A: Evidence of twist defects in nucleosomal core particles. Overlay of the crystal structures of nucleosomal DNA from a 147 base pair nucleosome core particle (pdb coordinates) and a 146 base pair nucleosome core particle (pdb coordinates). Phosphorus atoms within the DNA backbone are shown as spheres. The alternate colouring demonstrates a one base pair twist defect for the 146 base pair structure (red colour) within eleven DNA base pairs in relation to the 147 base pair structure (green colour). The figure was produced with PyMol (DeLano, 2002) using Protein Data Bank coordinate files 1kx5 and 1kx3 (Richmond and Davey, 2003). B, C: Models for ATP-dependent remodelling mechanisms. B: Twist diffusion model, C: Loop recapture model. See text for details.

2.4.3 The Rad54 ATPase domain

The ATPase domain of Swi2p/Snf2p is the founding member of the SNF2 family of ATPases, which belongs to the helicase superfamily 2 (SF2) (Eisen *et al.*, 1995). SF2-type ATPase domains consist of a set of seven ATPase/helicase motifs, which are organised in two subdomains. The N-terminal subdomain I includes motifs I, Ia, II, and III and has been implicated in ATP-binding and hydrolysis, whereas the C-terminal subdomain II contains motifs IV to VI and is thought to translate the ATP-derived energy into DNA rearrangements. Subdomain I is also present in the bacterial recombination protein RecA (Caruthers and McKay, 2002).

Rad54 is a SF2-type ATPase that functions in concert with the recombinase Rad51 in DNA double strand break repair. Its ATPase activity is stimulated by double stranded DNA, and like other members of the Swi2p/Snf2p family, it is able to translocate on DNA, to create negative superhelical torsion and to enhance accessibility to nucleosomal DNA (Jaskelioff *et al.*, 2003).

Recent crystal structures of two Rad54 ATPase domains from *Sulfolobus solfataricus* and zebrafish provide valuable insights in the mechanism of DNA translocation and energy transduction by Swi2p/Snf2p-type ATPases (Dürr *et al.*, 2005; Thomä *et al.*, 2005).

Both crystal structures confirm that the overall organisation of the Rad54 ATPase domain closely resembles other SF2-class ATPases. However, two helical subdomains, which are fused to the ATPase core, seem to be specific for the Swi2p/Snf2p type. This allows speculating that these domains might crucial for Swi2p/Snf2p function.

The structure of *Sulfolobus solfataricus* Rad54 in complex with DNA shows that Rad54 binds the DNA double helix at the backbone and suggests that it travels along the minor groove. During the translocation, the DNA double helix is rotated along its helical axis, or, in other words, negative superhelical torsion is created. A multi-subunit chromatin remodelling complex with further substrate binding sites in addition to the DNA binding site could therefore use both the translocation and the twisting of DNA to disrupt protein-DNA interactions (Dürr *et al.*, 2005).

The Swi2p/Snf2p ATPases are structurally related to DExx box helicases, although they do not display helicase activity. In contrast to the helicases, Rad54 does not possess any single strand binding domain and no wedge-like structures that could separate the two DNA strands.

The DNA-dependent stimulation of the ATPase activity can be explained with the help of the Rad54 structure. DNA binding triggers a conformational change within the Mg^{2+}-binding and ATP-hydrolysing motif II. Due to these structural rearrangements, a conserved glutamate residue adopts a conformation that allows ATP hydrolysis (Dürr *et al.*, 2005).

A detailed mutational analysis of several Swi2p/Snf2p family members has recently shown that mutations in the ATPase motif V have only minor effects on the DNA-stimulated ATPase activity, but destroy the remodelling activity. As a consequence, motif V is thought to couple the energy of ATP hydrolysis to the mechanical force required for chromatin remodelling (Smith and Peterson, 2005). Consistent with these observations, several mutations in this motif have also been reported to be implicated in various cancers (Medina *et al.*, 2004; Wong *et al.*, 2000).

2.4.4 SWI/SNF complexes

Several different remodelling activities have been reported for SWI/SNF and related complexes. SWI/SNF- and RSC complexes peel off the DNA from the histone octamer surface and have been shown to displace nucleosomes in *trans*, but also induce nucleosome sliding in *cis* (Jaskelioff *et al.*, 2000; Lorch *et al.*, 2001; Phelan *et al.*, 2000; Vicent *et al.*, 2004). Moreover, SWI/SNF disrupts regular nucleosomal arrays and forms noncovalently linked dinucleosome structures (Phelan *et al.*, 2000; Schnitzler *et al.*, 2001). It has also been reported that these complexes are able to displace H2A/H2B dimers from or exchange them between nucleosomes (Bruno *et al.*, 2003; Vicent *et al.*, 2004).

The subunit stoichiometry of the eleven-subunit SWI/SNF has been investigated in detail. For six out of the eleven subunits, including the ATPase subunit Swi2p/Snf2p, it could be shown by differential epitope tagging and quantitative tyrosine-iodination that only one copy is present in the complex. The rest of the subunits are present in duplicate or triplicate. The calculated molecular weight of SWI/SNF is therefore approximately 1.15 MDa, in agreement with scanning transmission electron microscopy studies (Smith *et al.*, 2003).

The structure of both SWI/SNF and RSC has been studied by electron microscopy (Asturias *et al.*, 2002; Schnitzler *et al.*, 2001; Smith *et al.*, 2003). The low resolution structures of both complexes show a disc-like shape with several prominent lobes and a central cavity large enough to accommodate a single nucleosome. Naturally, this pocket is the prime candidate for the nucleosome binding site (Asturias *et al.*, 2002; Smith *et al.*, 2003), see Figure 2.6.

Recently, Cairns and colleagues proposed a 'wave-ratchet-wave' mechanism for RSC-mediated remodelling, based on detailed biochemical studies (Saha *et al.*, 2005). According to this model, the ATPase Sth1p binds to nucleosomal DNA at an internal site, approximately two helical turns from the dyad axis. Upon ATP hydrolysis, the DNA is then translocated towards the dyad axis by pulling and twisting, which causes a first wave of one-dimensional diffusion of the DNA towards the Sth1p-binding site. The DNA is then released through a uni-directional ratchet and propagated in a second wave of DNA diffusion towards the distal linker.

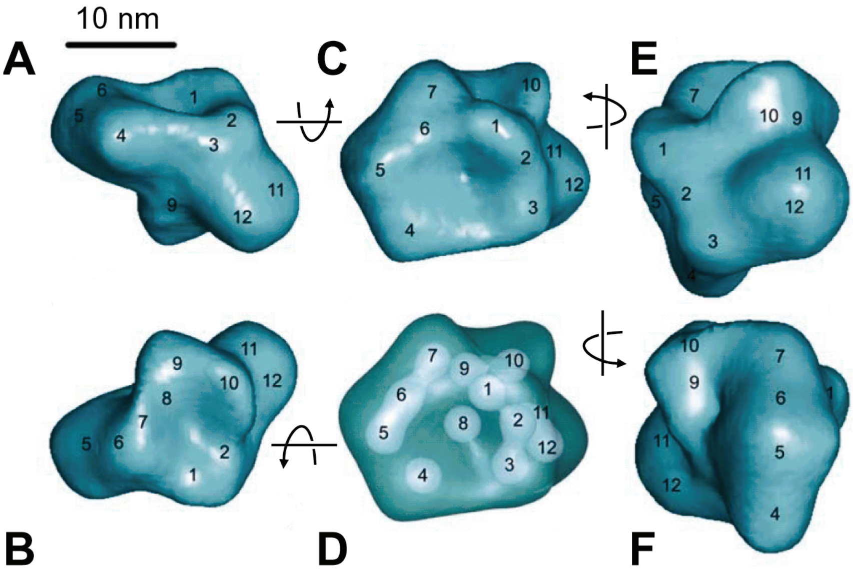

Figure 2.6: 3D structure of the *S. cerevisiae* SWI/SNF complex at 30 Å resolution. Numbers represent individual centres of mass. Panels C and D are shown in the same orientation, and the semi-transparent view in D shows the twelve centres of mass (white spheres). Panels A and B are 90° rotations around the horizontal axis in C and D and panels E and F are 90° rotations around the vertical axis in C and D. The rim of the conical depression, which is the putative nucleosome binding site, is surrounded by the mass centres 1 to 6. Centre 8 is located close to the base of the depression. From (Smith *et al.*, 2003).

2.4.5 ISWI-containing complexes

2.4.5.1 *ISWI complexes in* Drosophila

ISWI-type remodelling machines are able to induce the sliding of nucleosomes, i. e. they move histone octamers along the DNA sequence. In contrast, the transfer of nucleosomes to a competing DNA fragment by ISWI and its complexes has not been observed (Längst *et al.*, 1999). Nucleosome sliding can be catalysed by the ISWI subunit alone *in vitro*, but there is no evidence that ISWI functions as a monomer in the living cell. Indeed, the remodelling activity of ISWI is greatly enhanced and also qualitatively modulated, when it is in complex with its interaction partners (see below).

The N-terminal half of ISWI holds the SF2-type ATPase domain, while the C-terminal part contains a SANT domain and a SANT-like ISWI domain (SLIDE). The crystal structure of the ISWI C-terminus reveals a rather rigid, helical domain. It can be divided into four subdomains: The so-called HAND domain is a four-helix bundle with a novel fold. It is followed by the SANT domain, which is separated from the SLIDE domain by a long linker helix (Grüne *et al.*, 2003, see Figure 2.7).

SANT and SLIDE show homology to c-Myb DNA binding modules (Ogata *et al.*, 1994). However, it can be concluded from the crystal structure that SANT is not a *bona fide* DNA binding module, because several negatively charged and voluminous residues would interfere with DNA binding. In contrast, SLIDE should bind well to DNA. This postulate is strongly supported by biochemical data (Grüne *et al.*, 2003).

Drosophila ISWI requires linker DNA for stable nucleosome binding. The interaction of ISWI with the nucleosome core particle is not tight enough to form discrete complexes in bandshift assays (Brehm *et al.*, 2000; Whitehouse *et al.*, 2003). Interestingly, the ATPase activity of ISWI is only mildly stimulated by free DNA, whereas nucleosomal DNA is a potent activator of ATP hydrolysis.

Both the C-terminal SANT/SLIDE domain and the N-terminal ATPase domain bind to nucleosomal DNA *in vitro*, but the stimulatory effect of DNA or nucleosomes on ATPase activity is not seen with the ATPase domain alone. Therefore, the SANT/SLIDE module is considered to serve as a substrate-recognition module. The current model proposes the induction of a conformational change in the flexible linker between ATPase and SANT/SLIDE domain upon substrate binding, which consequently stimulates ISWI's ATPase activity (Grüne *et al.*, 2003).

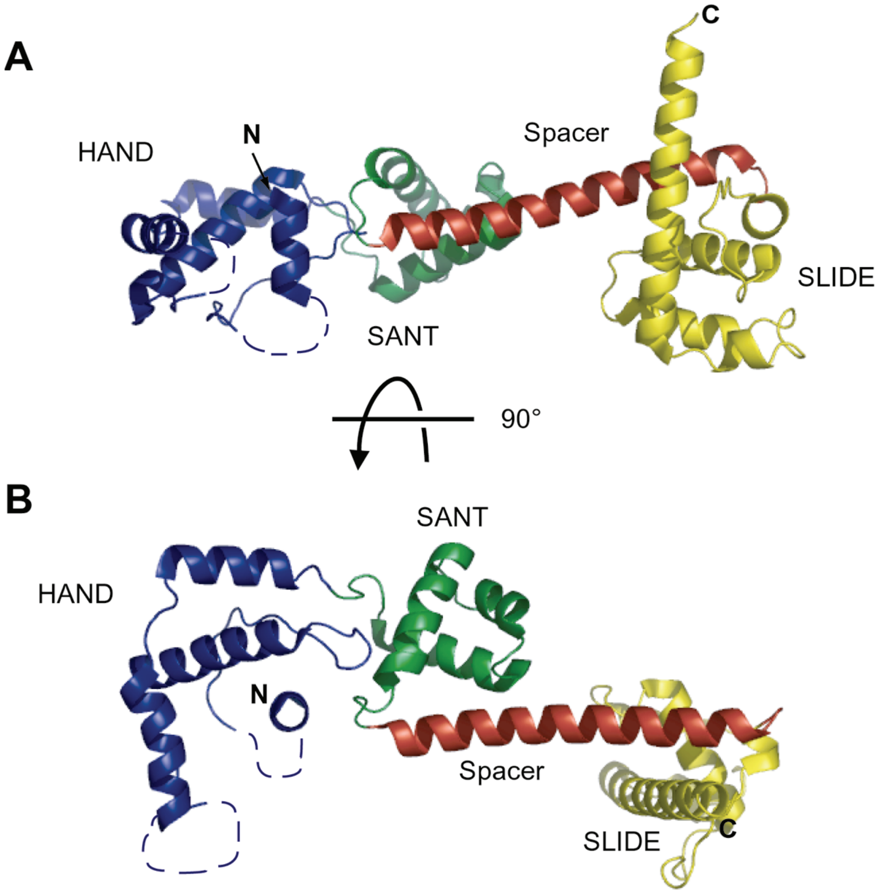

Figure 2.7: Crystal structure of the C-terminal ISWI fragment. The colours correspond to the subdomains as follows: blue: HAND domain; green: SANT domain; red: linker helix; yellow: SLIDE domain. The views in A and B are related by a 90° rotation around a horizontal axis. The figures were produced with the programme PyMol (DeLano, 2002). Adapted from (Grüne *et al.*, 2003).

ISWI binds asymmetrically to nucleosomal linker DNA, protecting only one end from DNase I activity (Längst and Becker, 2001a). Although the N-terminal histone H4 tail does not seem to affect the binding of ISWI to its nucleosomal substrate, it is required for the stimulation of ISWI's ATPase and nucleosome remodelling activity. A basic patch formed by the histone H4 residues $K_{16}R_{17}H_{18}R_{19}K_{20}$ is crucial for ISWI stimulation, and it is conceivable that ISWI interacts with H4 at this site (Clapier *et al.*, 2001; Clapier *et al.*, 2002).

The properties of ISWI-containing remodelling complexes are also modulated by other complex subunits. In fact, there are great qualitative and quantitative differences between free ISWI and ISWI residing in a remodelling complex: ISWI slides mononucleosomes on the 248 bp rDNA promoter fragment exclusively towards the ends of the DNA (Längst *et al.*, 1999). In contrast, the ACF complex (i. e. ISWI and ACF1) moves the nucleosomes towards the centre of the DNA fragment. ACF1 also increases the efficiency of nucleosome remodelling by an order of magnitude, although it does not stimulate the ATP hydrolysis rate of ISWI (Eberharter *et al.*, 2001). Presumably, the effect of ACF1 on ISWI activity is caused by direct interactions with the substrate. The ACF1 subunit interacts with DNA, although mapping of the DNA interaction domain has not been satisfying (Fyodorov and Kadonaga, 2002). Recently, it has been demonstrated that the PHD fingers of ACF1 interact with the nucleosomal core histones, and this contact is required for ACF-mediated remodelling (Eberharter *et al.*, 2004b). The PHD fingers can therefore be considered as an 'anchor point' on the nucleosomal substrate (see also 2.4.2).

There are also significant differences between the different types of ISWI-containing remodelling complexes. CHRAC and ACF distribute the nucleosomes in an array evenly, while NURF disrupts regularly spaced chromatin (Tsukiyama and Wu, 1995; Varga-Weisz *et al.*, 1997). The reason for this fundamental difference is unknown.

In agreement with the studies on the yeast ISW2 complex (Kagalwala *et al.*, 2004, see 2.4.5.2), hydroxyl radical footprinting has shown that the *Drosophila* NURF complex protects approximately 40 base pairs of linker DNA at the nucleosomal entry site and several sites close to the dyad axis, including the region proximal to the histone H4 tail (Schwanbeck *et al.*, 2004). This suggests that the remodelling mechanisms of various ISWI-containing complexes and also of RSC (see 2.4.4) closely resemble each other.

2.4.5.2 ISW2

ISW2 is the yeast orthologue of *Drosophila* ACF and consists of the two polypeptides Isw2p and Itc1p (Gelbart *et al.*, 2001; Tsukiyama *et al.*, 1999, see 2.3.5.2). It has been the subject of several mechanistic studies. Photo-crosslinking, DNase I and hydroxyl radical footprinting revealed that ISW2 binds the nucleosome at three distinct regions (Kagalwala *et al.*, 2004): Approximately 63 base pairs of linker DNA are bound predominantly by the regulatory subunit Itc1p. Both Itc1p and Isw2p contact approximately 20 bp at the entry site of the DNA into the nucleosome and another 10 to 20 bp close to the dyad axis, near the site where the histone H4 tail interacts with the nucleosomal DNA. Since the linker DNA is crucial for ISW2 binding, it has been suggested that the complex binds predominantly to the larger linker DNA fragment. Moreover, the nucleosome movement occurs towards the ISW2 binding site (Kagalwala *et al.*, 2004). Consistent with the ISW2 binding behaviour and directionality of nucleosome sliding, and in agreement with observations of the related *Drosophila* complexes ACF and CHRAC (see 2.4.5.1 and 2.5), ISW2 moves mononucleosomes towards the centre of the DNA fragment under equilibrium conditions (Kassabov *et al.*, 2002). Besides, nucleosomal arrays get regularly spaced upon ISW2-dependent remodelling (Tsukiyama *et al.*, 1999). Based on these observations, the following model of ISW2-dependent nucleosome sliding has been proposed. ISW2 might move nucleosomes along the DNA until the ISW2 complex encounters the neighbouring nucleosome particle, i. e. until the linker DNA length between the two nucleosomes equals the DNA length required for ISW2 binding (approximately 60 base pairs, see above). As a consequence, the nucleosomal repeat length of an ISW2-remodelled array would be approximately 200 base pairs (146 base pairs within the nucleosome and 60 base pairs of linker DNA), which is consistent with the experimentally determined repeat length (Kagalwala *et al.*, 2004; Tsukiyama *et al.*, 1999).

Studies with yeast *isw2Δ* strains that contained an inducible version of the yeast *ISW2* gene showed that the ISW2 complex (or yCHRAC) also catalyses nucleosome sliding *in vivo* without disrupting the nucleosome structure (Fazzio and Tsukiyama, 2003). In contrast to the nucleosomal spacing activity of ISW2 observed *in vitro*, the *in vivo* sliding specifically affects only few distinct nucleosomes and does not result in an evenly spaced array. These findings imply that additional factors are involved that direct the remodelling activity *in vivo* (Fazzio and Tsukiyama, 2003).

Other studies on ISW2 focused on the ATP-dependent reaction cycle of nucleosome remodelling (Fitzgerald *et al.*, 2004). In contrast to chromatin remodellers of the SWI/SNF type, ISW2 displays a very low translocation processivity on naked DNA; however, the processivity is increased on nucleosomal substrates due to additional binding components at the nucleosomal core. According to these studies, ADP promotes the release of DNA, while the absence of nucleotides or the presence of a non-hydrolysable ATP analogue allows DNA binding by ISW2. Furthermore, ISW2 adopts a more compact conformation in the presence of a non-hydrolysable ATP analogue than in the presence of ADP and thereby is likely to undergo a major conformational change upon ATP hydrolysis. Taken together, the following model of the reaction cycle can be formulated: The ISW2 complex is anchored on the nucleosome and binds to linker DNA in the absence of ATP. ATP-binding induces a conformational change within the ISW2 complex and thereby creates a DNA bulge. The release of this bulge towards the nucleosome leads to the propagation of the DNA around the histone octamer surface and causes the nucleosome to move along the DNA sequence by a defined step length (i. e. the size of the DNA bulge). In the following step, the hydrolysis of ATP releases ISW2 from its binding site on the linker DNA, thereby completing the reaction cycle (Fitzgerald *et al.*, 2004).

2.5 The Chromatin Accessibility Complex (CHRAC)

The Chromatin Accessibility Complex (CHRAC) was originally purified from *Drosophila* embryo extracts as an ISWI-containing remodelling factor. Its name reflects its ability to increase the overall DNA accessibility in chromatin. It also arranges irregularly spaced nucleosomes into a regular array in the presence of ATP (Varga-Weisz *et al.*, 1997). The largest CHRAC subunit of approximately 175 kDa was recognised as ACF1, which had been reported previously to interact with ISWI in the ACF complex (Eberharter *et al.*, 2001; Ito *et al.*, 1997). The remaining two CHRAC subunits were identified as small proteins with a molecular weight of 14 and 16 kDa, respectively. The two polypeptides had presumed histone folds, interacted with each other in a yeast two hybrid screen and seemed to be developmentally regulated (Corona *et al.*, 2000). Hence, ACF and CHRAC can be distinguished by the ‘diagnostic’ subunits p14 and p16 (Corona *et al.*, 2000). Figure 2.8 shows the four CHRAC components with their functional motifs in their relative sizes.

To date, remodelling complexes orthologous to *Drosophila* CHRAC have been characterised in human cells (Poot *et al.*, 2000), *Saccharomyces cerevisiae* (Iida and Araki, 2004) and *Xenopus laevis* (MacCallum *et al.*, 2002). Furthermore, the murine YBL1 and YCL1 histone fold proteins are true orthologues of the *Drosophila* and human CHRAC histone fold subunits and therefore substantiate the existence of murine CHRAC (Bolognese *et al.*, 2000).

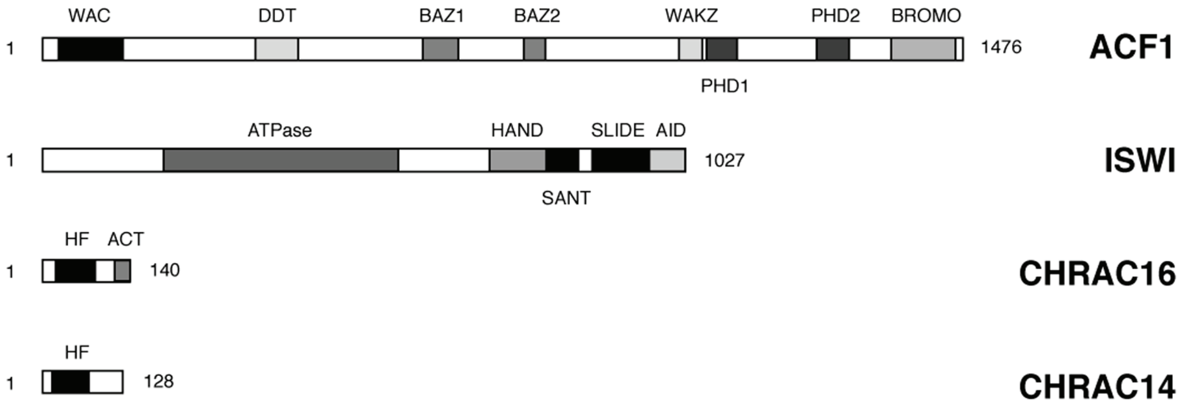

Figure 2.8: Topography of the four CHRAC subunits. AID: ACF1-interacting domain, HF: histone fold, ACT: acidic C-terminal tail.

Until recently, the two small subunits of the Chromatin Accessibility Complex were not subject to detailed analysis. Genetic studies in yeast revealed that yCHRAC is involved in telomeric position effects and that the CHRAC16 orthologue Dls1p is required for ISW2-dependent chromatin remodelling at some gene loci *in vivo* (Iida and Araki, 2004; McConnell *et al.*, 2004). One study on the human subunits hCHRAC17 and hCHRAC15 demonstrated an involvement in nucleosome mobilisation and chromatin assembly (Kukimoto *et al.*, 2004).

The CHRAC14 and CHRAC16 subunits from *Drosophila melanogaster* have been the subject of this dissertation. Several open questions such as the structure of the two polypeptides and their biochemical properties and functions within CHRAC have been addressed. Besides, first attempts were made to study them in the living organism. The findings of this work allow speculations about a more detailed model of chromatin remodelling by CHRAC.

3 Materials and methods

3.1 Materials

3.1.1 Solutions, buffers and media

Phosphate buffered saline (PBS)

137 mM NaCl
2.7 mM KCl
10 mM Na_2HPO_4
2 mM KH_2PO_4
adjust pH to 7.4 with HCl

PBS500

PBS with a final salt concentration of 500 mM (dissolve 21.06 g NaCl in 1 L of PBS)

HEMG buffer

25 mM HEPES-KOH pH 7.6
KCl in varying concentrations
1.5 mM $MgCl_2$
0.1 mM EDTA
10% glycerol

HEMG/imidazole

HEMG buffer containing 500 mM imidazole. pH is adjusted to 7.6 with HCl.

EX buffer

20 mM HEPES-KOH pH 7.6
KCl in varying concentrations
1.5 mM $MgCl_2$
0.5 mM EDTA
10 % glycerol

Glutathione elution buffer

100 mM Tris-HCl pH 8.0
30 mM reduced glutathione

5x SDS running buffer

15.1 g/L Tris base
72.0 g/L glycine
5.0 g/L SDS

5x SDS sample buffer

5x SDS sample buffer
0.45 M DTT
10 % SDS
0.4 M Tris-HCl pH 6.8
50 % glycerol
100 mg/L bromophenol blue

4x buffer for stacking gels

0.5 M Tris-HCl, pH 6.8
0.4% SDS

4x buffer for separating gels

1.5 M Tris-HCl, pH 8.8
0.4% SDS

5x Western transfer buffer

58 g/L Tris base
29.5 g/L glycine
For 1x Western transfer buffer, mix 100 mL 5x stock solution with 200 mL methanol and dilute to 1 L with H_2O (methanol: 20% final)

Tris-Borate-EDTA (TBE)

90 mM Tris-Borate
2 mM Na_2EDTA
pH 8.0

ATPase buffer

50 mM Tris-HCl pH 7.5
50 mM KCl
0.5 mM 2-mercaptoethanol
0.1 g/L BSA
0.67 mM $MgCl_2$

TMS buffer for four way junction DNA

10 mM Tris-HCl pH 7.5
100 mM NaCl
1 mM Na_2EDTA
10 mM $MgCl_2$
0.01% NP-40

Protease inhibitors

Where indicated, the following protease inhibitors were used at the given final concentrations:

0.2 mM PMSF
2 µg/mL aprotinin
0.7 µg/mL pepstatin
1 µg/mL leupeptin

Tris-EDTA (TE)

10 mM Tris-HCl pH 8.0
1 mM Na_2EDTA

10x DNA loading dye

0.1% bromophenol blue
0.1% xylene cyanol
50% glycerol

Sodium carbonate buffer for HAT-assay

15.9 g/L Na_2CO_3
71.4 g/L $NaHCO_3$
pH 9.3

Antibiotics

Where indicated, the following antibiotics were used at the given final concentrations:

100 µg/mL Ampicillin (AMP)
34 µg/mL Chloramphenicol (CHL)
50 µg/mL Kanamycin (KAN)

Media and plates for bacteria were prepared according to standard protocols (Sambrook and Russell, 2001).

Flies were raised at 25°C on a cornmeal molasses yeast agar tegosept medium containing propionic acid essentially as described in (Ashburner, 1989).

For culturing insect cells, the following commercially available solutions and media were used:

Sf-900 II SFM (Invitrogen)

Schneider's *Drosophila* medium (Invitrogen)

Fetal bovine serum (FCS, Sigma)

Penicillin/Streptomycin stock solution (Pen/Strep, 10000 U/mL penicillin, 10 mg/mL streptomycin, C. C. Pro)

3.1.2 Organisms, cells and strains

3.1.2.1 E. coli *strains*

DH5α (Invitrogen)
E. coli F^{-} *Φ*80*lac*ZΔM15 Δ(*lac*ZYA-*arg*F)U169 ***deo***R ***rec***A1 ***end***A1 ***hsd***R17(r$_{k}^{-}$, m$_{k}^{+}$) ***pho***A ***sup***E44 ***thi***-1 ***gyr***A96 ***rel***A1 λ^{-}

SURE (Stratagene)
E. coli e14^{-} (McrA^{-}) D(mcrCB-hsdSMR-mrr)171 endA1 supE44 thi-1 gyrA96 relA1 lac recB recJ sbcC umuC::Tn5 (Kan^{r}) uvrC [F' proAB lacI^{q}ZDM15 Tn10 (Tet^{r})]

XL1Blue (Stratagene)
E. coli recA1 endA1 gyrA96 thi-1 hsdR17 supE44 relA1 lac [F'proAB lacI^{q}ZDM15 Tn10 (Tet^{r})]

BL21(DE3)pLysS (Stratagene)
E. coli B F^{-}dcm ompT hsdS(r$_{B}^{-}$m$_{B}^{-}$) gal λ(DE3)[pLysS Cam^{r}]

3.1.2.2 Insect cells and fly lines

S2 cells (*Drosophila melanogaster*, embryonic cells, Invitrogen)

KC cells (*Drosophila melanogaster*, embryonic cells, Invitrogen)

Sf9 cells (*Spodoptera frugiperda*, Novagen)

Drosophila melanogaster yw flies described in FlyBase (http://flybase.bio.indiana.edu)

3.1.2.3 Baculoviral expression vectors

pFASTBAC (Invitrogen)

pFASTBACDual (Invitrogen)

3.1.3 Vectors, plasmids and oligonucleotides

3.1.3.1 Vectors and plasmids

Table 3.I: Vectors and plasmids

Plasmid name	**Description and comments**	**Primers used for cloning or mutagenesis (see Table 3.II)**
pBCEXMaJo	Derived from pGEX2T-CHRAC14 (Corona *et al.*, 2000), see 3.2.1.1 for details. Bicistronic transcript encodes full length GSTp14 and untagged p16	oFH1/oFH2
pBCMaJoHIS 1A	Derived from pBCEXMaJo, see 3.2.1.1 for details. Bicistronic transcript encodes full length GSTp14 and His$_8$p16. See Appendix for plasmid map.	oFH5/oFH6
pBCMaJoHIS 1B	Derived from pBCMaJoHIS 1A, nonsense mutation in CHRAC16 gene: D118STOP	oFH17/oFH18
pBCMaJoHIS 1C	Derived from pBCMaJoHIS 1A, nonsense mutation in CHRAC16 gene: H103STOP	oFH26/oFH27
pBCMaJoHIS 1D	Derived from pBCMaJoHIS 1A, nonsense mutation in CHRAC16 gene: N88STOP	oFH28/oFH29
pBCMaJoHIS 1E	Derived from pBCMaJoHIS 1A, deletion in CHRAC16 gene: ΔG2 – P9	oFH30/oFH31
pBCMaJoHIS 1F	Derived from pBCMaJoHIS 1A, deletion in CHRAC16 gene: ΔG2 – T18	oFH32/oFH33
pBCMaJoHIS 2A	Derived from pBCMaJoHIS 1A, nonsense mutation in CHRAC14 gene: S109STOP	oFH20/oFH21
pBCMaJoHIS 3A	Derived from pBCMaJoHIS 1A, nonsense mutation in CHRAC14 gene: S80STOP	oFH22/oFH23
pBCMaJoHIS 4A	Derived from pBCMaJoHIS 1A, deletion in CHRAC14 gene: ΔV2 – L8	oFH24/oFH25

pBCMaJoHIS 2B	Derived from pBCMaJoHIS 1A, nonsense mutations in CHRAC14 and CHRAC16 genes: CHRAC14 S109STOP and CHRAC16 D118STOP	oFH20/oFH21 and oFH17/oFH18
pIVTFH1	Derived from pING14A; for *in vitro*-translation of ACF1 aa 2-201.	100IVT.fw/oFH7
pIVTFH2	Derived from pING14A; for *in vitro*-translation of ACF1 aa 202-1476.	oFH8/oFH10
pIVTFH3	Derived from pING14A; for *in vitro*-translation of ACF1 aa 473-1476.	oFH9/oFH10
pMUT23EF	Derived from pET15b, the 581 base pair NcoI fragment of pBCMaJoHIS 1A was ligated into the pET15b NcoI site.	-
pMUTBCD	Derived from pBluescript KS II+, the 329 base pair XbaI/SacI fragment of pBCMaJoHIS 1A was ligated into the XbaI/SacI-cut pBluescript KS II+ vector.	-
pFBDMaJo corrected	The original pFastBacDual baculoviral expression plasmid pFBDMaJo was cloned by J. Brzeski and encodes for FLAG-CHRAC14 and His$_6$-CHRAC16, but it contains a point mutation in the CHRAC16 ORF (R113H). Here, this point mutation was corrected by site directed mutagenesis with wild type primers. A plasmid map of 'pFBDMaJo corrected' is given in the Appendix.	oFH15/oFH16
pFBDMaJo DNA mut corrected	Original plasmid created by J. Brzeski, derived from pFBDMaJo, several mutations of putative DNA binding residues are introduced into the CHRAC14- and CHRAC16 coding sequences. Here, the unintentional CHRAC16 point mutation R113H was corrected as described above. The plasmid was not used in this work.	oFH15/oFH16
pWIZ11-12	Derived from pWIZ (Lee and Carthew, 2003), plasmid for creating *Drosophila* fly lines carrying an inducible CHRAC14-specific RNAi knockout construct.	oFH11/oFH12
pWIZ13-14	Derived from pWIZ (Lee and Carthew, 2003), plasmid for creating *Drosophila* fly lines carrying an inducible CHRAC16-specific RNAi knockout construct.	oFH13/oFH14

3.1.3.2 *Oligonucleotides*

Table 3.II: Oligonucleotides

Oligo name	**Sequence**	**Description**
oFH1	5’-GGG GGT CTC GAA TTC AAT AAT TTT GTT TAA CTT TAA GAA GGA GAT ATA CAT *ATG GGC GAA CCA AGG AGC CAA*-3’	CHRAC16-ORF fw-primer used for creation of the bicistronic expression plasmid pBCEXMaJo. Contains the linker region upstream of the CHRAC16 ORF underlined: internal ribosomal entry site (IRES); italics: CHRAC16 ORF
oFH2	5’-GCC GGT CTC GAA TTC TAG A*CT ATT CAT CAG ACT CCG ATT C*-3’	CHRAC16-ORF rev-primer used for creation of the bicistronic expression plasmid pBCEXMaJo. italics: CHRAC16 ORF
oFH3	5’-CGG CGC ATA TGC ATC ACC ATC ACC ATC ACC ATC ACG AGA ATT TGT ATT TTC AGG GTG GCG AAC C-3’	fw-primer for His-tagging CHRAC16. Not used, see oFH5/oFH6
oFH4	5’-CCG TGG AGC TCT TCA TGA TCG TTC GC-3’	rev-primer for His-tagging CHRAC16. Not used, see oFH5/oFH6
oFH5	5’-TAT GGT TAA CCA TCA TCA CCA TCA CCA CCA TCA CGA GAA TTT GTA TTT TCA GGG TCA-3’	Oligonucleotide used for annealing with oFH6 and directly cloning the resulting 57bp linker containing a His$_8$-TEV tag into the NdeI restriction site of pBCEXMaJo. Resulting plasmid: pBCMaJoHIS
oFH6	5’-TAT GAC CCT GAA AAT ACA AAT TCT CGT GAT GGT GGT GAT GGT GAT GAT GGT TAA CCA-3’	Oligonucleotide used for annealing with oFH5 and directly cloning the resulting 57bp linker containing a His$_8$-TEV tag into the NdeI restriction site of pBCEXMaJo. Resulting plasmid: pBCMaJoHIS
100 IVT.fw	5’-GGG GCC ATG GGG CCC ATT TGC AAG CGG GAA GGA-3’	ACF1 fw-primer (A. Eberharter) for creating the *in vitro* translation construct pIVTFH1 (corresponding to ACF1 amino acids 2-201, WAC motif, see Table 3.I); rev-primer oFH7
oFH7	5’-CGG CGG AAT TCA ATT GCT CTT TAT AAA CAT ACT CAG G-3’	ACF1 rev-primer for creating the *in vitro* translation construct pIVTFH1, see primer 100IVT.fw (above) and Table 3.I

oFH8	5’-GGC CGG AAT TCG TAT CGC GGG TGG ATG GAC TT-3’	ACF1 fw-primer for creating the *in vitro* translation construct pIVTFH2 (corresponding to ACF1 amino acids 202-1476, ACF1ΔWAC, see Table 3.I); rev-primer: oFH10
oFH9	5’-GCG GCG GAT CCG GAG CTT TTG TAA ATG-3’	ACF1 fw-primer for creating the *in vitro* translation construct pIVTFH3 (corresponding to ACF1 amino acids 473-1476, ACF1ΔWAC/DDT, see Table 3.I); rev-primer: oFH10
oFH10	5’-GCG GCG AAT TCA GCA AGC TTT GAC TTC CCC-3’	ACF1 rev-primer including the ACF1 stop codon; for use with oFH8 and oFH9, see also Table 3.I
oFH11	5’-GCG GGT CTA GA*A TGG TCG AGC GCA TCG AG*-3’	CHRAC14 fw-primer with XbaI restriction site 5’ of start codon italics: CHRAC14 coding sequence
oFH12	5’-CGG GGT CTA GA*T CAC TCG GGG GCT TCC TC*-3’	CHRAC14 rev-primer with XbaI restriction site 3’ of stop codon italics: CHRAC14 coding sequence
oFH13	5’-GGG CCT CTA GA*A TGG GCG AAC CAA GGA GC*-3’	CHRAC16 fw-primer with XbaI restriction site 5’ of start codon italics: CHRAC16 coding sequence
oFH14	5’-CCG CGT CTA GA*C TAT TCA TCA GAC TCC GAT TC*-3’	CHRAC16 rev-primer with XbaI restriction site 3’ of stop codon italics: CHRAC16 coding sequence
oFH15	5’-CTG CGG CTA AAT CGC TCC GCC GGC AGC-3’	CHRAC16 fw-primer, spanning nucleotides 325 to 351 of CHRAC16 ORF (wt sequence)
oFH16	5’-GCT GCC GGC GGA GCG ATT TAG CCG CAG-3’	CHRAC16 rev-primer, complementary to oFH15
oFH17	5’-CTA AAT CGC TCC GCC GGC AGC TAG GAC GAC GAT GAC GAC-3’	fw-primer used for site directed mutagenesis of CHRAC16: mutated triplet underlined: (GAC→ TAG; corresponds to D118STOP) resulting expression plasmid: pBCMaJoHIS 1B, see Table 3.I
oFH18	5’-GTC GTC ATC GTC GTC CTA GCT GCC GGC GGA GCG ATT TAG-3’	rev-primer used for site directed mutagenesis of CHRAC16, mutated triplet underlined. See oFH17
oFH19	5’-CAA GCC ACG TTT GGT GGT GG-3’	fw-primer used for sequencing CHRAC14-CHRAC16 expression plasmids, prime site in GST coding sequence, approximately 40 bp upstream of CHRAC14 start ATG

oFH20	5'-GCC AGC AAG AAG GAT TGA AAC ACT GCC GAA AAT GCC-3'	fw-primer used for site directed mutagenesis of CHRAC14: mutated triplet underlined: (TCC→ TGA; corresponds to S109STOP) resulting expression plasmid: pBCMaJoHIS 2A, see Table 3.I
oFH21	5'-GGC ATT TTC GGC AGT GTT TCA ATC CTT CTT GCT GGC-3'	rev-primer used for site directed mutagenesis of CHRAC14: mutated triplet underlined. see oFH20
oFH22	5'-CCG AGC TAG ACT TCG AAT GAT TCG TGC CCT CTC TGA CG-3'	fw-primer used for site directed mutagenesis of CHRAC14: mutated triplet underlined (AGC→ TGA; corresponds to S80STOP) resulting expression plasmid: pBCMaJoHIS 3A, see Table 3.I
oFH23	5'-CGT CAG AGA GGG CAC GAA TCA TTC GAA GTC TAG CTC GG-3'	rev-primer used for site directed mutagenesis of CHRAC14: mutated triplet underlined. see oFH22
oFH24	5'-CCG CGT GGA TCC ATG AAC CTG CCG AAT GCC-3'	fw-primer used for site directed mutagenesis of CHRAC14: deletion of 21 bp encoding for amino acids V2 to L8 resulting expression plasmid: pBCMaJoHIS 4A, see Table 3.I
oFH25	5'-GGC ATT CGG CAG GTT CAT GGA TCC ACG CGG-3'	rev-primer used for site directed mutagenesis of CHRAC14. See oFH24
oFH26	5'-CCG CAA AAG ATC CGT GTA TAG CAG TTC CAG GAG ATG CTG-3'	fw-primer used for site directed mutagenesis of CHRAC16: mutated triplet underlined (CAC→ TAG; corresponds to H103STOP) resulting expression plasmid: pBCMaJoHIS 1C, see Table 3.I
oFH27	5'-CAG CAT CTC CTG GAA CTG CTA TAC ACG GAT CTT TTG CGG-3'	rev-primer used for site directed mutagenesis of CHRAC16: mutated triplet underlined. see oFH26
oFH28	5'-CAG GTG GTC AAT AAG AAC AAG TAG CTG GAG TTT CTG CTG CAG-3'	fw-primer used for site directed mutagenesis of CHRAC16: mutated triplet underlined (AAT→ TAG; corresponds to N88STOP) resulting expression plasmid: pBCMaJoHIS 1D, see Table 3.I
oFH29	5'-CTG CAG CAG AAA CTC CAG CTA CTT GTT CTT ATT GAC CAC CTG-3'	rev-primer used for site directed mutagenesis of CHRAC16: mutated triplet underlined. see oFH28

oFH30	5'-TTT CAG GGT CAT ATG GTG GAG CGT CCA CCG-3'	fw-primer used for site directed mutagenesis of CHRAC16: deletion of 24 bp encoding for amino acids G2 to P9 resulting expression plasmid: pBCMaJoHIS 1E, see Table 3.I
oFH31	5'-CGG TGG ACG CTC CAC CAT ATG ACC CTG AAA-3'	rev-primer used for site directed mutagenesis of CHRAC16. See oFH30
oFH32	5'-TTT CAG GGT CAT ATG TTT CTG CCC CTC AGC-3'	fw-primer used for site directed mutagenesis of CHRAC16: deletion of 51 bp encoding for amino acids G2 to T18 resulting expression plasmid: pBCMaJoHIS 1F, see Table 3.I
oFH33	5'-GCT GAG GGG CAG AAA CAT ATG ACC CTG AAA-3'	rev-primer used for site directed mutagenesis of CHRAC16. See oFH32
oFH34	5'-GAC AAG CTG TGA CCG TCT CCG-3'	rev-primer used for sequencing CHRAC14-CHRAC16 expression plasmids, prime site approximately 80 bp downstream of CHRAC16 stop codon
oFH35	5'-CCC TAT AAC CCC TGC ATT GAA TTC CAG TCT GAT AA-3'	oligonucleotide for generating four way junction DNA (Bianchi *et al.*, 1989)
oFH36	5'-AAC AGT AGC TCT TAT TCG AGC TCG CGC CCT ATC ACG ACT A-3'	see oFH35
oFH37	5'-GTA GTC GTG ATA GGT GCA GGG GTT ATA GGG-3'	see oFH35
oFH38	5'-TTT ATC AGA CTG GAA TTC AAG CGC GAG CTC GAA TAA GAG CTA CTG T-3'	see oFH35
oFH39	5'-TTT ATC AGA CTG GAA TTC AAT GCA GGG GTT ATA GGG-3'	oligonucleotide for annealing with oFH35 to generate linear control DNA fragment 1 (Bianchi *et al.*, 1989)
oFH40	5'-GTA GTC GTG ATA GGG CGC GAG CTC GAA TAA GAG CTA CTG T-3'	oligonucleotide for annealing with oFH36 to generate linear control DNA fragment 2 (Bianchi *et al.*, 1989)
oFH41	5'-TTA ATA CGA CTC ACT ATA GGG AGA ATG GTC GAG CGC ATC GAG G-3'	fw-primer for RNAi-knockdown of CHRAC14 expression underlined: T7 promoter sequence

oFH42	5’-TTA ATA CGA CTC ACT ATA GGG AGA TCA CTC GGG GGC TTC CTC TG-3’	rev-primer for RNAi-knockdown of CHRAC14 expression underlined: T7 promoter sequence
oFH43	5’-TTA ATA CGA CTC ACT ATA GGG AGA ATG GGC GAA CCA AGG AGC C-3’	fw-primer for RNAi-knockdown of CHRAC16 expression underlined: T7 promoter sequence
oFH44	5’-TTA ATA CGA CTC ACT ATA GGG AGA CTA TTC ATC AGA CTC CGA TTC-3’	rev-primer for RNAi-knockdown of CHRAC16 expression underlined: T7 promoter sequence
oFH45	5’-CAC GGA GGA ATT CGG CCA G-3’	CHRAC16 fw-primer including natural EcoRI site
oFH46	5’-GCC GCG GTA CCC TAT TCA TCA GAC TCC-3’	CHRAC16 rev-primer introducing KpnI and SacII restriction sites downstream of stop codon
oFH47	5’-GTT GGC TCC TTG GTT CGC CCA TAT GTA TAT CTC CTT CTT AAA GTT AAA CAA AAT TAT TGA ATT CGA GAC CCC C-3’	oligonucleotide used for annealing with oFH1 to generate a 72 bp linear DNA fragment for DNA bandshifts

3.1.3.3 Antibodies

Table 3.III: Primary antibodies and dilutions

Antibody	**Western Blot dilution**	**Immunofluorescence**			**Immuno-precipitation**
		dilution for S2 cells	**dilution for polytene chromo-somes**	**dilution for embryos**	
α-ISWI rabbit polyclonal (J. Tamkun)	1:5000	-	1:350	1:50	67 μL per 1 mL protein G sepharose
α-p14 and α-p16 rat monoclonal antibodies (E. Kremmer, see 4.2)	1:20 to 1:100	undiluted to 1:9	1:1 to 1:3	1:1 to 1:9	1 mL per 1 mL protein G sepharose
α-ACF1 rat monoclonal, clone 3B7 (E. Kremmer)	1:40 to 1:500	-	-	-	-
α-MOF (J. Lucchesi)	-	1:400	-	-	-
α-poly-glutamate, GT335 (Wolff *et al.*, 1992)	1:5000	-	-	-	-
α-pan-acetyl-lysine rabbit polyclonal (Cell signalling technologies)	1:1000	-	-	-	-
α-pan-methyl-lysine rabbit polyclonal (Abcam)	1:2000	-	-	-	-
9E10 α-myc (Sigma)	1:50	-	-	-	-
mouse α-FLAG-tag (Sigma)	1:5000	-	-	-	-
mouse α-His-tag (Qiagen)	1:1500	-	-	-	-

Table 3.IV: Secondary antibodies and dilutions

Antibody	**Western Blot dilution**	**Immunofluorescence**		
		dilution for S2 cells	**dilution for polytene chromosomes**	**dilution for embryos**
α-rabbit, HRP-conjugated (Biozol)	1:5000 to 1:10000	-	-	-
α-rat, HRP-conjugated (Dianova)	1:3000 to 1:5000	-	-	-
α-mouse, HRP-conjugated (Amersham)	1:5000	-	-	-
α-rabbit for infrared detection[a)] (Biomol)	1:10000	-	-	-
α-rat for infrared detection[a)] (Biomol)	1:10000	-	-	-
α-rabbit FITC-labelled (Dianova)	-	-	-	1:200
α-rat Cy3-labelled (Jackson)	-	1:2000	1:350	1:200
α-rat rhodamin-labelled (Jackson)	-	-	-	1:200
α-rabbit Cy3-labelled (Jackson)	-	1:500 to 1:1000		
α-rabbit Cy2-labelled (Jackson)	-		1:350	

[a)] antibodies labelled with either IRDye 800 or Alexa 680 dye, respectively.

3.2 Methods

3.2.1 Cloning of expression vectors

3.2.1.1 *Recombinant CHRAC14-CHRAC16 in* E. coli

For creation of a bicistronic CHRAC14-CHRAC16 expression vector, the coding sequence of CHRAC16 was amplified by PCR with the primers oFH1 and oFH2 from the plasmid pET24d-CHRAC16 (Corona *et al.*, 2000). A linker with an NdeI restriction site and an internal ribosomal entry site was introduced upstream of the CHRAC16 start codon by oFH1 (modified after (Lutzmann *et al.*, 2002)), and a XbaI restriction site was introduced downstream of the CHRAC16 STOP-codon by oFH2. Each end of the PCR product contained an EcoRI restriction site masked by a BsaI restriction site. The BsaI-treated PCR-fragment was then ligated into the EcoRI restriction site of the plasmid pGEX2T-CHRAC14 (Corona *et al.*, 2000), and the resulting plasmid was sequenced and named pBCEXMaJo.

The NdeI restriction site of pBCEXMaJo was used to add an N-terminal His_8-tag and a TEV cleavage site to the CHRAC16 ORF (57 bp fragment, annealed oligonucleotides oFH5 and oFH6). The resulting plasmid was named pBCMaJoHIS 1A and sequenced before protein expression (see Table 3.I and Appendix for plasmid map).

3.2.1.2 In vitro *translation of ACF1 deletion constructs*

Deletion variants of the ACF1 ORF were created by PCR using the plasmid pSPORT-ACF1 (A. Eberharter, I. Vetter) as a template, and the amplified fragments were cloned into the multiple cloning site (MCS) of the pING14A vector (Hagemeier *et al.*, 1993, see also Table 3.I).

3.2.2 Site-directed mutagenesis of expression vectors

The C- and N-terminal deletion variants of CHRAC14 and CHRAC16 were derived from the bicistronic expression vector pBCMaJoHIS and created with the QuikChange site-directed mutagenesis kit (Stratagene). All mutations were verified by sequencing and – whenever possible – by confirming changes in restriction endonuclease sites. An overview of the resulting plasmids is given in Table 3.I.

3.2.3 Expression and purification of recombinant CHRAC subunits from *E. coli*

Full-length CHRAC14-CHRAC16 and deletion variants were expressed in *E. coli* BL21(DE3)pLysS. Single colonies of the transformed bacteria grown on $LB_{AMP/CHL}$ plates were amplified overnight in $LB_{AMP/CHL}$ liquid medium. The overnight cultures were used to inoculate expression cultures ($LB_{AMP/CHL}$ liquid medium) at an OD_{600} of approximately 0.05 to 0.1. Bacteria were grown at 37°C to an OD_{600} of approximately 0.8. Protein expression was induced by addition of IPTG to a final concentration of 0.3 mM, and the bacterial cultures were shifted to 30°C for 3h. Bacteria were harvested and resuspended in 10 mL PBS/protease inhibitors (see 3.1.1) per litre of bacterial culture. This bacterial cell suspension was frozen in liquid nitrogen and stored at -80°C.

Cells were lysed by two freeze-thaw cycles and sonication (Branson digital sonifier 250 D, sonication 4-6 times for 20 s on ice, 50% amplitude), and insoluble components were removed by centrifugation for 30 min in the Sorvall SS34 rotor at 18000 rpm. The supernatant was passed over a Glutathione Sepharose 4B-column (Amersham) preequilibrated in PBS/0.05% NP40, with a bed volume of 1 mL beads per litre of bacterial culture. The column was washed with ten column volumes PBS/0.05% NP40, then with 20 column volumes PBS500/0.05% NP40 and again with ten column volumes PBS/0.05% NP40. The soluble and insoluble fractions after centrifugation, the column flowthrough and the Glutathione Sepharose beads were analysed by SDS-PAGE on 15% polyacrylamide gels.

The CHRAC14-CHRAC16 heterodimer was either eluted from the beads with glutathione elution buffer or it was cleaved off the beads, leaving the GST-tag behind. For cleavage, the beads were equilibrated with PBS/0.05% NP40/1 mM $CaCl_2$ and the bead slurry (bead volume : buffer volume = 1:1) was incubated with approximately 1 unit of bovine thrombin protease (Amersham) per 350 µg of GST fusion protein for 3 h on a rotating wheel at RT. The supernatant was collected and the beads were washed twice with PBS/0.05 % NP40. All fractions were pooled and passed over a 1 mL HiTrap chelating column (Amersham) that had been loaded before with Ni^{2+} according to the manufacturer's protocol. The heterodimer was eluted with an imidazole gradient (0-500 mM) in HEMG500 buffer (500 mM KCl). After elution, fractions were monitored by SDS-PAGE. The CHRAC14-CHRAC16 protein complex eluted at an imidazole concentration of approximately 170 mM.

For protein crystallisation, the CHRAC16 His_8-tag was cleaved off by TEV protease in EX50 buffer (50 mM KCl) or PBS containing 3 mM β-mercaptoethanol. CHRAC14-CHRAC16-containing fractions were pooled and dialysed against PBS/0.5 mM EDTA/2 mM 2-mercaptoethanol. Approximately 10 µg TEV protease per 1 mg protein were added, and cleavage was carried out for 3 h at RT. The protein was dialysed against PBS and passed again over the Ni^{2+}-loaded HiTrap chelating column. The cleaved protein eluted from the column in the flowtrough fraction and at low imidazole concentrations (<100 mM). Fractions were analysed by SDS-PAGE.

For gel filtration chromatography, protein-containing fractions were pooled, concentrated to a volume ≤ 0.5 mL and loaded either onto a Superdex 75 column (Amersham) or – if the GST-tag was still present – onto a Superdex 200 column (Amersham). Protein was eluted with EX200 buffer. Fractions were analysed by SDS-PAGE, and protein-containing fractions were pooled and concentrated in 6 mL spin concentrators (molecular weight cut-off: 5000 Da, Vivascience). If necessary, the buffer was adjusted appropriately for further applications during protein concentration. The protein concentration was determined by Bradford assay (BioRad) using BSA (Sigma) as a standard.

3.2.4 Expression and purification of recombinant CHRAC subunits from Sf9-cells

Various ISWI- and ACF1-constructs and CHRAC14-FLAG/His_6-CHRAC16 were expressed in baculovirus-infected Sf9 cells (Eberharter *et al.*, 2004a). Cells were either plated on 15 cm petri dishes ($1.2 \cdot 10^7$ cells/plate) or large-scale expressions of CHRAC14-CHRAC16 were performed in roller bottles ($1.8 \cdot 10^8$ cells/roller bottle). For infection, cells were carefully shaken at RT in Sf-900 II medium, 10% fetal calf serum and 1% Pen/Strep (see 3.1.1). After 1-2 hours, approximately 3 volumes of medium were added, and cells were either incubated at 26°C or rotated at RT for 48 h before harvesting. Cell pellets were washed in chilled PBS containing protease inhibitors (see 3.1.1), frozen in liquid nitrogen and stored at -80°C.

3.2.5 *in vitro*-translation

ACF1 variants (A. Eberharter, I. Vetter and this work, see Table 3.I) were translated *in vitro* using the TNT rabbit reticulocyte lysate system (Promega). Full length ACF1 was expressed from a pSPORT-derived plasmid (Invitrogen), whereas ACF1 deletion variants were expressed from pING14A vectors (Hagemeier *et al.*, 1993). During translation, the ACF1 variants were labelled with [^{35}S]methionine and [^{35}S]cysteine (ratio 70% to 30%).

3.2.6 SDS-PAGE and Western blotting

SDS-polyacrylamide gel electrophoresis (SDS-PAGE) was used for separation of denatured proteins (adapted from (Laemmli, 1970).

For Western blot analysis, proteins were electrophoretically transferred onto nitrocellulose or PVDF membrane (Amersham) for 1.5 h at 300 mA or overnight at 60 mA, respectively. The membranes were blocked in PBS/0.1% Tween/6% dry milk for 30 min at RT and incubated with the primary antibody (appropriately diluted in PBS/0.1% Tween/3% dry milk; for antibody dilutions, see Table 3.III) for 1 h at RT or overnight at 4°C. Membranes were washed three times in PBS/0.1% Tween for 10 min and incubated with the secondary antibody in PBS/0.1% Tween/3% dry milk (for dilution, see Table 3.IV). After 1 h, the membranes were washed again three times for 10 min in PBS/0.1% Tween. Depending on the type of secondary antibody, the membranes were analysed either by using ECL reagent (Amersham) and exposure to X-ray film (Fuji) or by scanning with the Odyssey infrared imaging system (LiCor Biosciences).

3.2.7 GST-pull-down assays

Glutathione-Sepharose 4B beads (Amersham) were equilibrated in EX250/0.05% NP-40 and loaded with recombinant, *E. coli*-expressed GST, GST-CHRAC14, GST-CHRAC14-CHRAC16 or various GST-tagged deletion variants of CHRAC14-CHRAC16. Binding of approximately 0.75 mg protein/mL bead volume occurred by rotating overnight at 4°C, and subsequently, the beads were washed twice with EX250/0.05% NP-40. To 25 µL aliquots of the protein-loaded beads, *in vitro*-translated ACF1 constructs were added, and samples were rotated in a total volume of 100 µL EX250/0.05% NP-40 for 3 h at 4°C. Unbound constructs were removed by washing the beads once with EX250, three times with EX500, once with EX250 and once with EX100, with 0.05% NP-40 in all buffers. Bead-bound protein was separated by SDS-PAGE, and signals of the radiolabelled ACF1-constructs were enhanced by incubation in Amplify solution (Amersham) for 30 min bevor drying. Signals were detected by exposure of X-ray film (Fuji) to the dried gels.

3.2.8 FLAG-co-immunoprecipitations from Sf9 cell extracts

Sf9 cells were co-infected with baculoviruses encoding for p14FLAG-His6p16 (pFASTBACDual, Invitrogen, J. Brzeski, see Table 3.I) and myc-tagged ACF1 full-length and deletion constructs (pFASTBAC, Invitrogen, (Eberharter *et al.*, 2004a) following the procedures described in 3.2.4. Lysis was carried out in EX100/protease inhibitors/0.05% NP-40 by two freeze-thaw-cycles and mild sonication, and cell debris was removed by centrifugation for 30 min at 3000 rpm and 4°C. The extracts were incubated with 10 µL anti-FLAG M2 beads (Sigma) per $12 \cdot 10^6$ cells for 3 h at 4°C on the rotating wheel. Unbound material was removed by washing the beads once in EX100, three times in EX500 and once in EX100, with protease inhibitors and 0.05% NP-40 in all buffers. Bound protein was eluted overnight using FLAG peptide (final concentration approximately 1 mg/mL), and myc-tagged ACF1-constructs were detected by Western blot analysis using the 9E10 anti-myc antibody (Sigma, see Table 3.III).

3.2.9 Production of monoclonal antibodies

Rat monoclonal antibodies against CHRAC14 and CHRAC16 were produced by E. Kremmer and coworkers (GSF, Munich) following standard techniques. Rats were immunised with recombinant GST-CHRAC14-CHRAC16 dimer expressed in *E. coli*. Screening for positive hybridoma cell supernatants was done by ELISA assay with the antigen (GST-CHRAC14-CHRAC16) immobilised via the GST-tag in the wells of 96-well plates (E. Kremmer). In two independent rounds of ELISA screening, 49 and 45 hybridoma cell supernatants gave a positive signal, respectively. The positive supernatants were tested in Western blotting both on recombinant GST-CHRAC14-CHRAC16 and on *Drosophila* nuclear embryo transcription extract (TRAX, embryo age: 0 to 16 h, (Nightingale *et al.*, 1998)) or *Drosophila* chromatin assembly extract (DREX, embryo age: 0 to 2 h, (Becker and Wu, 1992)), respectively. A total of fourteen supernatants out of the two rounds of ELISA screening gave a Western blot signal on the *Drosophila* extracts. The five most promising candidates were subcloned and the types of the antibodies were classified by E. Kremmer (see also 4.2 and Table 4.I).

3.2.10 Immunoprecipitation

Rat monoclonal antibodies directed against CHRAC14 and CHRAC16 and the rabbit polyclonal antibody directed against ISWI were coupled to protein G sepharose beads (Amersham). The beads (15 µL) were incubated for 1.5 h at 4°C with 50 µL *Drosophila* embryo nuclear extract from 0 to 4 h old embryos (TRAX, 2 µg protein/µL in EX100/0.0125% NP-40). The beads were washed three times with EX200/0.0125% NP-40 and once with EX100/0.0125% NP-40 and analysed by SDS-PAGE and Western blotting.

3.2.11 Immunofluorescence on S2 cells

$0.5 \cdot 10^6$ to $1 \cdot 10^6$ cells were seeded onto a coverslip and incubated for 2 h at 26°C in a humid chamber. After removing the medium, cells were washed briefly in PBS and fixed in PBS/2% paraformaldehyde for 7.5 min on ice. Cells were permeabilised in PBS/1% paraformaldehyde/0.25% Triton-X-100 for 7.5 min on ice and washed two times in PBS. Cells were blocked for 1 h in PBS/2 % BSA/5 % goat serum, incubated with the primary antibody diluted appropriately in blocking solution for 1h (see Table 3.III), washed two times in PBS for 5 min, incubated with the secondary antibody diluted appropriately in blocking solution (see Table 3.IV) for 1 h and washed again two times for 5 min in PBS. All incubations were performed at RT in a humid chamber. For DNA staining, cells were incubated for 2 min in PBS containing Hoechst dye (dilution 1:50000) and washed in PBS for 5 min. Cells were mounted with PBS/0.1 M n-propyl-gallate/50 % glycerol and coverslips were stored at 4°C in the dark.

3.2.12 Immunofluorescence on polytene chromosomes

D. melanogaster salivary glands were dissected from 3rd instar larvae in 0.7% NaCl solution and incubated for 10 min in fixing solution (45% acetic acid/1.85% formaldehyde) on a siliconised coverslip. The coverslip was taken up by a poly-lysine-treated slide and the glands were broken by regularly dotting the coverslip with the back end of a paintbrush in a spiral movement. Polytene chromosomes were spread by squeezing the slide and coverslip with the thumb. The polytene chromosome quality was checked by phase contrast microscopy, and acceptable slides were frozen in liquid nitrogen. The coverslip was removed from the frozen slide with a razor blade and the slide was washed in PBS for 5 min and in PBS/0.1% Triton-X-100 for 10 min.

For blocking, the slide was incubated in PBS/0.1% Triton-X-100/1% BSA. Subsequently, the slide was placed in a humid chamber, and the squashed polytene chromosomes were covered overnight at 4°C with 20 µL of the primary antibody dilution and a fresh coverslip. All antibodies were diluted in PBS/0.1% Triton-X-100/1% BSA (see Tables 3.III and 3.IV).

The next day, the slides were washed three times for 5 min in PBS and two times for 15 min in PBS/0.1% Triton-X-100/1% BSA before the polytene chromosomes were incubated with the appropriately diluted secondary antibody (Table 3.IV) as described before for 1 h at RT. Slides were washed two times for 10 min with PBS/0.1% Triton-X-100/1% BSA and three times for 5 min in PBS, before staining the DNA with Hoechst dye (1:20000 in PBS) for

2 min. The slides were washed two times for 5 min in PBS, mounted with PBS/0.1 M n-propyl-gallate/50 % glycerol and stored at 4°C in the dark.

3.2.13 Immunofluorescence on *Drosophila* embryos

D. melanogaster 0-12 h embryos were dechorionated in 25% sodium hypochlorite solution (Merck) for 3 min, rinsed five times with PBS/0.1% Tween 20, washed two times with water and transferred into a 10 mL glass jar containing 1.5 mL n-Heptane. The glass jar was shaken vigorously for 15 s before 1.5 mL of PBS/3.7% paraformaldehyde were added and the glass jar was shaken again for 30 s. The embryos were fixed for 20 min at RT. The lower fraction (PBS/paraformaldehyde) was removed and 2 to 3 volumes of methanol were added before shaking again for 30 s to remove the vitellin membrane. Subsequently, the embryos were transferred into an 1.5 mL Eppendorf tube, washed two times with methanol and stored overnight at 4°C in methanol.

The next day, the embryos were washed in subsequent steps with PBS/0.1% Tween 20 containing 80%, 50% and 20% methanol, respectively, and twice with PBS/0.1% Tween 20. The embryos were then incubated with the diluted primary antibodies for 12 to 72 h at 4°C (see Table 3.III).

The primary antibody was removed by washing five times for 10 min with PBS/0.2% Tween 20/0.2% Triton-X-100 before adding the secondary antibody (diluted in PBS/0.1% Tween 20, see Table 3.IV). After 3 h incubation at RT, the secondary antibody was removed by washing three times for 10 min with PBS/0.2% Tween 20/0.2% Triton-X-100. The embryos were then rinsed with PBS and DNA was stained with TOPRO 3 (1 mM stock solution, diluted 1:1000 in PBS) for 10 min in the dark. The embryos were washed with PBS/0.2% Tween 20/0.2% Triton-X-100 and with PBS before mounting them in VectaShield mounting medium (Vector Labs).

3.2.14 Crystallisation of recombinant CHRAC14-CHRAC16

Screening for crystallisation conditions of recombinant *E. coli*-expressed CHRAC14-CHRAC16 was performed with a Cartesian crystallisation robot (Genomic Solutions) at the EMBL Outstation, Grenoble. Drops of 0.2 μL of protein solution (35 mg/mL in EX50 without glycerol) were mixed with 0.2 μL of reservoir solution. Several conditions of the Index screen (Hampton Inc.) yielded protein crystals. The largest crystals grew as regular rhomboids with sizes of approximately 350 by 200 by 100 μm^3 in sitting drops above a reservoir containing 0.1 M citric acid, pH 3.5 and 2 M ammonium sulfate (condition 1, Index screen). These crystals belong to the space group $P3_221$, with unit cell dimensions of a = 76.0 Å, c = 166.1 Å, $\gamma = 120°$ (crystal form I). A second condition that generated crystals sufficiently large for data collection contained 0.1 M HEPES, pH 7.5, 12% (w/v) PEG 3350, 5 mM $CoCl_2$, 5 mM $NiCl_2$, 5 mM $CdCl_2$, 5 mM $MgCl_2$ (condition 64, Index screen) as reservoir solution. These crystals grew as cubes of approximately 100 by 100 by 100 μm^3 and possess space group $P42_12$, with unit cell dimensions of a = 130.5 Å, c = 59.7 Å (crystal form II).

3.2.15 Structure determination of recombinant CHRAC14-CHRAC16

A first data set of crystal form I (see 3.2.14) was collected at the ESRF beam line ID14-4 and diffracted to 2.4 Å resolution (see Table 4.II). Initial attempts to solve the structure by molecular replacement with the structure of NFYB-NFYC (Romier *et al.*, 2003) were unsuccessful (T. Grüne, C. Fernández-Tornero, C. Müller, Grenoble).

Hence, crystal form II (see 3.2.14) was used to solve the structure by single isomorphous replacement in combination with anomalous scattering (SIRAS) using data from a native crystal and a methylmercuryacetate derivative (C. Fernández-Tornero, C. Müller, Grenoble). Data for the second crystal form were collected at ESRF beam line ID29 (Table 4.II). Two major heavy atom sites were located and refined with the programme SOLVE (Terwilliger and Berendzen, 1999). The original SIRAS map was further improved by solvent flattening and histogram matching with the programme RESOLVE (Terwilliger, 2000). The two mercury atoms served as starting points for model building and turned out to be bound to Cys49 of CHRAC16 in both heterodimers present in the asymmetric unit. The structure was built manually with the programme O (Jones *et al.*, 1991) and refined with CNS (Brunger *et al.*, 1998) against native data of this crystal form. The refined model resulting from crystal form II was then used to locate both heterodimers of the asymmetric unit in crystal form I (see 3.2.14) with the programme AMORE (CCP4, 1994) and subsequent refinement with CNS to a final resolution of 2.4 Å. The models in both crystal forms possess excellent stereochemistry. Table 4.II summarises the final refinement statistics of the two crystal forms. The structure determination described here was performed by C. Fernández-Tornero and C. Müller, EMBL Outstation, Grenoble.

3.2.16 RT-PCR

Total RNA was isolated from *Drosophila* embryos using Trizol reagent (Invitrogen), treated with RQ1 RNase-free DNAse for 30 min at 37°C, extracted with phenol/chloroform and preciptiated with ethanol. Total RNA from KC- and S2-cells was isolated and DNase treated using the RNAeasy kit (Qiagen) according to the manufacturer's protocol.

Random primers and equal amounts of the different RNA preparations were used to produce cDNA with help of the Reverse Transcriptase kit (Invitrogen). Control reactions were carried out without Reverse Transcriptase.

Polymerase chain reactions were performed with gene-specific primers for 35 reaction cycles with an annealing temperature of 55°C, using 2 μL of the cDNA-templates or the control-templates, respectively.

3.2.17 Production of four way junction DNA

Four way junction DNA and linear control DNA was produced as described (Bianchi *et al.*, 1989). Oligonucleotide oFH35 and oligonucleotide oFH1 (see Table 3.II) were radioactively end-labelled with [^{32}P]phosphate following standard techniques (Sambrook and Russell, 2001) and purified over a G25 spin column (Amersham). Equal molar amounts of the oligonucleotides oFH36, oFH37 and oFH38 were annealed with the labelled oligonucleotide oFH35 to form the cruciform four way junction DNA (151 DNA bases total), whereas the labelled oligonucleotide oFH1 was annealed with oFH47 to form the linear control DNA fragment (145 DNA bases total, termed '72 base pair fragment'). After annealing, the four way junction DNA and the linear control DNA fragment were purified under native conditions on a 6% polyacrylamide gel in 0.5x TBE. The DNA was detected by exposure of the gel to X-ray film, excised from the gel, and extracted by shaking overnight at 4°C in TMS buffer.

3.2.18 Electrophoretic mobility shift assay (EMSA)

Approximately 60 fmol of radiolabelled 248 base pair DNA (labelled with α[^{32}P]CTP by PCR) or approximately 5 fmol of radiolabelled linear and cruciform DNA fragments (end-labelled with γ[^{32}P]ATP) were incubated with varying amounts of protein for 10 min at RT. DNA-protein complex formation was tested by native PAGE on 4.5 % to 6.5 % polyacrylamide/0.5x TBE gels. PAGE and autoradiography conditions were chosen as described for the nucleosome mobilisation assays (see 3.2.20).

3.2.19 DNA pull-down assay

TALON beads (BD Biosciences) were loaded with full length p14-His$_8$p16 and p14-His$_8$p16ΔC, respectively (both purified from *E. coli*, concentration of the heterodimer either 10 pmol/μL bead volume or 20 pmol/μL bead volume), or with no protein (mock). 10 μL of the beads were then incubated with approximately 0.6 ng (240 Bq) of radiolabelled 10 bp DNA ladder (Invitrogen) in EX50/0.005 % NP40 while shaking for 45 min at 26°C. The supernatant was saved, the beads were washed three times in EX50/0.005% NP40 and input, supernatant and beads were boiled in DNA loading dye before loading one third onto a DNA sequencing gel (8% acrylamide, 0.5x TBE, 7 M urea). The gel was run at 35 to 38 W (approximately 2200 V at the beginning), dried and exposed overnight to a phosphoimager screen. The intensity of the DNA bands between 10 and 100 bases was determined using AIDA software (Fuji).

3.2.20 Nucleosome mobilisation assay

Mononucleosomes with radiolabelled 248 base pair DNA were prepared according to (Eberharter *et al.*, 2004a) and were a gift from A. Eberharter. Approximately 60 fmol of positioned mononucleosomes were incubated with the remodelling complexes ISWI (approximately 3 to 30 fmol), ACF and ACFΔWAC (approximately 0.3 to 3 fmol) in EX50 buffer (50 mM KCl) containing 1 mM ATP and 0.2 g/L BSA. Where indicated, varying amounts of CHRAC14-CHRAC16 full length and deletion variants were titrated to the samples before starting the sliding reaction. The total reaction volume was 10 μL, and samples were incubated at 26°C for 45 min. Reactions were stopped by adding 0.5 μg plasmid DNA and chilling on ice. Samples were analysed by native PAGE on 4.5 % polyacrylamide/0.4x TBE gels. Gels were run for 3 to 5 h at 18°C and 100 to 120 V, and analysed by exposure of X-ray film or a phosphoimager screen (Fuji) to the dried gels.

3.2.21 ATPase assay

The ATPase activities of ISWI and ACF were measured using a modified protocol from (Corona *et al.*, 1999). The ATP hydrolysis rate of approximately 3 fmol ISWI and ACF, respectively, was determined in the presence of either 0.1 μg dsDNA or the same amount of chromatinised DNA (gift from A. Eberharter, A. Kiziltas). Standard reactions (15 μL) were performed in ATPase buffer and were started with a mix of 20 μM ATP and 35 kBq [γ-^{32}P]ATP (Amersham). Reactions were incubated at 26°C for 30 min. 1 μL of each reaction was spotted onto a cellulose thin-layer chromatography plate (Merck) and free phosphate was separated from ATP by chromatography with 0.5 M LiCl/1 M formic acid for 15 min. A phosphoimager screen (Fuji) was exposed to the dried gel for 10 min and the ratio of free phosphate and ATP was quantified with AIDA software (Fuji).

3.2.22 HAT-assay

The activity of different acetyltransferases (CBP, GCN5, MOF, p300) was tested on 2 µg of recombinant CHRAC14-CHRAC16. Acetyltransferase reactions (20 µL) contained 10 mM Tris-HCl pH 8.0, 0.1 mM EDTA and 3 µM (250 nCi) of [^{3}H]-Acetyl-Coenzyme A. The reactions were incubated for 30 min at 26°C. 10 µL of the reactions were analysed by SDS-PAGE and autoradiography; the SDS gels were incubated in Amplify solution (Amersham) for 30 min, dried and exposed to X-ray film for 6 weeks. The rest of the reactions (10 µL) was spotted onto P81 paper (Whatman), dried and washed three times with 50 mM sodium carbonate buffer pH 9.3 before determining the amount of bound radioactivity in the scintillation counter.

3.2.23 Standard molecular biology techniques

Standard techniques in molecular biology such as the transformation of bacteria, isolation of DNA/RNA, radiolabelling of DNA, restriction analysis, polymerase chain reaction (PCR), cloning of DNA, agarose gel electrophoresis etc. were performed essentially as described in (Sambrook and Russell, 2001)

4 Results

4.1 Expression of recombinant CHRAC14-CHRAC16

4.1.1 Establishment of a bicistronic expression system for CHRAC14-CHRAC16 in *E. coli*

All recombinant CHRAC14-CHRAC16 purified from *E. coli* used in this study was expressed from a bicistronic plasmid.

The two histone fold subunits had been co-expressed before from two separate plasmids (Corona *et al.*, 2000). However, this approach was unsatisfactory, because the proteins were never produced in stoichiometric amounts. Furthermore, it was impossible to express CHRAC16 alone, which was presumably due to toxic effects of the single histone fold protein (D. Corona, A. Eberharter, personal communication). In contrast, the expression of CHRAC14 alone was feasible, but a high percentage of the protein was insoluble.

For these reasons, a bicistronic expression vector was constructed (see 3.2.1.1) to ensure equivalent transcript levels of CHRAC14 and CHRAC16. Initially, CHRAC14 was expressed with an N-terminal GST-tag, whereas CHRAC16 had no affinity tag and was co-purified via the GST-tag of CHRAC14. Although the protein yield was improved by the bicistronic expression, the stoichiometry of the two proteins was still not equimolar, but there was an excess of GST-CHRAC14 over CHRAC16. Therefore, an eight-histidine (His_8) tag was introduced at the CHRAC16 N-terminus (see plasmid map of the bicistronic expression plasmid pBCMaJoHIS in the Appendix), and a purification scheme was established that makes successive use of both the GST- and the histidine affinity tag (see 3.2.3). This two-step strategy allows the purification of a highly pure CHRAC14-CHRAC16 complex with a 1:1 stoichiometry. Figure 4.1 shows a Coomassie-stained SDS-polyacrylamid-gel of purified CHRAC14-CHRAC16.

According to analytical ultracentrifugation studies, the two proteins form heterodimers, but no higher order aggregates in solution (N. Mücke, J. Langowski, unpublished observation).

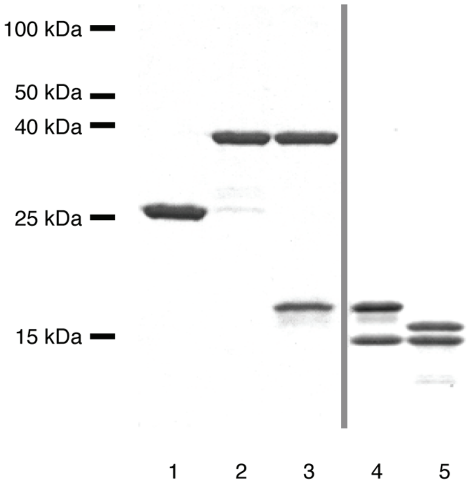

Figure 4.1: Purified recombinant CHRAC14 and CHRAC16 from *E. coli*. Coomassie-stained 15 % SDS-polyacrylamid-gel. Lane 1: GST. Lane 2: GST-CHRAC14. Lane 3: GST-CHRAC14-His$_8$CHRAC16. Lane 4: CHRAC14- His$_8$CHRAC16. Lane 5: CHRAC14-CHRAC16. Affinity tags were cleaved off by Thrombin protease (GST, lanes 4 and 5) and TEV protease (His$_8$, lane 5), respectively.

The expression plasmid pBCMaJoHIS was further used to produce several N- and C-terminal truncations of both CHRAC14 and CHRAC16 by site directed mutagenesis (see 3.2.2 and Table 3.I). An overview of the deletion constructs is given in Figure 4.2 A. However, not all of the constructs expressed equally well.

The C-terminal deletion variants CHRAC14-3 (aa 1-79) and CHRAC16-C (aa 1-102) were not expressed in detectable amounts, whereas the C-terminal deletion variant CHRAC16-D (aa 1-87) was expressed, but was highly unstable and rapidly degraded during purification. It is an interesting observation that the CHRAC16 deletion variant with the shorter C-terminus (CHRAC16-D) seems to be more stable than the deletion variant with the longer C-terminus (CHRAC16-C).

All other deletion variants could be expressed and purified. A total of four deletion variants have been studied in detail, each one lacking either the N-terminal tail or the C-terminal tail of CHRAC14 or CHRAC16. Since the two N-terminal deletion variants of CHRAC16 (CHRAC16-E and CHRAC16-F) are only slightly different (see Figure 4.2 A), most studies were done with CHRAC16-F, which has the larger N-terminal deletion. For simplicity, the four deletion variants used for further studies are referred to as CHRAC14ΔN, CHRAC14ΔC, CHRAC16ΔN and CHRAC16ΔC, respectively (see Figure 4.2 A). A polyacrylamide gel of the purified CHRAC14-CHRAC16 deletion variants is shown in Figure 4.2 B.

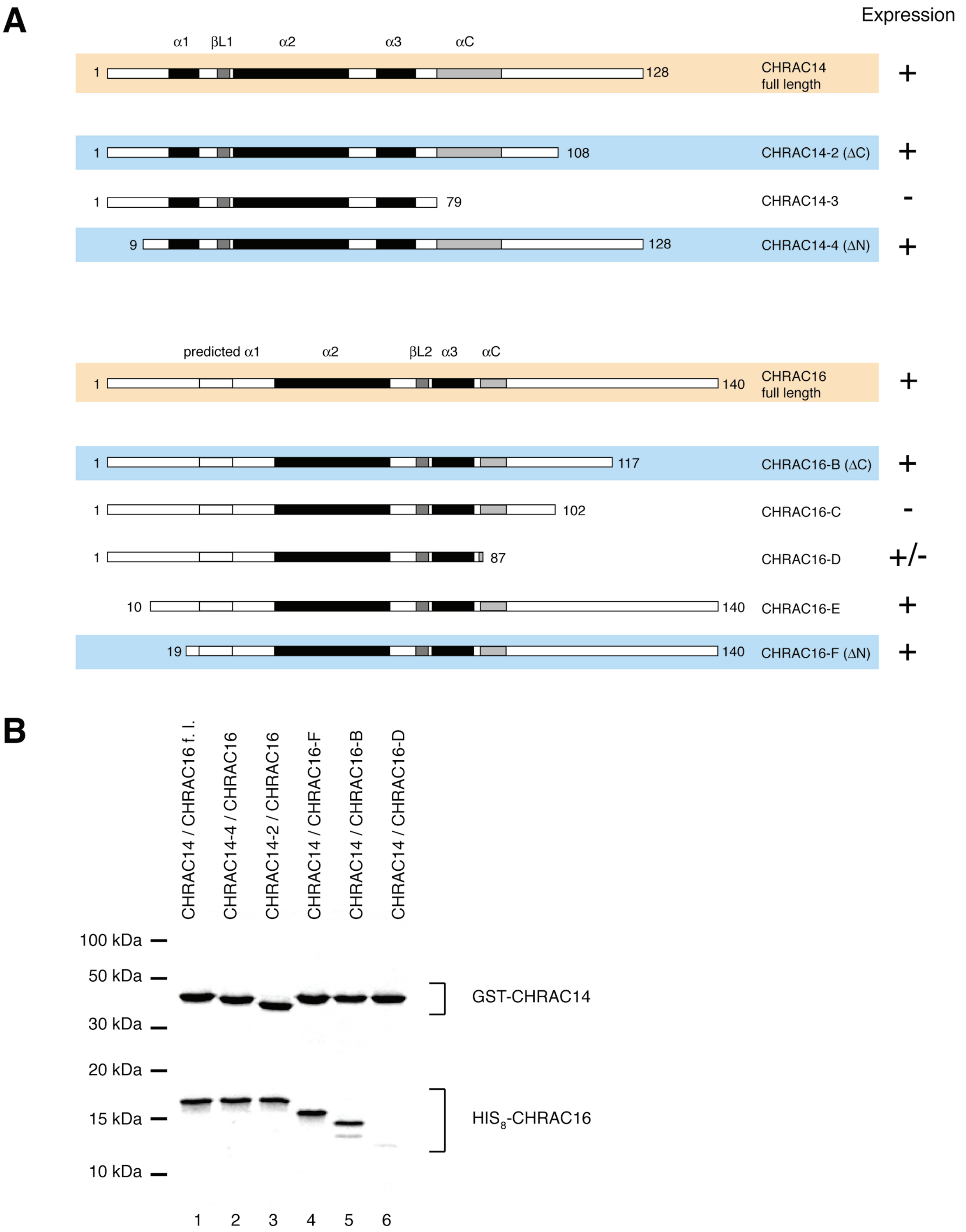
A
Expression
α1
βL1
α2
α3
αC
1
128
CHRAC14 full length
+
1
108
CHRAC14-2 (ΔC)
+
1
79
CHRAC14-3
-
9
128
CHRAC14-4 (ΔN)
+
predicted α1
α2
βL2
α3
αC
1
140
CHRAC16 full length
+
1
117
CHRAC16-B (ΔC)
+
1
102
CHRAC16-C
-
1
87
CHRAC16-D
+/-
10
140
CHRAC16-E
+
19
140
CHRAC16-F (ΔN)
+
B
CHRAC14 / CHRAC16 f. l.
CHRAC14-4 / CHRAC16
CHRAC14-2 / CHRAC16
CHRAC14 / CHRAC16-F
CHRAC14 / CHRAC16-B
CHRAC14 / CHRAC16-D
100 kDa
50 kDa
30 kDa
20 kDa
15 kDa
10 kDa
GST-CHRAC14
HIS8-CHRAC16
1
2
3
4
5
6

Figure 4.2: CHRAC14- and CHRAC16 deletion variants. A: Schematic overview. The ability to express the constructs is indicated on the right. Full length p14 and p16 are highlighted in orange, and the deletion variants used for further studies are highlighted in blue. B: Coomassie-stained SDS-gel with various GSTp14-p16 deletion constructs. Lane 1: full length GSTp14-p16. Lane 2: CHRAC14-4. Lane 3: CHRAC14-2. Lane 4: CHRAC16-F. Lane 5: CHRAC16-B. Lane 6: CHRAC16-D, which appears to be unstable and easily degraded (see text).

4.1.2 Expression of CHRAC14-CHRAC16 in a eukaryotic system (Sf9-cells)

4.1.2.1 Post-translational modification

The two histone fold CHRAC subunits were expressed in Sf9 cells by infection with a baculovirus construct encoding for C-terminally FLAG-tagged CHRAC14 and N-terminally His_6-tagged CHRAC16 (vector by J. Brzeski, sequenced and corrected for a point mutation in CHRAC16, see Table 3.I). Purification of the heterodimer occured via the CHRAC14-FLAG tag. Surprisingly, the two subunits migrated as a single band on SDS-polyacrylamide gels (see Figure 4.3 A lane 1). The presence of both protein subunits in the single band was verified by mass spectrometry (MALDI-TOF) and Western blot analysis with the rat monoclonal antibodies 5C7, 7D6 (directed against p14) and 6G6 (directed against p16), respectively (see 4.2.1 for antibody details). The aberrant migration behaviour could not exclusively be explained by the presence of the FLAG and His_6 affinity tags. Therefore, the proteins were inspected for post-translational modifications with different approaches.

First, it was tried to determine the exact molecular mass of the histone fold subunits by Electrospray Ionisation mass spectrometry (ESI-TOF). For this analysis, the full length CHRAC14-CHRAC16 heterodimers purified either from *E. coli* or from Sf9 cells were examined in parallel and compared with their calculated molecular masses. Only the CHRAC14 subunit, but not the CHRAC16 subunit, was detected in the ESI-TOF analysis, which was probably due to the high negative charge of CHRAC16. The measured molecular weight of *E. coli*-expressed CHRAC14 was 13989 Da, which was consistent with the theoretical molecular weight of 13988 Da. The molecular weight for Sf9-expressed FLAG-CHRAC14 was 15318 Da, but the theoretical molecular weight is 15448 Da. The difference between the measured and the theoretical value can be explained by the absence of the start-methionine (131 Da), which is frequently observed in eukaryotic expression systems. As a consequence, CHRAC14 is unlikely to be post-translationally modified in Sf9 cells.

In parallel, the overall acetylation-, methylation- and poly-glutamination state of the two CHRAC subunits was checked by Western blotting with anti-pan-acetyl-lysine-, anti-pan-methyl-lysine and anti-poly-glutamine antibodies, respectively (see Table 3.III). The antibodies detected several bands in HeLa cell extract, which served as a positive control (gift from C. Regnard), but none of them gave a signal for CHRAC14 and CHRAC16 purified from Sf9 cells (data not shown). The absence of lysine acetylation was also confirmed by a histone acetyl-transferase (HAT) assay. The tested HAT enzymes (CBP, GCN5, MOF, p300) were not able to acetylate CHRAC14-CHRAC16 from *E. coli* and from Sf9-cells, whereas auto-acetylation of the HATs and histone acetylation (positive control) could be observed (data not shown).

Finally, a potential CHRAC14-CHRAC16 phosphorylation was tested by incubation of the heterodimer with two different phosphatases. Incubation with λ-protein-phosphatase (not shown) as well as with calf intestine phosphatase (CIP) resulted in partitioning of the single CHRAC14-CHRAC16 band into a doublet during SDS-PAGE (Figure 4.3 A, lane 2). The phosphatase-induced division of the single band could be suppressed by the presence of phosphatase inhibitors (Figure 4.3 A, lane 3). In contrast, *E. coli*-expressed p14-p16 was neither affected by phosphatase nor phosphatase inhibitors (Figure 4.3 A, lanes 4 to 6).

The phosphatase-treated protein was also analysed by Western blotting. Figure 4.3 B shows Western blot signals from membranes probed with the 5C7- and 7D6 antibodies (anti-CHRAC14, see 4.2.1) and the 6G6 antibody (anti-CHRAC16, see 4.2.1). A phosphatase-dependent shift of the p16 signal (Figure 4.3 B, compare lanes 4 and 6 with lane 5), but not of the p14 signal (Figure 4.3 B, lanes 1 to 3) revealed p16 to be phosphorylated. This is consistent with the finding that p14 has been found unmodified in the ESI-TOF analysis.

The p16 phosphorylation site has not been mapped in detail. However, it is likely to be located at the acidic C-terminal tail, since there are two potential casein kinase II (CK II) phosphorylation sites. There was no functional difference between the phosphorylated and the dephosphorylated state of the heterodimer in DNA bandshifts and nucleosome sliding assays. However, these experiments have to be interpreted carefully, because the protein preps were contaminated with an ATP-dependent remodelling activity (see 4.1.2.2).

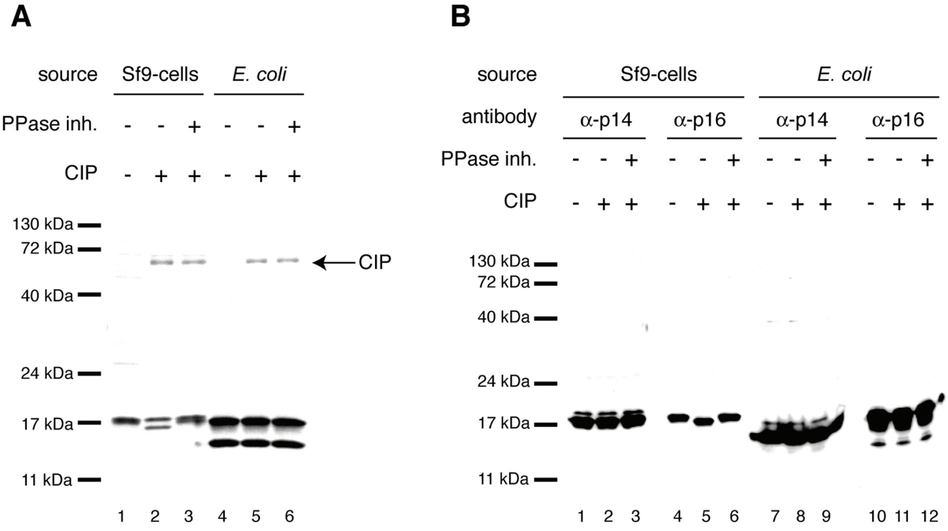

Figure 4.3: The CHRAC histone fold dimer is phosphorylated in Sf9-cells. A: Coomassie-stained 15% polyacrylamid gel. Dephosphorylation of the heterodimer leads to division of the single protein band into a doublet (lane 2), which can be repressed by phosphatase inhibitors (lane 3). Neither phosphatase nor phosphatase inhibitors influence p14-p16 from *E. coli* (lanes 4 to 6) CIP: calf intestine phosphatase. B: Western blot of phosphatase-treated p14-p16. Only the signal for p16 is shifted upon phosphatase-treatment (compare lane 4 with lane 5), but not the p14-signal (compare lane 1 with lane 2).

4.1.2.2 Co-purification of an ATP-dependent remodelling activity from Sf9-cells with recombinant CHRAC14-CHRAC16

Judged by Coomassie-stained SDS-gels, the CHRAC14-CHRAC16 protein preparations from Sf9 cells appeared to be rather pure, with hardly any additional protein band visible (see Figure 4.3 A, lane 1). Besides, the protein preparations from *E. coli* and from Sf9 cells had approximately the same DNA binding properties, suggesting that there was no obvious contamination by other DNA binding proteins.

However, at least some of the Sf9-expressed p14-p16 preps were contaminated by an ATPase activity (Figure 4.4 A). The ATPase was tightly associated with the p14-p16 dimer, since it resisted washes with 1 M KCl. When tested in the nucleosome mobilisation assay (see 4.6.1 for details), it became clear that the contamination in the CHRAC14-CHRAC16 preparations from Sf9 cells was able to mobilise a mononucleosome from the end of the DNA fragment towards the centre of the DNA fragment (Figure 4.4 B, lanes 5 to 7), and that this nucleosome movement was dependent on the presence of ATP (Figure 4.4 B, lanes 9 to 11). Therefore, the contamination turned out to be an endogenous chromatin remodelling activity from the Sf9 cells, which displayed a remarkably high performance in the *in vitro* assays. Consequently, the CHRAC14-CHRAC16 preparations from Sf9 cells were not used in further experiments, since p14-p16-specific effects would have been concealed by the effects of the co-purified remodelling activity.

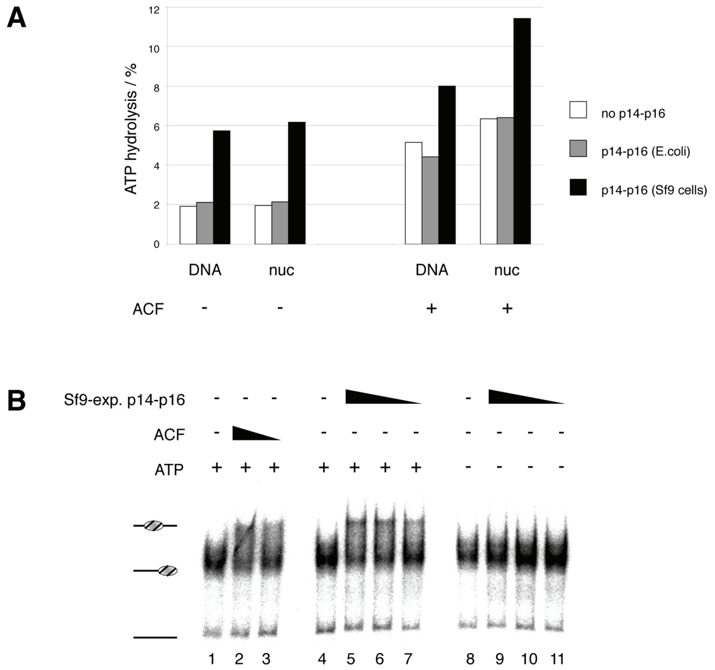

Figure 4.4: Sf9-expressed CHRAC14-CHRAC16 is contaminated by an ATP-dependent chromatin remodelling factor. A: ATPase-assay. The ATP hydrolysis rate of recombinant p14-p16 purified from *E. coli* and from Sf9 cells (both 1.3 µM) was determined in the absence and in the presence of ACF (0.2 nM). The ATPase activity was stimulated either by free DNA or by the same amount of chromatinised DNA (nuc). B: Nucleosome mobilisation assay. End-positioned mononucleosomes were incubated either with ACF (0.3 nM and 0.1 nM, lanes 2 and 3) or with recombinant p14-p16 purified from Sf9 cells (2.4 µM, 1.2 µM, 0.6 µM) in the presence of ATP (lanes 5 to 7) and in the absence of ATP(lanes 9 to 11). For a detailed description of the principle of the nucleosome mobilisation assay, see 4.6.1.

4.2 Characterisation of monoclonal antibodies directed against CHRAC14 and CHRAC16

4.2.1 Western blotting

The polyclonal rabbit antibodies that had been raised against GSTp14 and GSTp14-p16 previously (Corona *et al.*, 2000) appeared not to be very specific and of low affinity. Therefore, a new attempt was started to raise monoclonal rat antibodies against CHRAC14 and CHRAC16 (see 3.2.9), and the hybridoma cell supernatants were tested in two independent ELISA screens (E. Kremmer, GSF). 49 and 45 supernatants produced a signal in the two ELISA screens, respectively. These supernatants were further analysed by Western blotting. Although the majority of the hybridoma supernatants recognised the recombinant protein, there was only one supernatant from the first ELISA screen and 13 supernatants from the second screen that gave a signal with *Drosophila* nuclear embryo extract (TRAX, Nightingale *et al.*, 1998) or *Drosophila* chromatin assembly extract (DREX, Becker and Wu, 1992). Of these supernatants, only one was specific for CHRAC16, the others recognised CHRAC14. The p16-specific hybridoma cell clone and the four clones that appeared to have the highest specificity and affinity for p14 were then chosen to be further subcloned, and the IgG subtype was determined for each antibody (E. Kremmer).

Table 4.I summarises the properties of the five monoclonal antibodies, and Figure 4.5 shows Western blot analyses with recombinant CHRAC14-CHRAC16 or DREX probed with the monoclonal antibodies.

In general, all monoclonal antibodies give only a very poor Western blot signal on embryo extracts, and the signal is even weaker or undetectable on *Drosophila* cell extracts (not shown). Most likely, this observation can be explained by the lower abundance of p14 and p16 in cultured cells than in embryos (see also 4.2.2, 4.2.3.2 and 4.2.4). Besides, the 4F7 and the 5C7 antibodies recognise additional bands on TRAX and DREX (see Figure 4.5). As a consequence, the applicability of the antibodies is very limited in Western blotting.

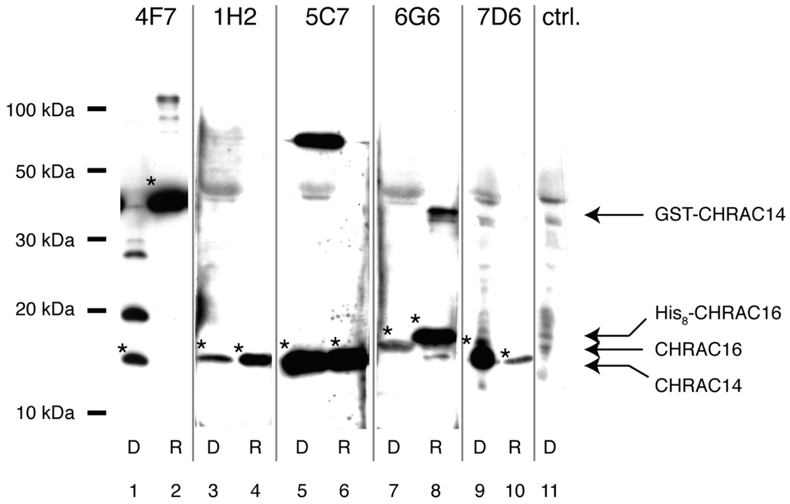

Figure 4.5: Western blots of the different monoclonal antibodies directed against p14 and p16. D: DREX, R: recombinant p14-p16 with GST-tag (lanes 2 and 8) or without GST-tag (lanes 4, 6 and 10), ctrl.: control lane (secondary antibody only). Asterisks mark the specific signal for p14 (4F7, 1H2, 5C7 and 7D6 antibodies) and p16 (6G6 antibody), respectively. Note that due to the His_8 affinity tag, the signal for recombinant p16 is slightly shifted (compare lanes 7 and 8).

Table 4.I: Properties of the rat monoclonal antibodies directed against CHRAC14 and CHRAC16.

name	**4F7**	**1H2**	**5C7**	**6G6**	**7D6**
derived from ELISA screen	first screen	second screen	second screen	second screen	second screen
directed against	CHRAC14	CHRAC14	CHRAC14	CHRAC16	CHRAC14
antibody class	IgG 2a	IgG 2c	IgG 2a	IgG 1	IgG 2a
number of performed subclonings	3	2	2	2	4
epitope location	central	C-terminal	central	central	N-terminal
Immunoprecipitation	(+)	+	-	-	-
Immunofluorescence on S2 cells	-	-	-	-	-
Immunofluorescence on polytene chromosomes	n/d	(+/-)	-	+	-
Immunofluorescence on embryos	-	-	+	-	-

For epitope mapping, the monoclonal antibodies were further tested on the C- and N-terminal deletion mutants of CHRAC14 and CHRAC16. The Western blot shown in Figure 4.6 indicates that the epitope of the 1H2 antibody is situated at the C-terminus of CHRAC14, since it does not recognise the CHRAC14ΔC deletion variant (lane 3). In contrast, the epitope of the 7D6 antibody seems to be at the CHRAC14 N-terminus (see lane 11). The 4F7 and 5C7 antibodies appear to recognise more central epitopes, because they give a signal with full length CHRAC14 as well as with the C- and N-terminal deletion variants (lanes 4 to 6 and 7 to 9, respectively). The 6G6 antibody recognises an epitope in the central part of CHRAC16 (lanes 13 to 15).

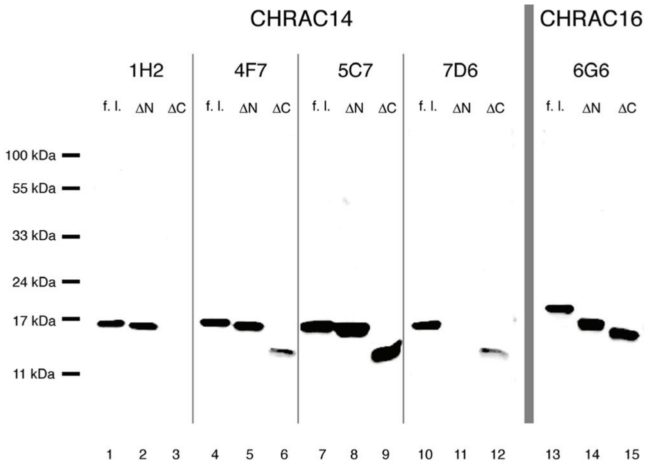

Figure 4.6: Western blot with p14- and p16 deletion variants.

4.2.2 Immunoprecipitation

The rat monoclonal antibodies were tested for their ability to immunoprecipitate CHRAC subunits from TRAX made from zero to four hour old embryos. This kind of extract was chosen because CHRAC is most abundant in early embryos (Corona *et al.*, 2000; Eberharter *et al.*, 2001, see also 4.2.4). The immunoprecipitations were analysed by Western blotting using antibodies against CHRAC14 (5C7 antibody), CHRAC16 (6G6 antibody), ACF1 (rat monoclonal antibody 3B7, A. Eberharter) and ISWI (rabbit polyclonal antibody, J. Tamkun). However, CHRAC14, CHRAC16 and ACF1 were not detected by the rat monoclonal antibodies.

When the membrane was probed with the anti-ISWI antibody, the ISWI signal was not only detected in the positive control (Figure 4.7, lane 7), but also in the immunoprecipitations with the 1H2 antibody and – with a very weak intensity – with the 4F7 antibody (Figure 4.7, lanes 1 and 2, respectively). Since CHRAC14-CHRAC16 have been found to interact with ACF1, but not with ISWI (see 4.4), this observation suggests that the 1H2 and 4F7 antibodies are able to co-immunoprecipitate ISWI via the ACF1 subunit, although ACF1 could not be detected. Interestingly, the epitope of the 1H2 antibody has been mapped to the C-terminal tail of CHRAC14 (see 4.2.1 and Figure 4.6), which suggests that the epitope is more accessible for antibody binding in the native CHRAC14-CHRAC16 complex.

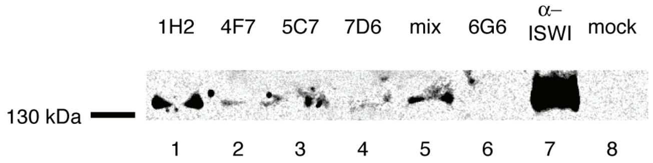

Figure 4.7: Western blot of immunoprecipitations from DREX with the anti-ISWI antibody. The antibodies used for immunoprecipitation are indicated above. Lane 6 (mix): IP with all four antibodies directed against p14 (1H2, 4F7, 5C7, 7D6).

4.2.3 Immunofluorescence

4.2.3.1 *S2-cells and polytene chromosomes*

Whereas no specific nuclear signal for CHRAC14 or CHRAC16 was observed with any of the monoclonal rat antibodies on S2 cells (Figure 4.8 A), the 6G6 antibody (and to some extent the 1H2 antibody, not shown) stained some bands on *Drosophila* polytene chromosomes. Some of the bands co-localised with the ISWI-staining, whereas others did not (Figure 4.8 B). However, the signals were weak and the level of background staining was very high. Therefore, it cannot be excluded that the bands seen on polytene chromosomes, or at least some of them, are non-specific.

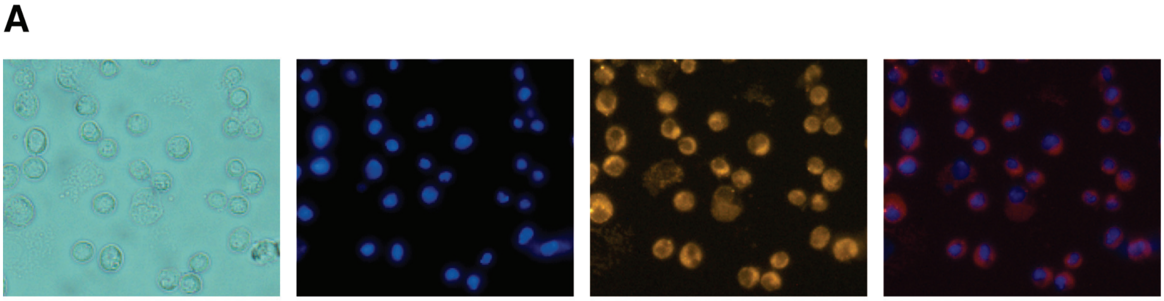

Nomarski DNA (Hoechst) p14 (Cy3) merge

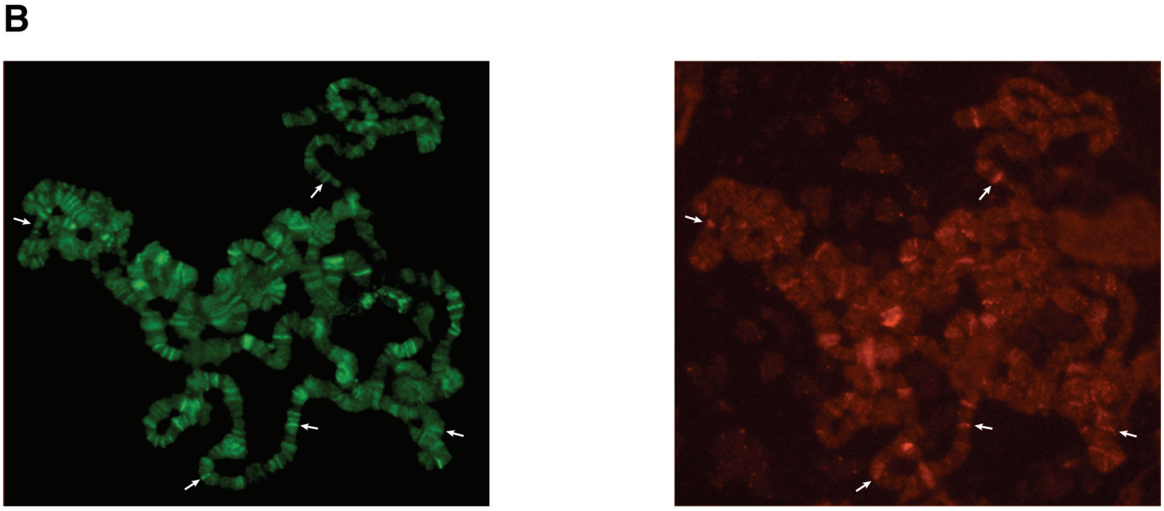

ISWI (Cy2) p16 (Cy3)

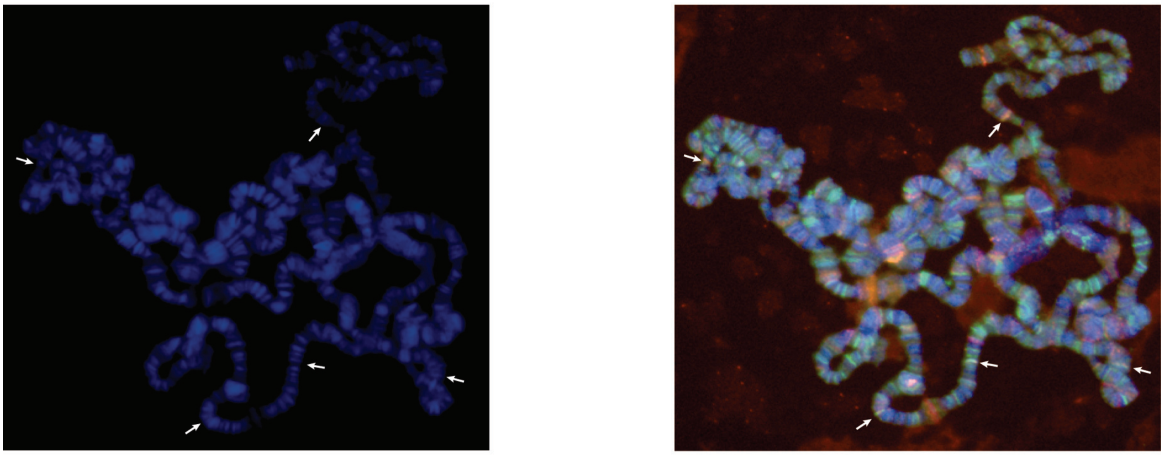

DNA (Hoechst) merge

Figure 4.8: A: Immunostaining of S2-cells with the α-p14 antibody 1H2. B: Co-immunostaining of polytene chromosomes with α-ISWI antibody (green) and the α-p16 antibody 6G6 (red). Some of the overlapping signals are marked with arrows.

4.2.3.2 *Drosophila embryos*

Also the immunostainings of *Drosophila* embryos with the monoclonal antibodies directed against p14 and p16 were hard to interpret. As already seen on polytene chromosomes, there was a high level of non-specific staining with most of the antibodies. Different developmental stages displayed different degrees of background staining, with a tendency of later stages (after cellularisation) being stained more intensively than earlier stages. In the early stages (until blastoderm), a shell at the embryo surface and the area surrounding the nuclei was stained particularly strong by the antibodies. Although the embryo surface staining is likely to be non-specific, it cannot be easily decided whether the staining around the nuclei contains a p14-p16-specific component.

Pre-incubation of the p16-specific antibody 6G6 with immobilised recombinant GSTp14-p16 suppresses the overall staining of the embryos (Figure 4.9, compare panels A and B). This can be seen in all developmental stages and suggests that the observed signal is indeed due to the 6G6 staining; however it does not necessarily mean that the staining is specific for p16. In fact, in some embryos, this antibody stains certain speckles that are clearly non-specific, since they co-localise neither with the ISWI staining nor the DNA staining (Figure 4.9 C). However, it cannot be ruled out that the antibody recognises p16 that is not associated with ISWI, but with another unknown factor. Whatever may be the case, it is very difficult to gain a credible p16 staining with the 6G6 antibody.

The only antibody that gave a definite signal was the anti-p14 antibody 5C7 (Figure 4.9 D). In very early developmental stages after only few nuclear divisions, it clearly stains the nuclei and co-localises with the ISWI staining. During mitosis, the antibody stains the centromeres (Figure 4.9 E), and the staining is very similar to the ACF1 staining on mitotic chromosomes (M. Chioda, unpublished observation). However, the signal intensity decreases with embryo age, whereas the intensity of the background staining increases, so that no distinct signal can be observed after the blastoderm stage. This suggests that CHRAC14-CHRAC16 are most abundant in the early developmental stages of the *Drosophila* embryo. Unfortunately, this monoclonal antibody recognises an additional band with a molecular weight of approximately 70 kDa on Western blots with embryo extracts (see Figure 4.5). Hence, although the signal co-localises with ISWI and shows a similar pattern than ACF1, it cannot be excluded that the immunostainings performed with this antibody do not solely reflect CHRAC14, but also another unknown protein.

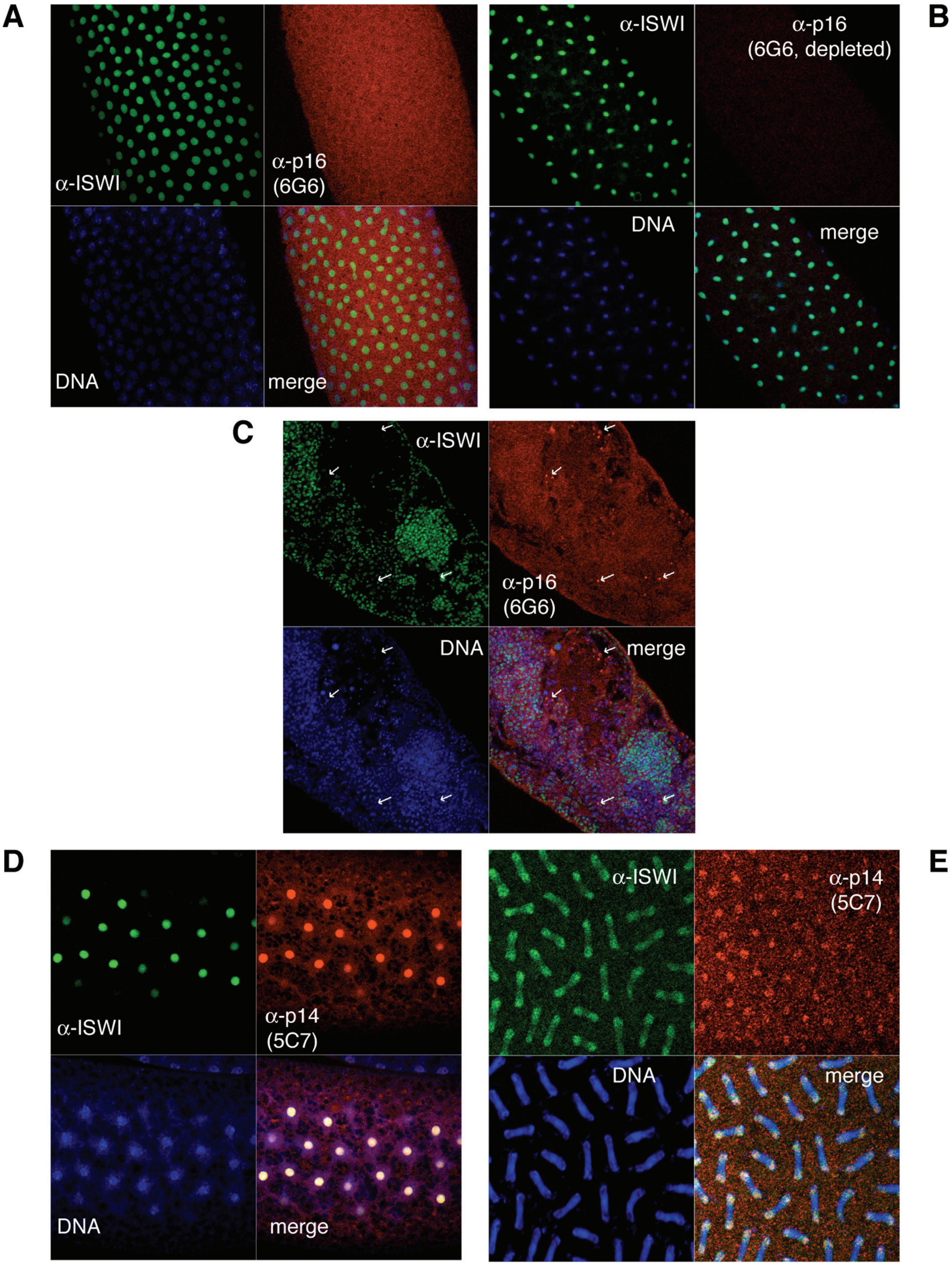
A
α-ISWI
α-p16
(6G6)
DNA
merge
B
α-ISWI
α-p16
(6G6, depleted)
DNA
merge
C
α-ISWI
α-p16
(6G6)
DNA
merge
D
α-ISWI
α-p14
(5C7)
DNA
merge
E
α-ISWI
α-p14
(5C7)
DNA
merge

Figure 4.9: Immunofluorescence on *Drosophila* embryos with the monoclonal antibodies directed against p14 and p16. The 6G6 antibody-staining (A) can be competed away by pre-incubation with recombinant p14-p16 (B), but gives non-specific signals in some embryos (C, see arrowheads). The signal 5C7 antibody signal co-localises with the ISWI-signal in early embryos (D) and stains the centromeres on mitotic chromosomes (E) (Panel E shows synchronous nuclear divisions during anaphase).

4.2.4 RT-PCR

For most applications, the monoclonal antibodies raised against CHRAC14 and CHRAC16 are not very reliable (see 4.2.1 to 4.2.3). Whereas the antibodies recognised CHRAC14 and CHRAC16 in *Drosophila* embryos, the detection in *Drosophila* cell lines was less successful (see 4.2.1 and 4.2.3.1). Therefore, the expression levels of the two small CHRAC subunits were checked by RT-PCR in KC and S2 cells. These cell lines are derived from *Drosophila* embryos, but possibly the expression pattern differs from the original embryonic tissues. It is imaginable that the expression of the small CHRAC subunits has been altered or downregulated.

Figure 4.10 shows the result of a typical RT-PCR reaction. Whereas there is a strong signal for both CHRAC14 and CHRAC16 from embryonic RNA (lanes 7 and 13), the signals from KC- cell RNA (lanes 9 and 15) and S2-cell RNA (lanes 11 and 17) are significantly weaker. The control RT-PCR with primers specific for the gene of the chromosomal kinase JIL-1 (lanes 1 to 6) indicates that this difference in mRNA levels is specific for the CHRAC14- and CHRAC16 subunits, because in the case of JIL-1, the difference in signal intensity between embryonic RNA and RNA from KC- and S2-cells is less pronounced (compare lanes 1, 3 and 5). The same result was obtained when primers specific for U6-RNA had been used for the control RT-PCR (not shown).

These experiments show that CHRAC14-CHRAC16 are expressed in KC and S2 cells, but – compared to *Drosophila* embryos – to a lesser extent. This could explain why it is difficult to detect the proteins in these cells with the weak monoclonal rat antibodies. The elevated mRNA levels in the embryos might not solely be due to higher expression, but also due to mRNA deposition by the mother (maternal contribution).

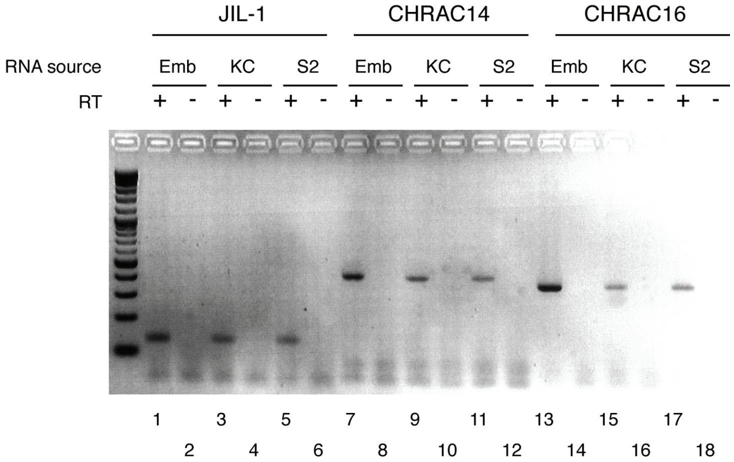

Figure 4.10: RT-PCR with primers specific for JIL-1 (lanes 1 to 6), CHRAC14 (lanes 7 to 12) and CHRAC16 (lanes 13 to 18). The CHRAC14 and CHRAC16 mRNA levels are significantly lower in KC- and S2 cells than in *Drosophila* embryos (compare lanes 9/11 with lane 7 and lanes 15/17 with lane 13).

4.3 Protein-protein interactions of CHRAC14-CHRAC16 with ACF1

4.3.1 Mapping of the interaction domain with ACF1

4.3.1.1 Co-expression studies in Sf9 cells

It has been reported previously that p14-p16 interact with ISWI in a GST pull-down assay (Corona *et al.*, 2000). However, this interaction appears to be stable only at salt concentrations lower than 50 mM and is almost completely abolished at salt concentrations higher than 100 mM (Corona *et al.*, 2000). However, p14-p16 remain stably associated with the Chromatin Accessibility Complex even at 1 M salt concentrations (A. Eberharter, unpublished observation), and hence it is unlikely that ISWI is the bona fide interaction partner of p14-p16 in CHRAC. Consequently, the interaction of p14-p16 with the ACF1 subunit was studied in several experiments.

Different myc-tagged ACF1 constructs (see Figure 4.11 A) were expressed in Sf9 cells together with p14-p16 heterodimer carrying a FLAG tag at the p14 C-terminus and a His_6-tag at the p16 N-terminus. A FLAG pull-down was performed under stringent conditions (500 mM KCl) from the Sf9 whole cell extract. The full length ACF1 construct (aa 1-1476) as well as a C-terminal ACF1 deletion construct (aa 1-1064) co-precipitated and were detected by Western blotting with anti-myc antibody (Figure 4.11 B, lanes 6 and 7). However, an N-terminal ACF1 deletion construct (aa 497-1476) failed to interact with CHRAC14-CHRAC16 in the FLAG pull-downs (Figure 4.11 B, lane 8), although it was expressed at higher levels than full length ACF1 and the C-terminal deletion construct (Figure 4.11 B, compare lane 4 with lanes 2 and 3). This finding suggests that CHRAC14-CHRAC16 bind to an N-terminal ACF1 site. Interestingly, the anti-myc antibody detected also several bands that were likely to be N-terminal degradation products in the input, but not in the pull-down fractions, which argues also for a N-terminal binding site.

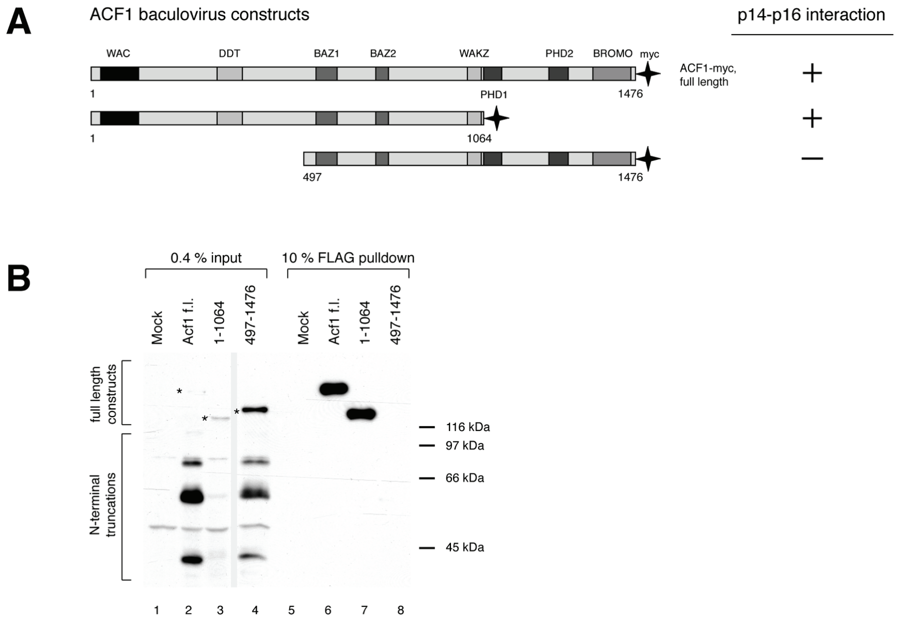
A
ACF1 baculovirus constructs
p14-p16 interaction
WAC
DDT
BAZ1
BAZ2
WAKZ
PHD2
BROMO
myc
PHD1
ACF1-myc, full length
1
1476
+
1
1064
+
497
1476
–
B
0.4 % input
10 % FLAG pulldown
Mock
Acf1 f.l.
1-1064
497-1476
Mock
Acf1 f.l.
1-1064
497-1476
full length constructs
N-terminal truncations
*
*
*
116 kDa
97 kDa
66 kDa
45 kDa
1
2
3
4
5
6
7
8

Figure 4.11: Co-immunoprecipitation of baculovirus-encoded ACF1 constructs with p14FLAG-His_6p16. A: myc-tagged ACF1 derivatives. Interaction with p14-p16 as determined in panel B is indicated to the right (+). B: Western blot of the FLAG affinity purification, probed with anti-myc antibody. In the mock-infection (lane 1), the cells were transfected with p14FLAG-His_6p16 alone. Bands corresponding to the ACF1 constructs in the input are marked with (*).

4.3.1.2 Interaction studies with in vitro*-translated ACF1 constructs*

A more precise mapping of the ACF1 interaction site with p14-p16 was performed with a series of *in vitro*-translated ACF1 derivatives (Figure 4.12 A). These proteins were tested for binding to immobilised GSTp14-p16 expressed in *E. coli*. Full length ACF1 and truncated versions of ACF1 that included the N-terminus were found to interact with GSTp14-p16 (Figure 4.12 B, lanes 1 to 3) whereas the ACF1 derivatives lacking the 201 N-terminal amino acids did not bind (Figure 4.12 B, lanes 4 to 8).

To ensure that the observed interactions were direct and not mediated by nucleic acids, the samples were DNase- and RNase-treated, which did not influence the results (Figure 4.12 C, lanes 4 and 5). Interestingly, GSTp14 alone does not interact with ACF1 (Figure 4.12 C, lanes 2 and 3), which reveals an important role of p16 in ACF1 binding (see also 4.3.2).

The ACF1 N-terminus contains a so-called WAC motif (WSTF, ACF1, cbp146), which has been found in several BAZ/WAL family proteins (Ito *et al.*, 1999; Xiao *et al.*, 2001), but its function is poorly understood. The data presented above imply that the WAC motif is part of a CHRAC14-CHRAC16 binding element. However, a construct consisting exclusively of the 201 N-terminal amino acids of ACF1 gave variable results in the GST pull-down assays, which was probably due to improper folding of the *in-vitro*-translated deletion construct. Therefore, it cannot be excluded that neighbouring sequences of the WAC motif, such as the DDT motif (Doerks *et al.*, 2001) are also involved in CHRAC14-CHRAC16 binding. However, it has been shown recently that the N-terminal 128 amino acids of human ACF1, which contain the WAC motif, are sufficient for the interaction with the human CHRAC14-CHRAC16 homologues hCHRAC17-hCHRAC15 (Kukimoto *et al.*, 2004).

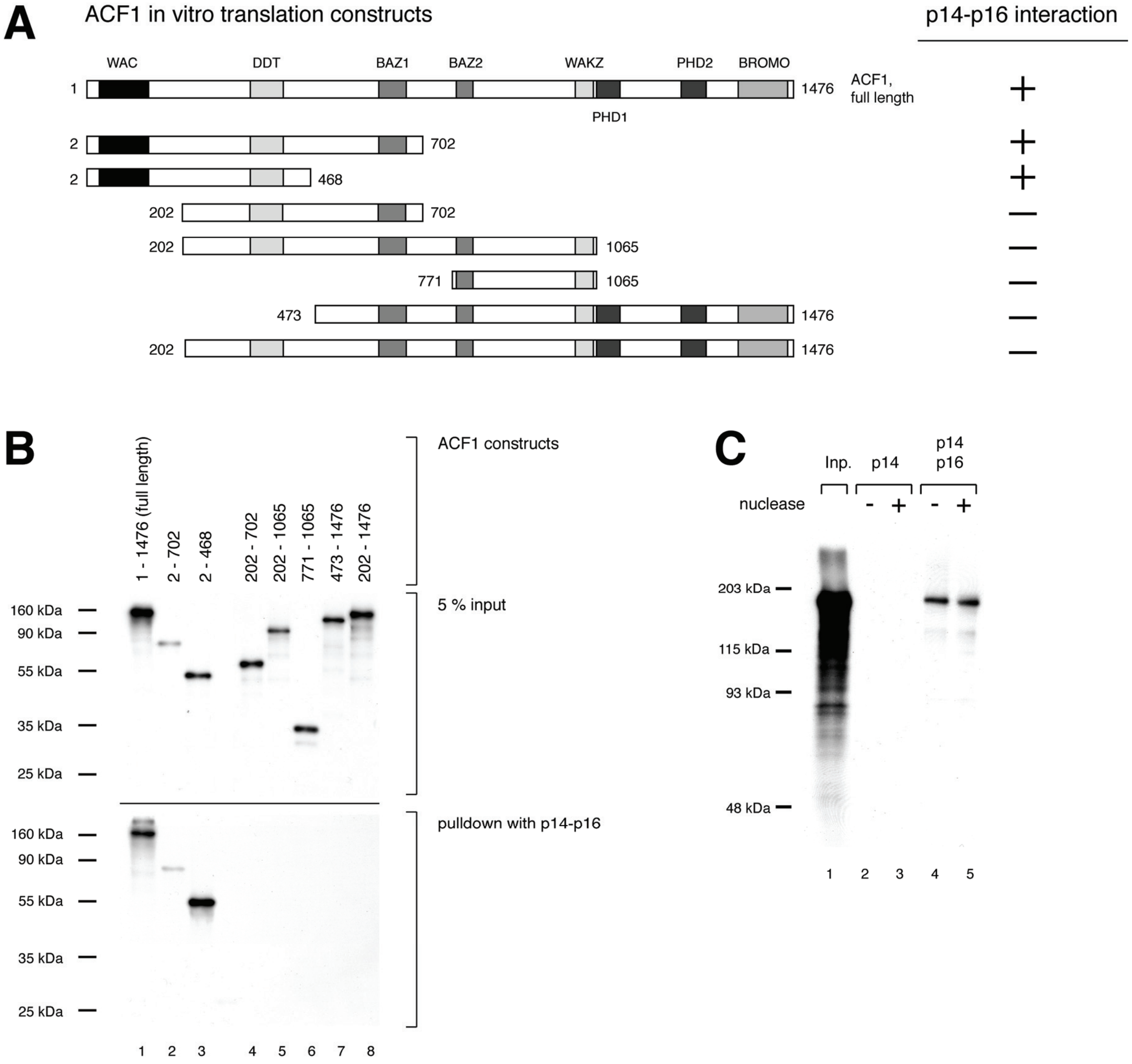
A
ACF1 in vitro translation constructs
p14-p16 interaction
WAC
DDT
BAZ1
BAZ2
WAKZ
PHD2
BROMO
PHD1
1
1476
ACF1, full length
+
2
702
+
2
468
+
202
702
—
202
1065
—
771
1065
—
473
1476
—
202
1476
—
B
1 - 1476 (full length)
2 - 702
2 - 468
202 - 702
202 - 1065
771 - 1065
473 - 1476
202 - 1476
ACF1 constructs
5 % input
pulldown with p14-p16
160 kDa
90 kDa
55 kDa
35 kDa
25 kDa
1 2 3 4 5 6 7 8
C
Inp.
p14
p14 p16
nuclease
- + - +
203 kDa
115 kDa
93 kDa
48 kDa
1 2 3 4 5

Figure 4.12: GST-pull-down of *in vitro*-translated ACF1-constructs. A: *in vitro*-translated ACF1 constructs. Interaction with p14-p16 as determined in panel B is indicated to the right (+) B: GST-pull-down. Top panel: 5% of input. Bottom panel: pull-down with recombinant GSTp14-His$_8$p16 heterodimer. C: ACF1 does not interact with GSTp14 alone, but only with the GSTp14-His$_8$p16 heterodimer in a nuclease-independent manner. *In vitro*-translated ACF1 was treated with DNase and RNase before incubation with glutathione beads loaded with either GSTp14 or GSTp14-His$_8$p16 . Degradation of nucleic acids upon nuclease treatment was monitored by agarose gel electrophoresis (not shown). The nuclease treatment of ACF1 does not have any influence on the interaction with GSTp14-p16 (lanes 4 and 5). Moreover, ACF1 interacts with p14-p16, but not with p14 alone (lanes 2 and 3).

4.3.2 Interaction of ACF1 with CHRAC14-CHRAC16 deletion variants

In another set of experiments, the CHRAC14-CHRAC16 N- and C-terminal deletion variants (see 4.1.1) were tested for interaction with *in-vitro*-translated ACF1 constructs (Figure 4.13). As expected, none of the CHRAC14-CHRAC16 variants interacted with ACF1 constructs lacking the N-terminal 201 amino acids (see also 4.3.1). The deletion of only seven amino acids at the CHRAC14 N-terminus led to a reduced binding of full length ACF1 and completely eliminated the binding of the construct containing amino acids 2 to 468 of ACF1. (Figure 4.13, lane 3).

These data suggest a role of the CHRAC14 N-terminus in ACF1 binding, but it is unlikely to be the only part involved in this interaction. In fact, CHRAC14 alone does not bind to ACF1 (Figure 4.12 C, lanes 2 and 3), which proposes that CHRAC16 residues participate in the interaction as well and suggests that the p14-p16 heterodimer is one functional entity.

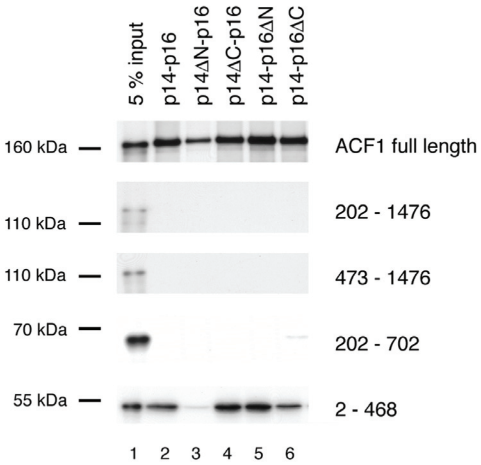

Figure 4.13: GST-pull-down of *in vitro* translated ACF1-constructs with p14-p16 deletion variants (see Figure 4.2 and Figure 4.12 A). Lane 1: 5% of input. The p14-p16 derivatives used for the pull-down are indicated above the lanes. The *in vitro*-translated ACF1 derivatives assayed for interaction are indicated to the right.

4.4 Composition and structure of the CHRAC14-CHRAC16 heterodimer

4.4.1 Sequence homology with different histone fold proteins

The central domains of CHRAC14 and CHRAC16 show striking sequence similarity with histone fold proteins of the histone H2A-H2B type. The highest similarity is observed between CHRAC14-CHRAC16 and the NFYB and NFYC subunits of the heterotrimeric transcription factor Nuclear Factor Y (NF-Y). This transcriptional activator binds to the CCAAT box of promoters (Maity and de Crombrugghe, 1998, see also 2.2.2.4). The histone fold domains of CHRAC14 and CHRAC16 share 32% and 27% identical residues with NFYB and NFYC, respectively, whereas they share only 9% and 15% identical amino acids with H2B and H2A. Figure 4.14 shows an alignment of the *Drosophila* CHRAC14 and CHRAC16 amino acid sequences with their direct homologues in human and mouse and with NFYB-NFYC and H2B-H2A, respectively. Although the sequences of the central domains of CHRAC14 and CHRAC16 clearly resemble typical histone folds, the N- and C-terminal extensions have no sequence similarity to other known histone-like proteins. In fact, with exception of the rather short N-terminus of CHRAC14, the two CHRAC subunits do not even show any sequence similarity with their direct homologues from other species within the N- and C-terminal tails (see Figure 4.14). Moreover, it seems that the acidic C-terminal tail of *Drosophila* CHRAC16 is exchanged between the two subunits in other species, so that the homologues of *Drosophila* CHRAC14 carry the more acidic C-terminal tail (Figure 4.14).

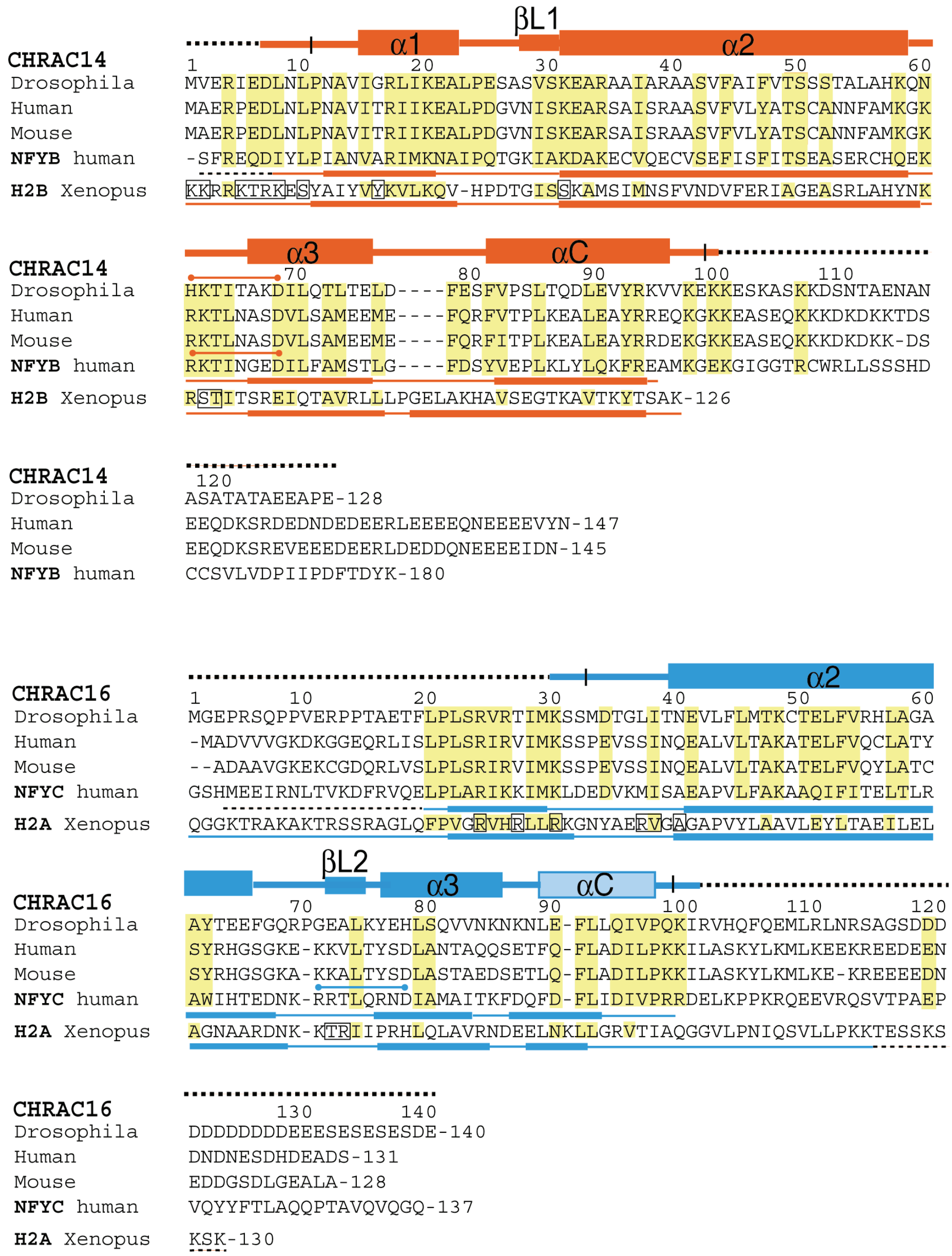
βL1
α1
α2
CHRAC14
1 10 20 30 40 50 60
Drosophila MVERIEDLNLPNAVIGRLIKEALPESASVSKEARAAIARAASVFAIFVTSSSTALAHKQN
Human MAERPEDLNLPNAVITRIIKEALPDGVNISKEARSAISRAASVFVLYATSCANNFAMKGK
Mouse MAERPEDLNLPNAVITRIIKEALPDGVNISKEARSAISRAASVFVLYATSCANNFAMKGK
NFYB human -SFREQDIYLPIANVARIMKNAIPQTGKIAKDAKECVQECVSEFISFITSEASERCHQEK
H2B Xenopus KKRRKTRKESYAIYVYKVLKQV-HPDTGISSKAMSIMNSFVNDVFERIAGEASRLAHYNK
α3
αC
CHRAC14
70 80 90 100 110
Drosophila HKTITAKDILQTLTELD----FESFVPSLTQDLEVYRKVVKEKKESKASKKDSNTAENAN
Human RKTLNASDVLSAMEEME----FQRFVTPLKEALEAYRREQKGKKEASEQKKKDKDKKTDS
Mouse RKTLNASDVLSAMEEME----FQRFITPLKEALEAYRRDEKGKKEASEQKKKDKDKK-DS
NFYB human RKTINGEDILFAMSTLG----FDSYVEPLKLYLQKFREAMKGEKGIGGTRCWRLLSSSHD
H2B Xenopus RSTITSREIQTAVRLLLPGELAKHAVSEGTKAVTKYTSAK-126
CHRAC14
120
Drosophila ASATATAEEAPE-128
Human EEQDKSRDEDNDEDEERLEEEEQNEEEEVYN-147
Mouse EEQDKSREVEEEDEERLDEDDQNEEEEIDN-145
NFYB human CCSVLVDPIIPDFTDYK-180
α2
CHRAC16
1 10 20 30 40 50 60
Drosophila MGEPRSQPPVERPPTAETFLPLSRVRTIMKSSMDTGLITNEVLFLMTKCTELFVRHLAGA
Human -MADVVVGKDKGGEQRLISLPLSRIRVIMKSSPEVSSINQEALVLTAKATELFVQCLATY
Mouse --ADAAVGKEKCGDQRLVSLPLSRIRVIMKSSPEVSSINQEALVLTAKATELFVQYLATC
NFYC human GSHMEEIRNLTVKDFRVQELPLARIKKIMKLDEDVKMISAEAPVLFAKAAQIFITELTLR
H2A Xenopus QGGKTRAKAKTRSSRAGLQFPVGRVHRLLRKGNYAERVGAGAPVYLAAVLEYLTAEILEL
βL2
α3
αC
CHRAC16
70 80 90 100 110 120
Drosophila AYTEEFGQRPGEALKYEHLSQVVNKNKNLE-FLLQIVPQKIRVHQFQEMLRLNRSAGSDDD
Human SYRHGSGKE-KKVLTYSDLANTAQQSETFQ-FLADILPKKILASKYLKMLKEEKREEDEEN
Mouse SYRHGSGKA-KKALTYSDLASTAEDSETLQ-FLADILPKKILASKYLKMLKE-KREEEEDN
NFYC human AWIHTEDNK-RRTLQRNDIAMAITKFDQFD-FLIDIVPRRDELKPPKRQEEVRQSVTPAEP
H2A Xenopus AGNAARDNK-KTRIIPRHLQLAVRNDEELNKLLGRVTIAQGGVLPNIQSVLLPKKTESSKS
CHRAC16
130 140
Drosophila DDDDDDDDEEESESESESDE-140
Human DNDNESDHDEADS-131
Mouse EDDGSDLGEALA-128
NFYC human VQYYFTLAQQPTAVQVQGQ-137
H2A Xenopus KSK-130

Figure 4.14: Alignment of *Drosophila* CHRAC14 and CHRAC16 with human and mouse homologues, NFYB and NFYC subunits of the human transcription factor NF-Y and *Xenopus* histones H2A and H2B. Conserved or conservatively substituted residues within the p14-p16 families and compared to NFYB-NFYC are highlighted in yellow. In addition, residues conserved or conservatively substituted in H2A-H2B compared to p14-p16 and NFYB-NFYC are also highlighted in yellow. Secondary structure elements in the p14 and p16 subunits were determined by manual inspection. The non-canonical p16 helix αC (see 4.4.2) is indicated in light blue. Secondary structure elements of NFYB-NFYC and H2A-H2B are depicted as published (Luger *et al.*, 1997; Romier *et al.*, 2003). Disordered regions present in the initial constructs are indicated by broken lines and are not included in the final structure (see 4.4.2). H2A-H2B residues forming hydrogen bonds with nucleosomal DNA are framed in black. Intra-chain salt bridges conserved between p14 and NFYB (red), but not between p16 and NFYC (blue) are indicated. The alignment was performed in collaboration with C. Müller and C. Fernández-Tornero, taken from (Hartlepp *et al.*, 2005).

4.4.2 Crystal structure of CHRAC14-CHRAC16

Crystals were obtained from one protein batch under several crystallisation conditions in collaboration with C. Müller and colleagues (EMBL Outstation, Grenoble) (see 3.2.14). However, due to unintentional proteolytic trimming during the protein preparation, a fragment of approximately 2.5 kDa was cleaved off the p16 subunit. Despite several attempts with different protein preparations, crystallisation could not be repeated with the full-length protein. Crystallisation yielded two crystal forms (Table 4.II). Initial attempts to solve the crystal structure by molecular replacement with the NFYB-NFYC crystal structure (Romier *et al.*, 2003) were unsuccessful. Instead, the structure of the p14-p16 heterodimer was solved in crystal form II by single isomorphous replacement using a methylmercuryacetate derivative (Table 4.II, C. Müller and C. Fernández-Tornero, EMBL Outstation, Grenoble). An initial model was built and refined in this crystal form at 2.8 Å resolution. Subsequently, this model was used for solving crystal form I by molecular replacement and for refinement of the structure at 2.4 Å resolution (see 3.2.15 and Figure 4.15).

The final model obtained in crystal form I contains p14 residues 7 to 98 (2nd molecule in the asymmetric unit: residues 11 to 99) and p16 residues 30 to 100 (2nd molecule in the asymmetric unit: residues 33 to 98), 39 water molecules and three sulphate ions. The heterodimer structure of crystal form II is very similar, although the ordered N- and C-terminal extensions are slightly shorter. Figure 4.15 shows the overall structure of the p14-p16 heterodimer. The two core domains of each protein adopt the predicted histone-like fold and interact with each other in the typical 'hand-shake' manner, packing head-to-tail against each other. The p14 core histone motif (helix α1 - loop L1 - helix α2 - loop L2 - helix α3) is extended by a long fourth helix αC, characteristic for the H2B family. Also p16 contains a C-terminal helical region following helix α3, similar to other H2A-related proteins. However, compared to canonical α- or 3_{10}-helices, the conformation of the p16 αC helix is rather irregular.

The predicted p16 helix α1 is missing in the crystal structure, which is most likely due to the partial proteolytic trimming during protein preparation (mentioned above). Presumably, this N-terminal cleavage of p16 causes the residues preceding helix α2 to adopt a conformation that is different from other histone fold proteins. In both crystal forms, two p14-p16 heterodimers related by a non-crystallographic dyad form a heterotetramer via the same, extensive interface of 3050 Å^2. To form this interface, the p16 helix α1 gets displaced from its canonical histone-fold-like position and instead, the p14 helix α2 of the neighbouring heterodimer is inserted into this groove. Presumably, this displacement occurred only under the experimental conditions used here, thus allowing crystallisation. Most likely, the N-terminal p16 helix α1 resides in its classical histone-fold position under physiological conditions. The fact that no crystals were obtained with the full length protein also argues for this hypothesis (discussed in 5.1.2).

Table 4.II: Data collection, structure solution and refinement of CHRAC14-CHRAC16. Done in collaboration with C. Müller and C. Fernández-Tornero and adapted from (Hartlepp *et al.*, 2005).

	Crystal form I	**Crystal form II**	
		native	Hg derivative
Data collection			
Space group	$P3_221$	$P42_12$	
Cell dimensions (Å)	$a = 76.0$, $c = 166.1$	$a = 130.5$, $c = 60.1$	$a = 130.5$, $c = 59.7$
Wavelength (Å)	0.9393	0.9795	0.9795
ESRF beamline	ID14-4	ID29	
Resolution (Å)[a]	24.0-2.4 (2.5-2.4)	30.0-2.8 (2.95-2.80)	35.0-3.0 (3.2-3.0)
Measurements[a]	130,593 (18,682)	186,423 (27,241)	142,145 (20,824)
Unique reflections[a]	22,490 (3,257)	13,325 (1,902)	10,828 (1,536)
Completeness (%)[a]	99.9 (99.9)	99.9 (99.9)	99.9 (99.9)
$I/\sigma(I)$[a]	4.4 (3.0)	5.6 (1.6)	5.3 (2.1)
R_{meas} (%)[a,b]	6.9 (26.4)	12.8 (47.5)	13.2 (36.8)
Structure determination			
Number of Hg sites (found/total)			2/2
R_{iso} (%)[c]			21.3
Z-score[d]			11.5
Figure of merit (before/after solvent flattening)			0.33/0.78
Refinement			
Resolution (Å)	20-2.4	30-2.8	
Total number of atoms	2519	2348	
Number of protein atoms	2465	2324	
Number of water molecules	39	21	
Bound ions	3 sulfate	3 Cd^{2+}	
R.m.s.d. from ideal geometry			
bond length (Å)	0.008	0.007	
bond angles (°)	1.261	1.193	
R_{cryst} (%)[e] (reflections)	23.7 (20214)	21.7 (11861)	
R_{free} (%)[f] (reflections)	27.8 (2231)	27.1 (1363)	

a) values in parentheses correspond to the highest resolution shell.

b) $R_{meas} = \Sigma_h (n_h/(n_h-1))^{1/2} \Sigma_h\Sigma_i |I_i(h)-<I(h)>| / \Sigma_h\Sigma_i I(h,i)$ with $<I(h)>$: mean of the I observations of reflection h, n: multiplicity of reflection h.

c) $R_{iso} = \Sigma\, |F_{PH} - F_P| / \Sigma\, F_P$, where F_{PH} and F_P are the derivative and native structure factor amplitudes, respectively.

d) calculated with program SOLVE (Terwilliger and Berendzen, 1999)

e) $R_{cryst} = \Sigma\, |F_o - F_c| / \Sigma\, F_o$, where F_o and F_c are the observed and calculated structure factor amplitudes, respectively.

f) R_{free} was calculated for crystal form I and II using 9.9% and 10.3% of the reflections, respectively.

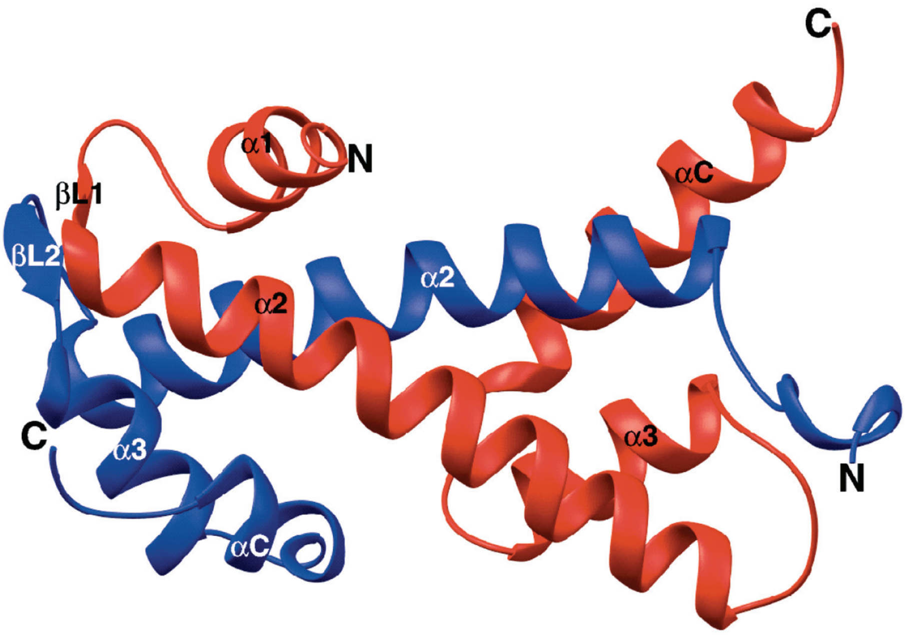

Figure 4.15: Ribbon representation of the p14-p16 heterodimer. CHRAC14 and CHRAC16 are depicted in red and blue, respectively. The figures 4.15, 4.16 and 4.18 were produced with programme Ribbons (Carson, 1991) by C. Müller and C. Fernández-Tornero and are taken from (Hartlepp *et al.*, 2005).

The CHRAC14-CHRAC16 overall structure closely resembles that of other histone-like protein pairs like the NFYB-NFYC heterodimer (Romier *et al.*, 2003) of the heterotrimeric transcription factor NF-Y (r.m.s.d.=1.68 Å, 143 C_α-atoms) and histone pairs H2A-H2B (Luger *et al.*, 1997) (r.m.s.d.=1.87 Å, 127 C_α-atoms). The main differences to the NFYB-NFYC and H2A-H2B heterodimers are in the C-terminal end of CHRAC16 helix α2 and in the conformation of the following loop L2 (Figure 4.16). Compared to NFYC, helix α2 of p16 is shorter by two residues, whereas loop L2 contains one additional residue. As a consequence, loop L2 adopts a different conformation and the CHRAC16 residues 72-74 are able to form a short two-stranded sheet with the βL1 residues 28-30 of CHRAC14. Additional differences between CHRAC14-CHRAC16 and H2A-H2B are a longer loop between helices α3 and αC in CHRAC14 compared to H2B and differently positioned helices α3 and αC in p16 compared to H2A. Hence, the histone fold core regions of CHRAC14-CHRAC16 are more similar to NFYB-NFYC than to H2A-H2B, which is also reflected by their primary sequence similarities (see 4.4.1). However, neither the CHRAC14-CHRAC16 structure nor the NFYB-NFYC structure contains the non-conserved N- and C-terminal extensions, since they are either disordered (CHRAC) or were essentially omitted from the crystallised constructs (NF-Y).

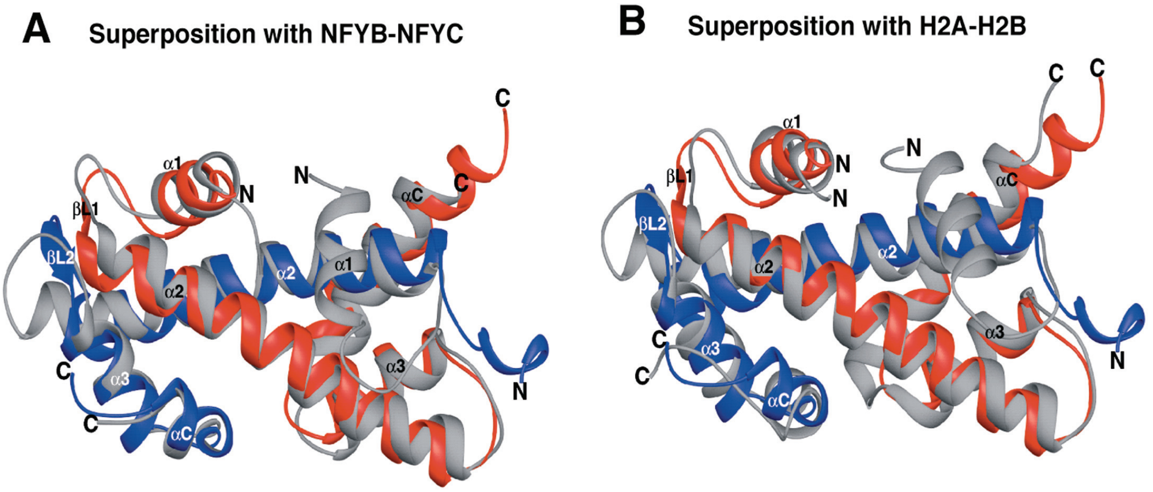

Figure 4.16: Comparison of the CHRAC p14-p16 heterodimer with other histone-like pairs. CHRAC14-CHRAC16 colour code as in Figure 4.15. A: Superposition of p14-p16 with NFYB-NFYC (grey). B: Superposition of p14-p16 with H2B-H2A (grey).

4.5 DNA-binding properties of CHRAC14-CHRAC16

4.5.1 Structural considerations

The electrostatic surface potentials of the p14-p16, NFYB-NFYC and H2A-H2B histone pairs were calculated by C. Müller and C. Fernández-Tornero and are given in Figure 4.17. The surface charge distribution of the p14-p16 dimer coincides well with the surface charge distributions of the other two heterodimers shown in Figure 4.17. In particular the H2A-H2B surface that faces the DNA shows a similar overall basic charge in p14-p16 and NFYB-NFYC (Figure 4.17), whereas the opposite surface is rather negatively charged (not shown). Binding of p14-p16 to DNA therefore probably involves a similar surface, so that it is feasible to model the CHRAC14-CHRAC16 heterodimer bound to DNA after the H2A-H2B-DNA complex (Figure 4.18, courtesy of C. Müller and C. Fernández-Tornero). However, the H2A-H2B side chains directly involved in DNA contacts are only poorly conserved in p14-p16 (Figure 4.14). This might be one of the reasons for the different DNA affinites of the two heterodimers (see also 4.5.2)

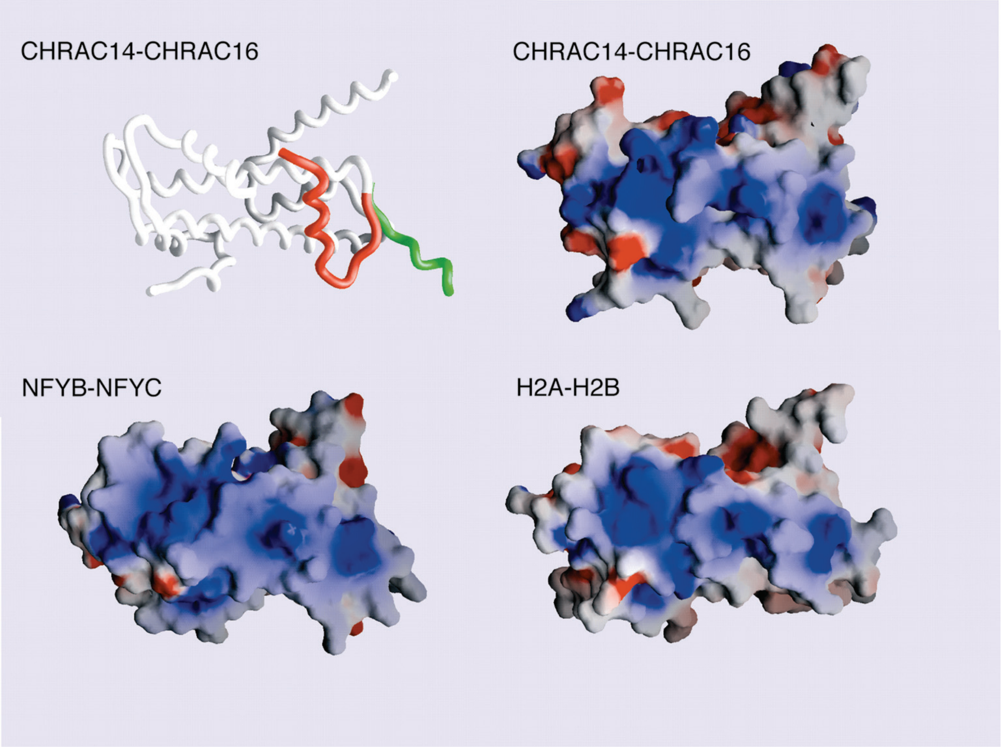

Figure 4.17: Surface charge distribution of p14-p16 compared to NFYB-NFYC and H2A-H2B heterodimers calculated with GRASP (Nicholls *et al.*, 1993). Negative and positive potentials ($\pm 15\ k_B T$ (k_B, Boltzmann constant; T, temperature)) are depicted in red and blue, respectively. The orientation of the three protein pairs is identical and corresponds to that shown for the p14-p16 worm model. Helix α1 of CHRAC16 was modelled onto NFYC and is depicted in red (compare also Figure 4.18). The figure was created by C. Müller and C. Fernández-Tornero and is taken from (Hartlepp *et al.*, 2005)

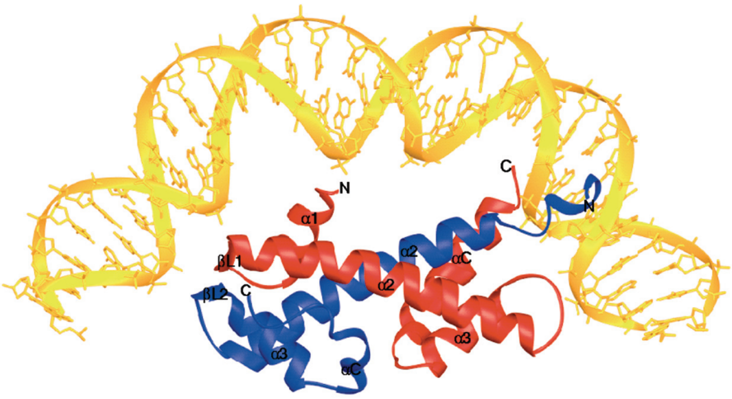

Figure 4.18: Model of DNA bound to a CHRAC14-CHRAC16 heterodimer. For this representation CHRAC14-CHRAC16 was superimposed onto histones H2A-H2B in the nucleosome (Luger *et al.*, 1997). The depicted DNA corresponds to the nucleosomal DNA contacted by histones H2A-H2B. Compared to Figure 4.17, the heterodimer was rotated by 90º around a horizontal axis.

4.5.2 Influence of the CHRAC14-CHRAC16 C-terminal tails on DNA binding

Histones bind to DNA tightly and independently of the DNA sequence. In contrast, hCHRAC17-hCHRAC15, the human counterparts of CHRAC14-CHRAC16, bind to DNA with weak affinity and do not bind to mononucleosomes *in vitro* (Poot *et al.*, 2000). Here, the DNA binding properties of *Drosophila* CHRAC14-CHRAC16 have been studied in detail.

Electrophoretic mobility shift assays (EMSA) with a radiolabelled 248 bp rDNA fragment (Längst *et al.*, 1999) revealed that also CHRAC14-CHRAC16 bind to DNA weakly and non-specifically (Figure 4.19). The full length heterodimer shifts the DNA only at relatively high concentrations (Figure 4.19 A, lanes 2-6): A bandshift is observed at an approximately 300-fold molar excess of protein heterodimer over DNA.

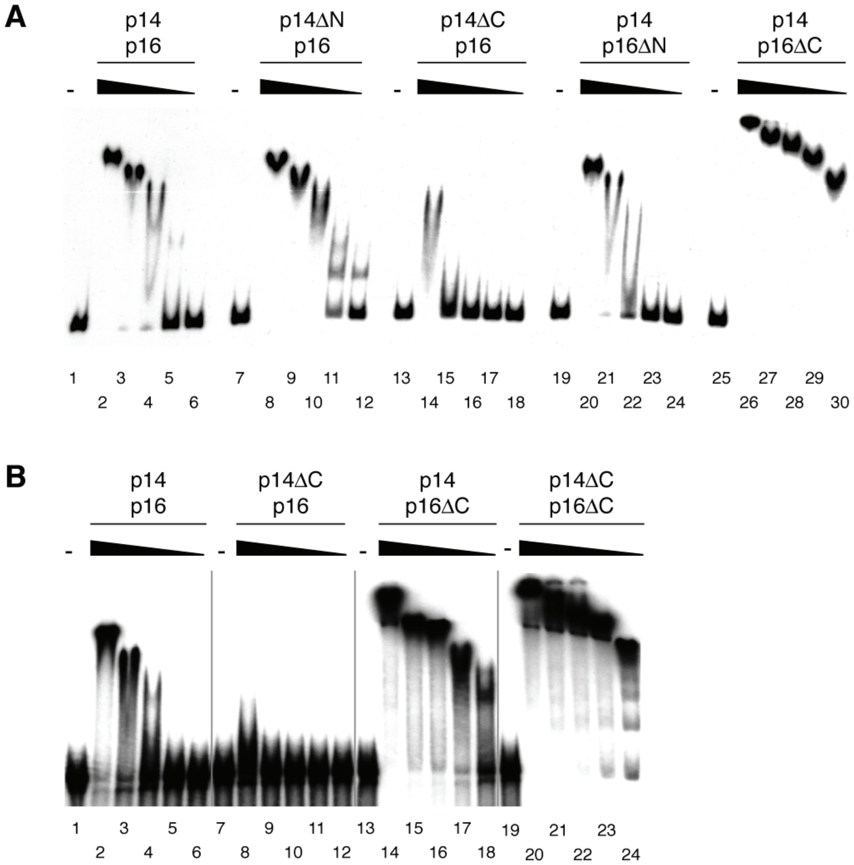
A
p14 p16
p14ΔN p16
p14ΔC p16
p14 p16ΔN
p14 p16ΔC
-
1 2 3 4 5 6 7 8 9 10 11 12 13 14 15 16 17 18 19 20 21 22 23 24 25 26 27 28 29 30
B
p14 p16
p14ΔC p16
p14 p16ΔC
p14ΔC p16ΔC
1 2 3 4 5 6 7 8 9 10 11 12 13 14 15 16 17 18 19 20 21 22 23 24

Figure 4.19: EMSA with wt p14-p16 and p14-p16 deletion mutants. 6 nM of radiolabelled 248 bp DNA were incubated with the respective p14-p16 derivatives (20, 5, 2, 0.5 and 0.2 µM) before complexes were resolved on a native polyacrylamide gel. A: The C-terminal deletions of p14 and p16 have opposite effects on DNA binding, whereas N-terminal deletions show no effect. B: The p14ΔC-p16ΔC double deletion variant has the same DNA binding properties as the p14-p16ΔC deletion variant.

The influence of the C- and N-terminal tails of p14 and p16 on DNA binding has also been tested by EMSA (Figure 4.19). Deletion of the N-terminal tails of either p14 (Figure 4.19 A, lanes 8-12) or p16 (Figure 4.19 A, lanes 20-24) has no influence on the DNA binding of the p14-p16 heterodimer. However, DNA binding is diminished by a C-terminal tail deletion of CHRAC14 (Figure 4.19 A, lanes 14-18). This argues either for a direct involvement of the p14 C-terminal tail in DNA binding or for an indirect contribution, e.g. through a structural stabilisation of the p14-p16 DNA binding surface.

In contrast, the deletion of the C-terminal tail of CHRAC16 leads to a strong increase in DNA binding (Figure 4.19 A, lanes 26-30). The affinity to DNA is increased at least by a factor of 25 to 30. The p16 C-terminal tail is extremely acidic, consisting of a stretch of 23 glutamates, aspartates and serines. Deletion of this tail causes a dramatic shift in the protein's theoretical pI from 4.47 to 9.30. This suggests that the negatively charged tail interferes with the negatively charged DNA and prevents a tight DNA binding of the p14-p16 dimer, either by repulsion or by folding back onto the DNA binding surface and thereby masking it. Possibly, both effects contribute (discussed in 5.2.1, see Figure 5.1).

To learn more about the nature of p14-p16 DNA binding, the double deletion variant p14ΔC-p16ΔC was also tested in EMSAs (Figure 4.19 B). The DNA binding affinities of the double deletion variant and the p14-p16ΔC variant were comparable. This result indicates that the negative effect of the p16 C-terminal tail on DNA binding is dominant over the positive effect of the p14 C-terminal tail. Since the N-terminal tails of p14 and p16 do not seem to play any role in DNA binding (see above), this suggests that the histone fold core of the CHRAC14-CHRAC16 dimer binds to DNA reasonably well and that the DNA binding properties of the core are modulated by the C-terminal extensions of both CHRAC14 and CHRAC16.

4.5.3 Dependence of the CHRAC14-CHRAC16-DNA interaction on DNA fragment length

CHRAC14-CHRAC16 bind to DNA in a non-specific manner. As a consequence, more than one heterodimer can bind to the same DNA double helix if the fragment is long enough. This binding behaviour results in indistinct, blurred bands in EMSAs, especially if the DNA binding is not very strong and the protein-DNA complex dissociates during gel electrophoresis. Indeed, this can be observed in Figure 4.19.

Therefore, the dependence of p14-p16 DNA binding on DNA fragment length was tested in a DNA pull-down assay. For this analysis, full length p14-p16 and p14-p16ΔC were immobilised on sepharose beads and incubated with a radiolabelled 10 base pair DNA ladder. Bead-bound DNA and DNA in the supernatant was separated by denaturing gel-electrophoresis and quantified (see 3.2.19, Figure 4.20 A). The data for the full length heterodimer were hard to interpret, because the portion of DNA that remained bound to the beads was below 3% for each fragment within the analysed range of DNA fragments between 10 and 100 bp (Figure 4.20 B).

However, both the full length and the p14-p16ΔC heterodimer bound only traces of the ten base pair DNA fragment (Figure 4.20 A lanes 11 to 14 and Figure 4.20 B, C). These results suggest that the minimal DNA fragment length required for p14-p16 binding is more than ten base pairs. This is consistent with the model of CHRAC14-CHRAC16 DNA binding derived from the nucleosome structure (Figure 4.18). According to this model, approximately 30 DNA base pairs span the surface of the p14-p16 histone fold core.

For the p14-p16ΔC deletion variant, the amount of interacting DNA increased in the range between 30 and 70 base pairs, until it reached a plateau and no further increase was observed (Figure 4.20 C). However, the supernatant was depleted to a great extent of DNA fragments larger than 70 base pairs in these experiments (see Figure 4.20 A lanes 7/8 and Figure 4.20 C), and therefore it is likely that the interaction with DNA still increases with DNA length for fragments larger than 70 base pairs.

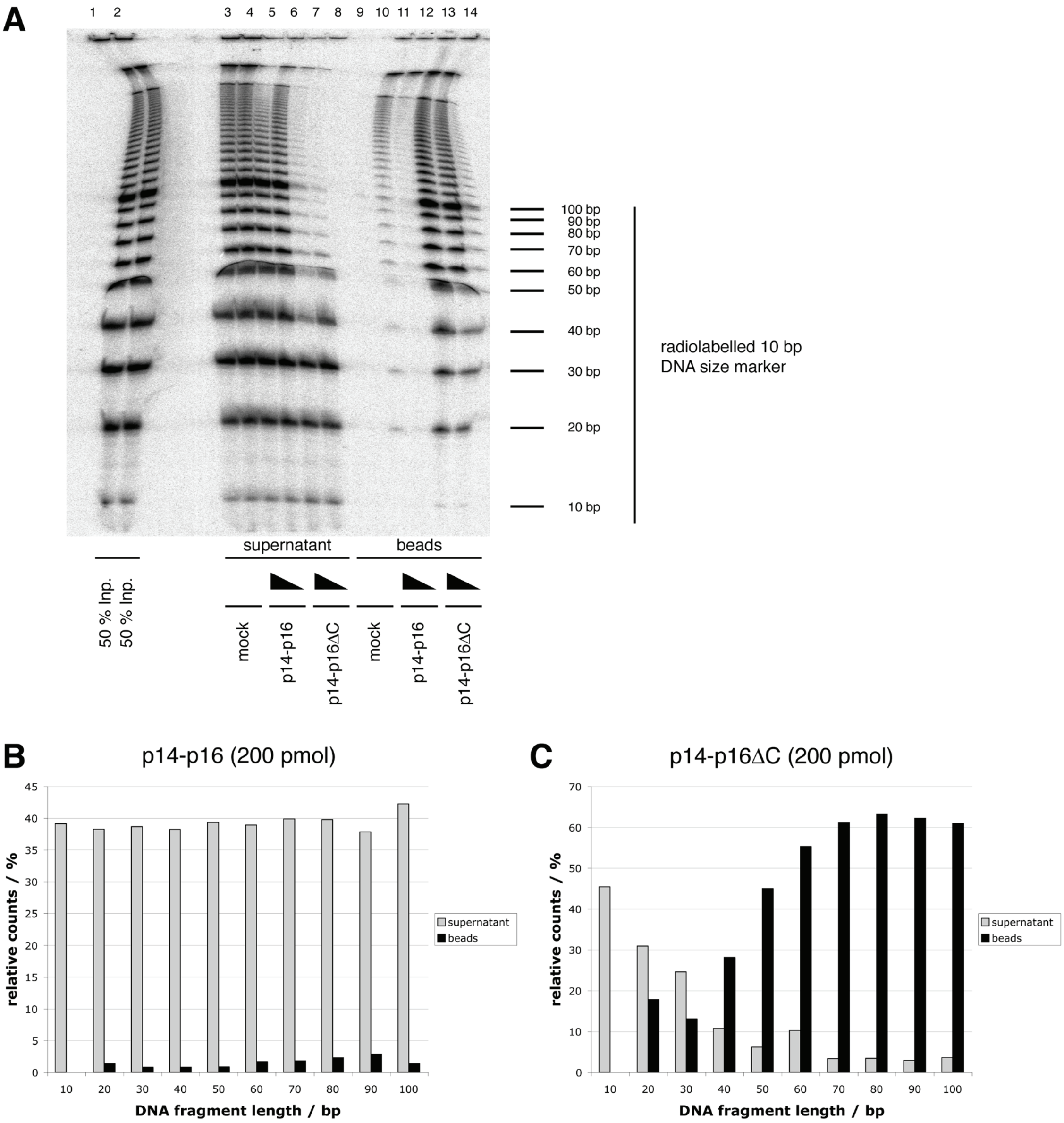

Figure 4.20: Determination of the length-dependence of p14-p16 DNA binding. A: Autoradiography of a DNA pull-down assay. Input (lanes 1 and 2), supernatant (lanes 3 to 8) and beads (lanes 9 to 14) are analysed on a 8 % denaturing gel. Mock: TALON beads only (10 µL, lanes 3/4 and 9/10). Total amount of protein on TALON beads: 200 pmol (lanes 5/11 and 7/13, respectively) and 100 pmol (lanes 6/12 and 8/14, respectively). B: Quantification of DNA pull-down with 200 pmol p14-p16. Unbound fraction: supernatant, lane 5 in panel A; bound fraction: beads, lane 11 in panel A. C: Quantification of DNA pull-down with 200 pmol p14-p16ΔC. Unbound fraction: supernatant, lane 7 in panel A; bound fraction: beads, lane 13 in panel A.

The electrophoretic mobility shift assay shown in Figure 4.21 argues for such a scenario. Full length CHRAC14-CHRAC16 does not shift the 35 base pair DNA fragment (lanes 2-6), and the 72 base pair fragment (lanes 8-12) is shifted only at relatively high protein concentrations (>4 µM), whereas the 248 base pair fragment (lanes 14-18) is shifted already at lower protein concentrations of 1 µM. The same trend can be seen for the CHRAC14-CHRAC16ΔC heterodimer, although the overall DNA binding of this deletion variant is increased and it shifts already the 35 base pair DNA fragment (lanes 20 to 24).

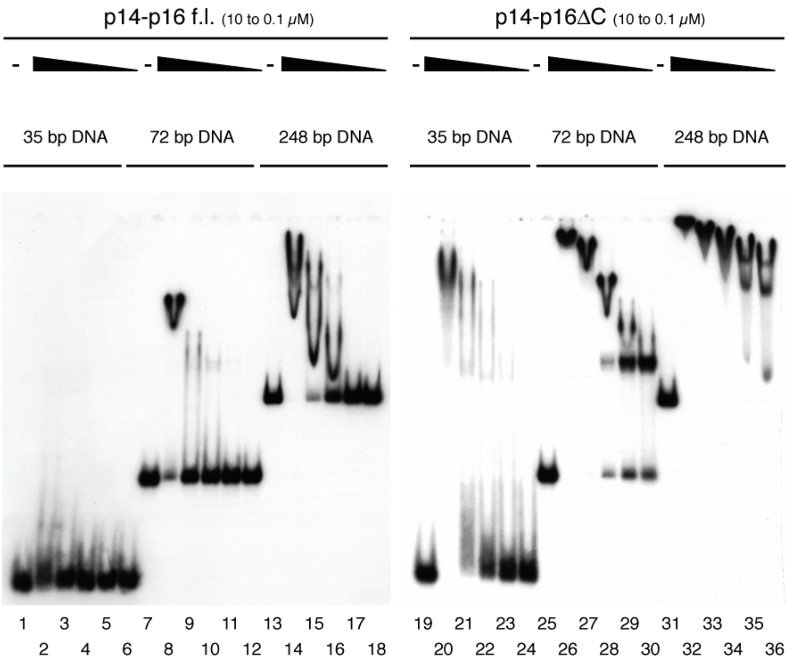

Figure 4.21: DNA-binding of p14-p16 is dependent on DNA length. EMSA of 0.5 nM radiolabelled (end-labelled) DNA with fragment sizes of 35 bp, 72 bp and 248 bp, respectively. Protein concentrations used were 10, 4, 1, 0.4 and 0.1 μM for both full length p14-p16 and p14-p16ΔC. Full length p14-p16 is unable to shift the 35 bp DNA fragment under the assay conditions (lanes 2 to 6). Bandshifts with distinct shifted species are only observed with 72 bp DNA (lanes 9/10 and 28 to 30, respectively).

The strength of protein-DNA interactions is often given as a dissociation constant (K_D). The K_D can be determined by the Langmuir model if the interaction can be described as a simple 1:1 complex formation. The binding of more than one protein (or protein complex) to the same DNA fragment or allosteric effects are not taken into consideration by the Langmuir model.

Hence, it is not trivial to determine an accurate K_D value for p14-p16 DNA binding. However, for short DNA fragments it can be assumed that there is only one p14-p16 binding site per DNA fragment and therefore it is feasible to make use of the Langmuir model and determine an approximate K_D value. As the full length CHRAC14-CHRAC16 heterodimer did not bind to 35 base pair DNA in the electrophoretic mobility shift assay (Figure 4.21), the K_D values for both the full length heterodimer and the p14-p16ΔC heterodimer were determined for the 72 base pair DNA fragment in four independent experiments like the one shown in Figure 4.22 A. The DNA binding could be approximated by a hyperbolic Langmuir curve (Figure 4.22 B, C). The K_D value for full length CHRAC14-CHRAC16 was 2.3 μM, reflecting its weak DNA affinity, and the K_D value for CHRAC14-CHRAC16ΔC was 57 nM. This means that the deletion variant binds about 40 times stronger to DNA than the full length heterodimer.

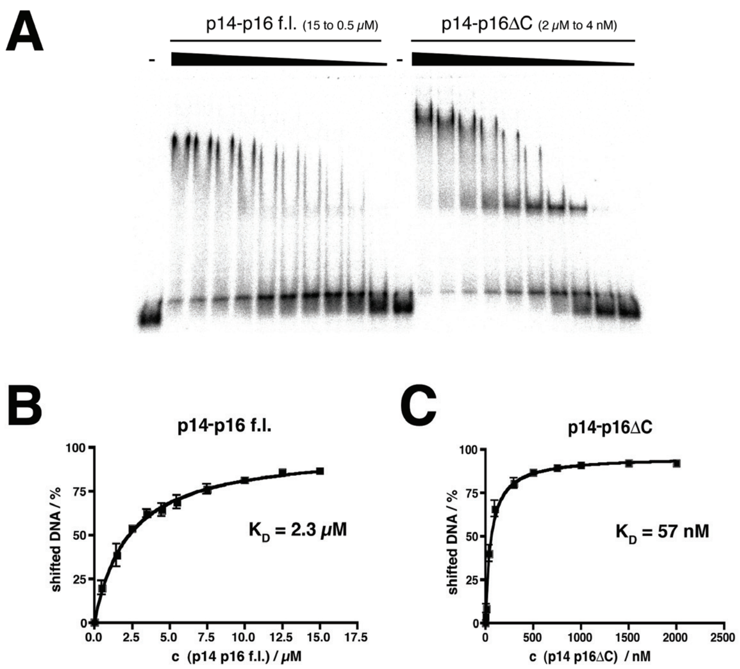

Figure 4.22: A: EMSA with fine titrations of full length p14-p16 and p14-p16ΔC to 0.5 nM radiolabelled 72 bp DNA for determination of their DNA binding constants. Protein concentrations were 15, 12.5, 10, 7.5, 5.5, 4.5, 3.5, 2.5, 1.5 and 0.5 µM for the full length heterodimer and 2, 1.5, 1, 0.75, 0.5, 0.3, 0.1, 0.04, 0.01 and 0.004 µM for the heterodimer with the C-terminal deletion of p16.
B: Quantification of the electrophoretic mobility shifts caused by full length p14-p16 and determination of the approximate DNA binding constant. In four independent experiments such as the one shown in panel A, the percentage of unshifted DNA was determined using AIDA software (Raytest). The non-linear curve fit was performed with the programme Prism (GraphPad).
C: Quantification of the electrophoretic mobility shifts caused by p14-p16ΔC and determination of the approximate DNA binding constant. The data analysis was performed as described for panel B.

4.5.4 Interaction with four-way junction DNA

Some proteins such as HMGB1 or ISWI have been shown to bind perferentially to four-way junction DNA, which resembles a stable Holliday junction. This cruciform DNA is widely used as a model for structured or distorted DNA (Bianchi *et al.*, 1989; Grüne *et al.*, 2003). The binding of p14-p16 to four way junction DNA was compared to the binding to a linear 72 base pair DNA fragment that had approximately the same size as the cruciform DNA (74 base pairs). Neither the full length p14-p16 heterodimer nor the p14-p16ΔC deletion variant had a higher affinity for four way junction DNA than for the linear 72 base pair control DNA fragment (Figure 4.23).

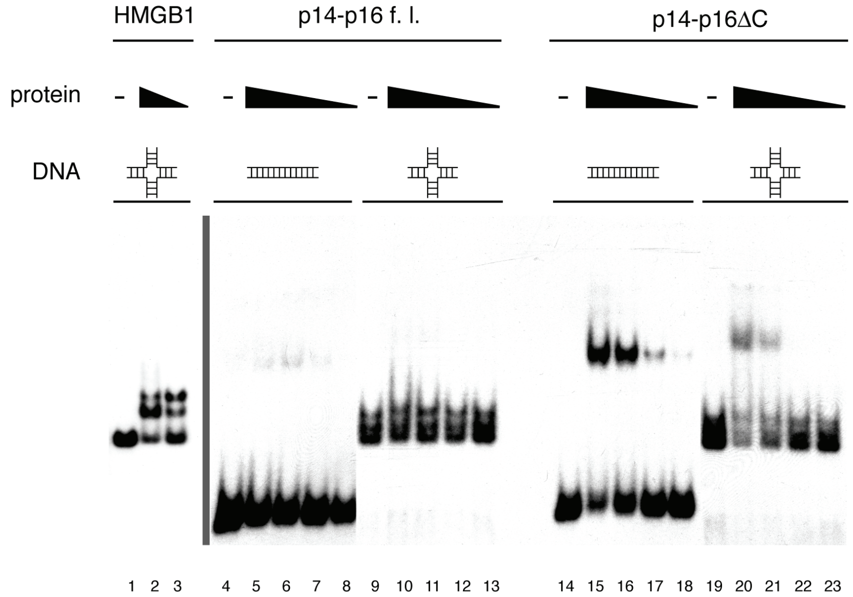

Figure 4.23: EMSA with four-way junction-DNA (cruciform symbol) and linear DNA (72 bp). 0.5 nM radiolabelled DNA was incubated with HMGB1 (0.25 and 0,1 µM, lanes 2, 3), with p14-p16 (5, 2, 0.5 and 0.2 µM, lanes 5-8 and 10-13, respectively), and with p14-p16ΔC (0.25, 0.1, 0.025 and 0.01 µM, lanes 15-18 and 20-23, respectively). Neither p14-p16 nor p14-p16ΔC bind better to four-way junction DNA than to linear DNA.

4.6 Influence of CHRAC14-CHRAC16 on ACF-driven nucleosome mobilisation

4.6.1 Enhancement of the ACF-mediated nucleosome sliding activity by CHRAC14-CHRAC16

Chromatin remodelling factors such as ACF/CHRAC and their ATPase subunit ISWI are able to move mononucleosomes along a DNA fragment without disruption of the histone octamer (Eberharter *et al.*, 2001; Längst *et al.*, 1999).

Mononucleosomes that are situated at the end of a DNA fragment have a different electrophoretic mobility than mononucleosomes at the centre of the DNA fragment. Therefore, a movement of the histone octamer along the DNA can be monitored by the altered migration behaviour of the nucleosome in native gel electrophoresis. The nucleosome sliding assay takes advantage of this effect. In an ATP-dependent reaction, ISWI catalyses the movement of a mononucleosome from the centre-position towards the end of the DNA fragment. In contrast, ACF/CHRAC move the mononucleosome in the opposite direction, i. e. from the end of the DNA fragment towards the centre. Besides, the nucleosome mobilisation by ACF is by an order of magnitude more efficient than ISWI-mediated nucleosome mobilisation (Eberharter *et al.*, 2001); see also 2.4.5.1).

The effect of the two small CHRAC subunits on nucleosome sliding was examined by titrating increasing amounts of recombinant, *E. coli*-expressed p14-p16 heterodimer into ACF-catalysed sliding reactions (Figure 4.24). At high ACF concentrations, i.e. at maximal nucleosome mobilisation levels, no effect of p14-p16 could be observed (Figure 4.24, lanes 3 to 6). At limiting ACF concentrations however, p14-p16 significantly stimulated the nucleosome repositioning (Figure 4.24, lanes 17 to 20 and lanes 23 to 26). This observation was dependent on the presence of ATP (Figure 4.24, lanes 8 to 14), and p14-p16 had no effect on mononucleosome mobility in the absence of ACF (Figure 4.24, lanes 7 and 14). This argues against a simple change in nucleosome mobility upon p14-p16 binding, but rather for a true stimulation of ACF remodelling. Since p14-p16 do not influence the ATPase activity of ACF *in vitro* (see Figure 4.27), the heterodimer stimulates the efficiency of ACF-mediated nucleosome mobilisation by another unknown mechanism.

However, the sliding enhancement was only observed at high p14-p16 concentrations. The excess of the heterodimer over the ACF complex present in the mobilisation reactions ranged from 3,300- to 270,000-fold. Despite several attempts with different protein preparations, the ratio between ACF and the small subunits stayed essentially the same. One possible explanation for that observation could be improper folding of the p14-p16 heterodimer when it is produced recombinantly in *E. coli* and not in its physiological context (see also 5.2.2).

Similar stimulatory effects of the human homologues hCHRAC17-hCHRAC15 on human ACF have been reported by Varga-Weisz and colleagues (Kukimoto *et al.*, 2004).

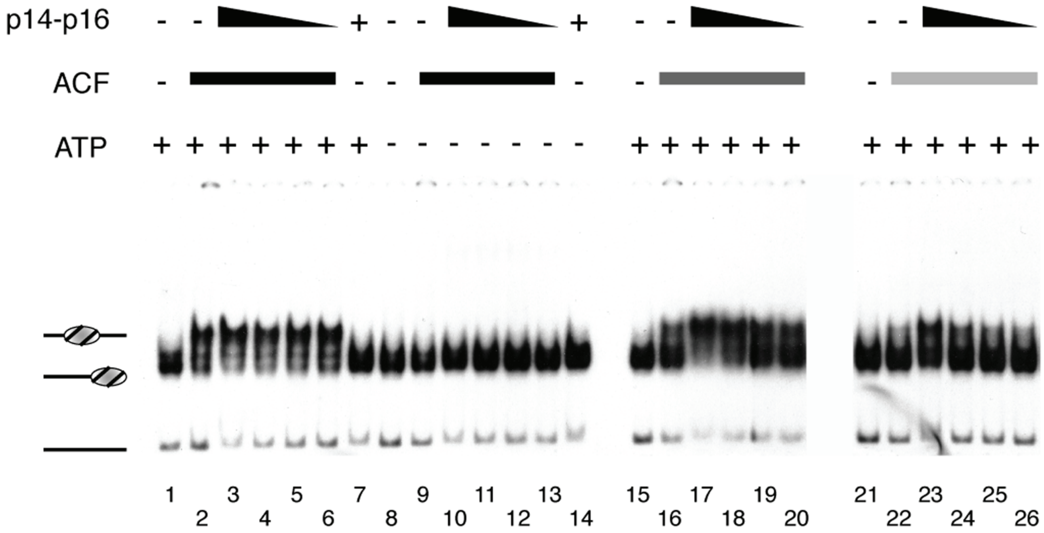

Figure 4.24: p14-p16 enhance ACF-catalyzed nucleosome sliding. Radiolabelled end-positioned nucleosomes (6 nM) were incubated with ACF (approximately 0.3, 0.09 and 0.03 nM, decreasing shading of bar). To the reactions, decreasing amounts of p14-p16 (8, 4, 2, 1 μM) were added. With high ACF concentrations (0.3 nM), sliding is maximal and no further enhancement due to p14-p16 is seen (lanes 2-6). With lower ACF concentrations (0.09 and 0.03 nM, lanes 16-20 and 22-26, respectively), an enhancement of nucleosome sliding can be observed in the presence of p14-p16. Nucleosomes do not slide in the absence of ATP (lanes 9-13), and p14-p16 alone do not affect the migration of the nucleosomes (lane 7 and 14).

4.6.2 Dependence of the nucleosome sliding enhancement on the ACF1 WAC motif

Since the CHRAC14-CHRAC16 interaction with the remaining CHRAC subunits has been mapped to the N-terminus of the large subunit ACF1 (see 4.3.1), an ACFΔWAC complex with an ACF1 subunit lacking the amino acids 4 to 111 was reconstituted and its nucleosome sliding activity was tested in the presence of CHRAC14-CHRAC16 (Figure 4.25 A, B). The protein concentrations and ATPase activities of wild type ACF and ACFΔWAC had been matched carefully. In the absence of p14-p16, the two complexes showed the same remodelling activity. In the presence of p14-p16, however, the nucleosome sliding activity of the ACFΔWAC complex was enhanced only very weakly. This result suggests that the direct interaction between ACF1 and p14-p16 is required for the nucleosome sliding enhancement.

The effects of the human homologues hCHRAC17-hCHRAC15 have also been shown to be dependent on the WAC motif of human ACF1 (Kukimoto *et al.*, 2004).

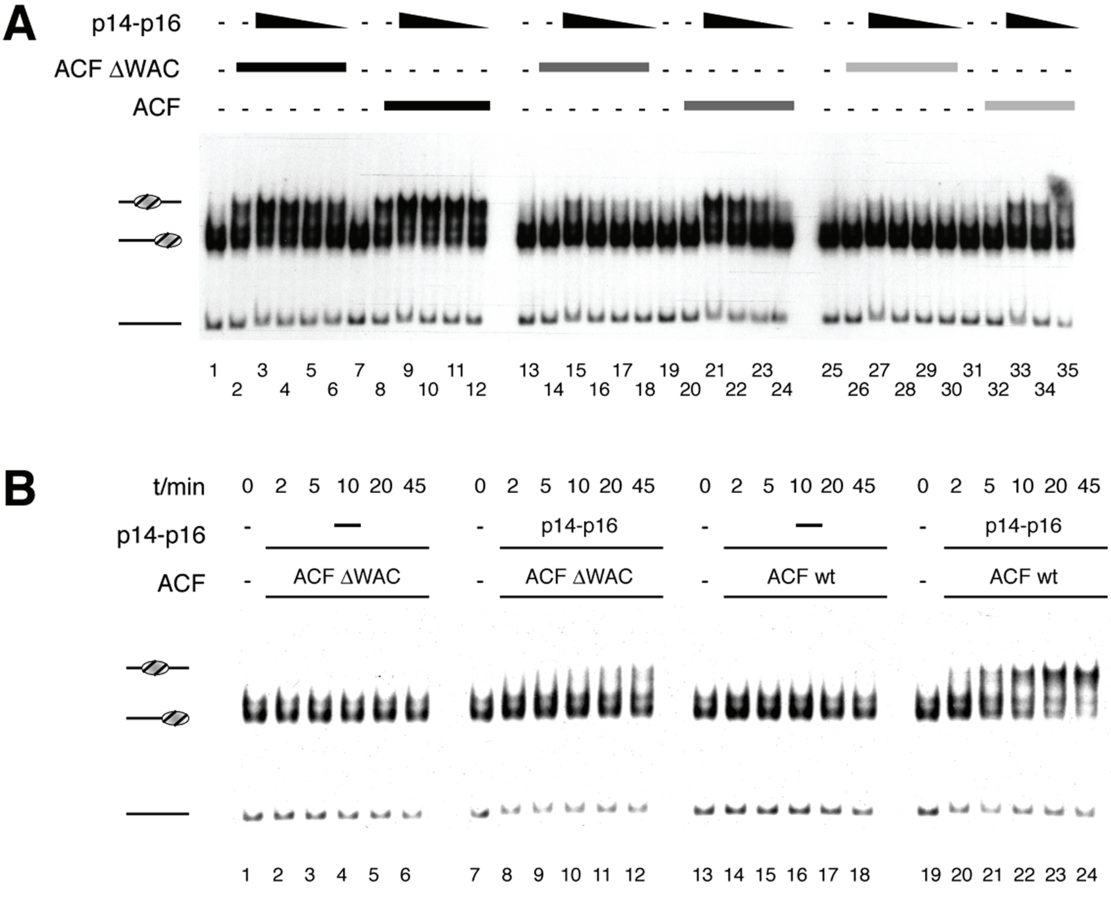
A
p14-p16
ACF ΔWAC
ACF
1 2 3 4 5 6 7 8 9 10 11 12 13 14 15 16 17 18 19 20 21 22 23 24 25 26 27 28 29 30 31 32 33 34 35
B
t/min
0 2 5 10 20 45
p14-p16
ACF
ACF ΔWAC
ACF wt
1 2 3 4 5 6 7 8 9 10 11 12 13 14 15 16 17 18 19 20 21 22 23 24

Figure 4.25: The p14-p16 sliding enhancement requires the ACF1 WAC domain.
A: Protein titrations. Nucleosome sliding is catalyzed by ACF or ACFΔWAC (0.3, 0.075 and 0.0375 nM, respectively, decreasing shading of bar) in the presence of decreasing amounts of p14-p16 (8, 4, 2, 1 µM) as indicated.
B: Time course. Reactions are performed with concentrations of ACF and ACFΔWAC complex (approx. 0.18 nM), which do not suffice to slide nucleosomes in the absence or presence of p14-p16 (approx. 8 µM). Time points are taken after 0, 2, 5, 10, 20 and 45 minutes.

4.6.3 Behaviour of C- and N-terminal deletion mutants of CHRAC14 and CHRAC16 in nucleosome mobilisation

The role of the N- and C-terminal tails of CHRAC14 and CHRAC16 in ACF-mediated nucleosome remodelling has been tested as well in this study. CHRAC14-CHRAC16 deletion variants were titrated into nucleosome sliding reactions with low (Figure 4.26 A, B) and with high ACF concentrations (Figure 4.26 C). It turned out that the N-terminal deletions of both p14 and p16 did not show any effect on the nucleosome remodelling activity (Figure 4.26 A, B and C, compare lanes 9 to 12 and 21 to 24 with lanes 3 to 6), although the p14ΔN-p16 heterodimer has a slightly reduced ACF1 binding affinity in GST pull-down assays (see 4.3.2).

The p14ΔC-p16 deletion variant, which hardly binds to DNA (see 4.5.2), was not able to stimulate nucleosome mobilisation (Figure 4.26 A, B, lanes 15 to 18). This finding suggests that the ability of the p14-p16 heterodimer to bind DNA is crucial for its nucleosome sliding enhancement, although the affinity for DNA is rather weak.

Due to its increased DNA binding (see 4.5.2to 4.5.4), the p14-p16ΔC deletion variant could not be analysed accurately in the nucleosome sliding assay under the standard conditions. The tight binding of the heterodimer caused the mononucleosomes to shift, so that the results were hard to interpret and not reproducible. Consistent results were only obtained when the p14-p16ΔC concentration was lowered and the ACF concentration was raised at the same time, so that the histone fold heterodimer did not shift the nucleosomes anymore and the ACF complex mobilised the nucleosomes to the maximal extent already in the absence of p14-p16 (Figure 4.26 C).

Although the concentrations of the full length p14-p16 heterodimer and of the other deletion variants were kept at their original levels (four times higher than the p14-16ΔC concentrations), none of them showed an effect on the sliding reaction at these high ACF concentrations (Figure 4.26 C). However, the p14-p16ΔC deletion variant inhibited nucleosome mobilisation under these conditions (Figure 4.26 C, lanes 27 to 30). This result suggests that CHRAC activity is blocked by too tight DNA binding of the p14-p16 heterodimer, whereas the ATPase activity of ACF is not affected (Figure 4.27). Hence, the acidic p16 C-terminal tail seems to allow a weak, but vital DNA binding of the p14-p16 dimer and thereby prevents sliding inhibition.

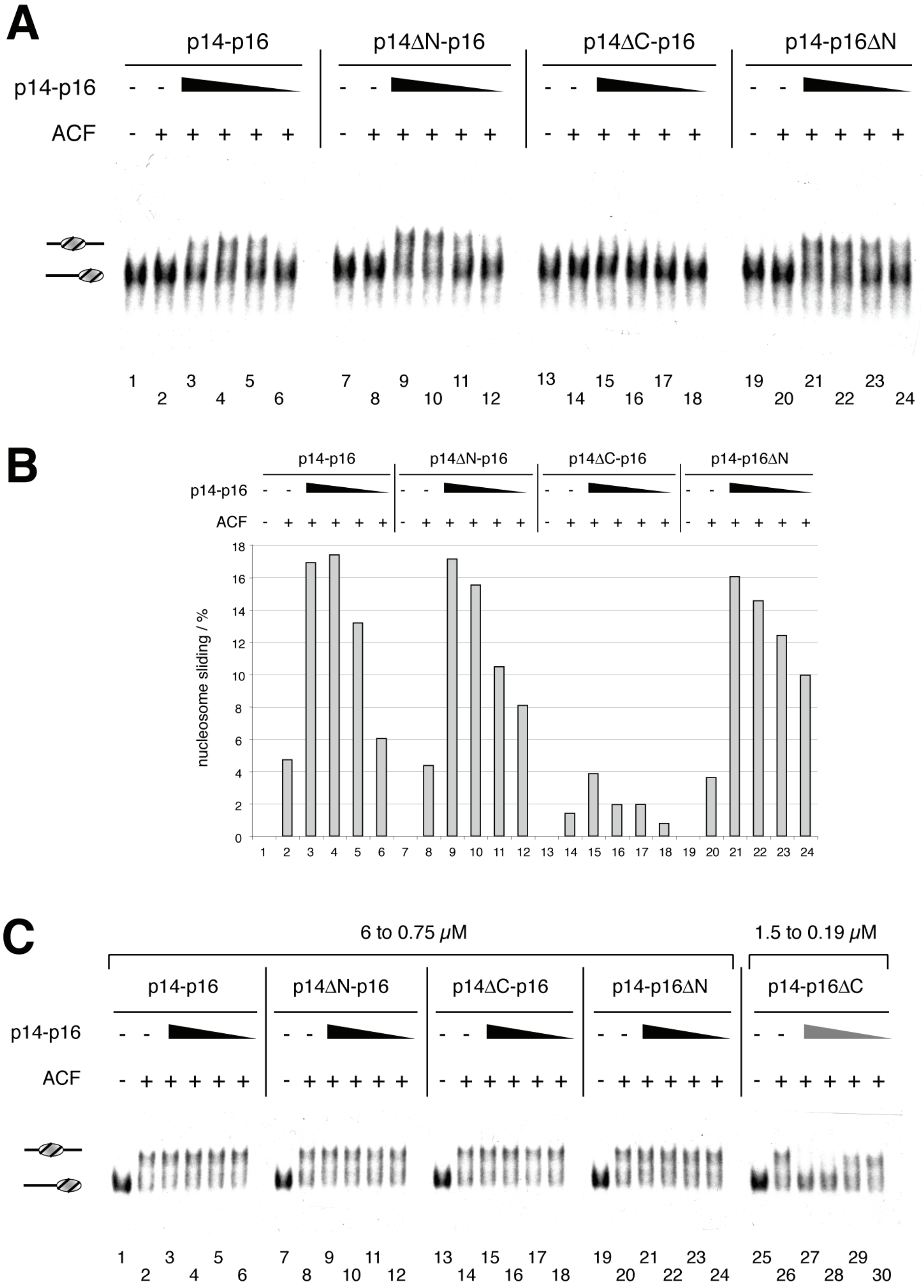

Figure 4.26: Effect of p14-p16 tails on nucleosome sliding

A: Deletion of the p14 C-terminus leads to loss of sliding enhancement. Sliding reactions contained 6 nM of end-positioned nucleosome, 37.5 pM ACF and 8, 4, 2 and 1 µM of intact p14-p16 (lanes 3-6), or p14ΔN-p16 (lanes 9-12), or p14ΔC-p16 (lanes 15-18) or p14-p16ΔN (lanes 21-24).

B: Quantification of nucleosome sliding. The percentage of nucleosomes that had been moved from the end- to the center-position was determined using a phosphoimager (Fuji). The graph shows the average sliding of two independent experiments.

C: Deletion of the p16 C-terminus inhibits of ACF-catalyzed nucleosome sliding. Sliding reactions contained 6 nM of end-positioned nucleosome, 0.3 nM ACF and different p14-p16 derivatives (6, 3, 1.5 and 0.75 µM) with exception of p14-p16ΔC, for which 1.5, 0.75, 0.375 and 0.1875 µM were used (lanes 26 – 30).

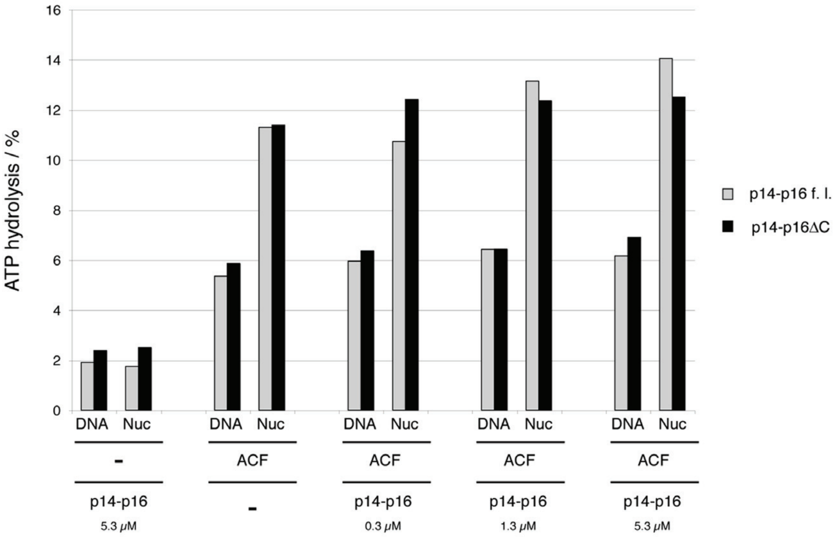

Figure 4.27: The ATPase activity of ACF (0.2 nM) is not influenced by the presence of various amounts of full length p14-p16 or p14-p16ΔC. The quantification of a typical ATPase assay is shown. Stimulation of the ACF ATPase activity is achieved either by free DNA or by the same amount of chromatinized DNA (Nuc). Concentrations of p14-p16 protein added to the ATPase assay are indicated.

5 Discussion

5.1 How do CHRAC14 and CHRAC16 interact?

5.1.1 Conclusions based on co-expression in *E. coli*

The histone fold motif is an exclusive feature of archeal and eukaryotic proteomes and does not exist in bacterial proteins (Pereira and Reeve, 1998). Overexpression of recombinant histones or histone fold proteins in bacteria can cause difficulties. The core histones can be expressed in *E. coli* as insoluble aggregates, which can be refolded (Luger *et al.*, 1999), but the production of several other histone fold proteins, such as histone fold TAFs in bacteria, results in poor expression levels or expression followed by rapid protein degradation (Fribourg *et al.*, 2001). However, the simultaneous expression of two interacting proteins leads to soluble and stable complexes in many cases, even if the complex components cannot be expressed individually. This co-expression strategy is not only restricted to histone fold proteins, but works also with other dimerisation domains and has been proven to be a useful tool for mapping interaction domains and for crystallisation of protein complexes (Baumli *et al.*, 2005; Fribourg *et al.*, 2001).

The CHRAC subunit p14 can be expressed recombinantly in the absence of p16 in a partially soluble form. In the light of the co-expression studies mentioned above, this leads to speculations about the formation of p14-homodimers. Histone fold homodimers with physiological relevance have been described in archea (Grayling *et al.*, 1996; Sandman *et al.*, 1994), and it is also known that the orthologues of p14 in yeast and human interact with more than one histone fold partner (Iida and Araki, 2004; Li *et al.*, 2000, see also 5.3.2.2). In the context of CHRAC, however, the potential existence of a p14 homodimer is probably irrelevant, because p14 does not interact with ACF1 in the absence of p16 (see Figure 4.12 C). Nevertheless, the p14 N-terminus appears to be involved in binding of the p14-p16 heterodimer to ACF1 (see Figure 4.13), suggesting that both p14 and p16 contribute to the interaction with ACF1.

In contrast to p14, the p16 subunit cannot be expressed alone in bacteria and even appears to have toxic effects. Expression is only accomplished when both proteins are produced simultaneously. The use of a bicistronic expression plasmid guaranteed identical transcript levels for the two polypeptides. This new strategy improved the expression levels and solubility of both proteins significantly, but still, an equimolar ratio could not be achieved. The excess of p14 over p16 might be caused by the toxicity of p16 for the bacteria. Likewise, p16 translation might be reduced due to a lowered frequency of translation initiation from the internal ribosomal entry site of the bicistronic mRNA. Only the establishment of a purification scheme with a different affinity tag on each subunit allowed the purification of a stoichiometric p14-p16 complex (see 3.2.3.1).

The crystal structure of CHRAC14-CHRAC16 (see 4.4.2 and 5.1.2) confirmed the interaction of the two proteins through their histone fold domains, which had been postulated for a long time (Corona *et al.*, 2000; Poot *et al.*, 2000). According to the observations made with p14 and p16 deletion variants, sequences outside the histone fold region might also contribute to the stability of the heterodimer. Several C-terminal tail deletion mutants of both p14 and p16 could not be expressed at all or were insoluble or unstable, even though the full-length interaction partner was co-expressed (see 4.1.1 and Figure 4.2). Therefore, regions adjacent to the αC helices (see Figures 4.2 and 4.14) are possibly involved in the proper formation of the p14-p16 heterodimer.

5.1.2 Heterodimer formation by CHRAC14-CHRAC16

In both crystal forms of CHRAC14-CHRAC16, the proteins formed a tetramer through dimerisation of two heterodimers, which were related by a non-crystallographic dyad axis. However, the tetramerisation seems to be an artefact of the crystallisation process and probably caused by partial proteolytic removal of the p16 N-terminus (see 4.4.2). Several reasons argue for the existence of CHRAC14-CHRAC16 dimers instead of tetramers in solution:

In analytical ultracentrifugation studies, purified recombinant CHRAC14-CHRAC16 behave as a heterodimer, but not as a tetramer (N. Mücke, J. Langowski, unpublished data). Furthermore, the CHRAC16 residues preceding the long helix α2 of the histone fold are highly conserved within the CHRAC16 orthologues, but also other histone fold proteins like H2A and NFYC, whose crystal structure has been solved (Luger *et al.*, 1997; Romier *et al.*, 2003, see also Figure 4.16). It is therefore unlikely that these residues adopt a different conformation in CHRAC16, meaning that helix α1 of the CHRAC16 histone fold prevents the tetramerisation observed in the crystal structure. Besides, the residues in question can even be modelled into the typical histone fold position without causing any steric clashes, when the structure of the NFYC helix α1 is used as a guideline (C. Fernández-Tornero, C. Müller, see Figure 4.17). Finally, secondary structure predictions of CHRAC16 strongly argue for an α-helical structure of residues 22-30 (Rost, 1996; Rost and Sander, 1994), which is also supported by the fact that the last ordered N-terminal residues in the crystal structure adopt a helical conformation (Figure 4.15).

In principle, the interaction with other partners could cause a displacement of the CHRAC16 helix α1, and further analysis is required to evaluate whether this hypothesis is biologically relevant or not. However, the conformation of the CHRAC16 N-terminus in the crystal structure is most likely caused by the fortuitous partial proteolysis.

A similar 'partial histone fold' has been described for the hTAF4-hTAF12 heterodimer. In this crystal structure, helix α3 of hTAF4 is missing, but this helix might just be separated from the rest of the histone fold by a remarkably long loop region of about 100 residues (Werten *et al.*, 2002).

5.2 How do the histone fold subunits function within CHRAC?

5.2.1 Functional similarities of histone-fold CHRAC subunits to other histone-like proteins and HMGB1

The chromosomal protein HMGB1 (see 2.3.4) has been shown to facilitate chromatin remodelling through transient interactions with nucleosomal linker DNA (Bonaldi *et al.*, 2002). Interestingly, HMGB1 shares some striking functional similarities with the CHRAC p14-p16 subunits. HMGB1 and p14-p16 bind to DNA only weakly and without sequence preference, and both enhance the nucleosome sliding activity of ACF *in vitro*. Furthermore, HMGB1 and CHRAC16 have an acidic C-terminal tail, and in both cases, deletion of this tail leads to a strong increase in DNA binding affinity. Besides, without the charged C-termini, ACF-mediated nucleosome sliding is not activated but inhibited, suggesting that the tight interactions with DNA lock the nucleosome positions in a way similar to the binding of linker histones (Hill and Imbalzano, 2000; Horn *et al.*, 2002; Pennings *et al.*, 1994).

It has been speculated that HMGB1 serves as a 'DNA chaperone' that is able to assist chromatin remodelling factors through distortion of the linker DNA (Bonaldi *et al.*, 2002). Likewise, CHRAC could bring along p14-p16 as its own built-in DNA chaperone, which might function in a fashion similar to HMGB1 and provide an alternative, temporary DNA binding surface (see 5.2.3).

Several HMG box-containing proteins are either subunits of SWI/SNF-type remodelling factors or have been shown to interact with subunits of remodelling complexes, which demonstrates their important role for chromatin remodelling *in vivo*. In yeast, the HMGB1-related transcription factor Nhp6p interacts both physically and functionally with the actin-related protein (ARP) subunits of SWI/SNF and RSC, and its binding to nucleosomes is facilitated by RSC (Szerlong *et al.*, 2003). *Drosophila* BAP111 and Polybromo and their mammalian homologues BAF57 and BAF180 are HMG box-containing subunits of the *Drosophila* BAP/PBAP and mammalian BAF/PBAF complexes, respectively (Mohrmann *et al.*, 2004; Papoulas *et al.*, 2001; Wang *et al.*, 1998), see Table 2.I). Important functions have been assigned to some of these subunits. For instance, transheterozygotes for *BAP111* and *brahma* (*brm*, the gene encoding for the SWI/SNF-type ATPase subunit) show an enhanced *brm* phenotype (Papoulas *et al.*, 2001), and mutations within the HMG domain of BAF57 impair the regulation of BAF target genes (Chi *et al.*, 2002). The HMG box-containing subunits of SWI/SNF-type remodelling complexes have been proposed to facilitate alterations in chromatin architecture by their ability to distort DNA (see 2.3.4). The CHRAC histone fold subunits might function in a similar way (discussed below). Therefore, the SWI/SNF class and the ISWI class of remodelling factors might have chosen different types of proteins – HMG box and histone fold proteins – to carry out similar tasks during chromatin remodelling.

Recent structural and biochemical data suggest that the so-called SWIRM domain is yet another sequence motif that might play a role in chromatin remodelling similar to HMG box proteins and CHRAC histone fold units. The SWIRM domain is found in the subunits Swi3, Rsc8 and Moira of SWI/SNF-type remodelling complexes, as well as in several other proteins associated with chromosomal regulation. It has been described previously as a putative protein-protein interaction domain (Mohrmann and Verrijzer, 2005). The recent NMR structure of the Ada2α SWIRM domain reveals a structural similarity to winged helix DNA-binding motifs as found in E2F4 and the linker histones H1 and H5 (Qian *et al.*, 2005). Indeed, the SWIRM motif was shown to bind to free DNA and nucleosomal linker DNA with moderate affinity, and moreover, it is able to facilitate ACF-mediated chromatin remodelling *in vitro* (Qian *et al.*, 2005). These findings suggest that SWIRM domain-containing proteins might assist ATP-dependent chromatin remodelling factors in a way similar to HMG box proteins and CHRAC histone fold subunits. Strikingly, SWI/SNF-type remodelling complexes contain both HMG box subunits and subunits containing SWIRM domains (Mohrmann and Verrijzer, 2005). Hence, variants of three different structural motifs – the HMG box, the histone fold and the winged helix DNA binding motif – could have co-evolved independently to fulfil similar functions in these proteins.

The C-terminal tail of CHRAC16 prevents strong DNA binding through its negative charge, which interferes with the negatively charged phosphate groups of the DNA backbone. Likewise, the flexible C-terminal domain of p16 might fold back onto the histone fold domain of the p14-p16 heterodimer, which offers a predominantly positive surface charge (Figure

4.17), so that its potential DNA binding surface would be covered by the negatively charged tail (Figure 5.1 B). This hypothesis is supported by the observation that the flexible acidic tail of HMGB1 binds to HMG box A within the same molecule, thereby masking one of the two HMG boxes in an intramolecular fashion (Knapp *et al.*, 2004; Muller *et al.*, 2001; Ramstein *et al.*, 1999). Both effects – the interference with the negatively charged DNA and the masking of the DNA binding surface – would contribute to the weak DNA binding of p14-p16.

In a nucleosomal context, however, this flexible and unstructured tail might have additional functions. The C-terminal acidic tail of the *Drosophila* HMGB1/2 homologue HMG-D has been shown to increase the affinity for deformed DNA (Payet and Travers, 1997), and it has been pointed out that the acidic tails of HMGB proteins are suited for interactions with the positively charged histones (Travers, 2003), Figure 5.1 A). Therefore, the CHRAC16 C-terminal tail could also serve as a histone binding entity, which might either interact with the flexible, lysine- and arginine-rich N-terminal histone tails or with the basic regions of the core octamer structure (Figure 5.1 C, D). These proposed histone contacts could potentially stabilise the interaction of the p14-p16 heterodimer with the nucleosome.

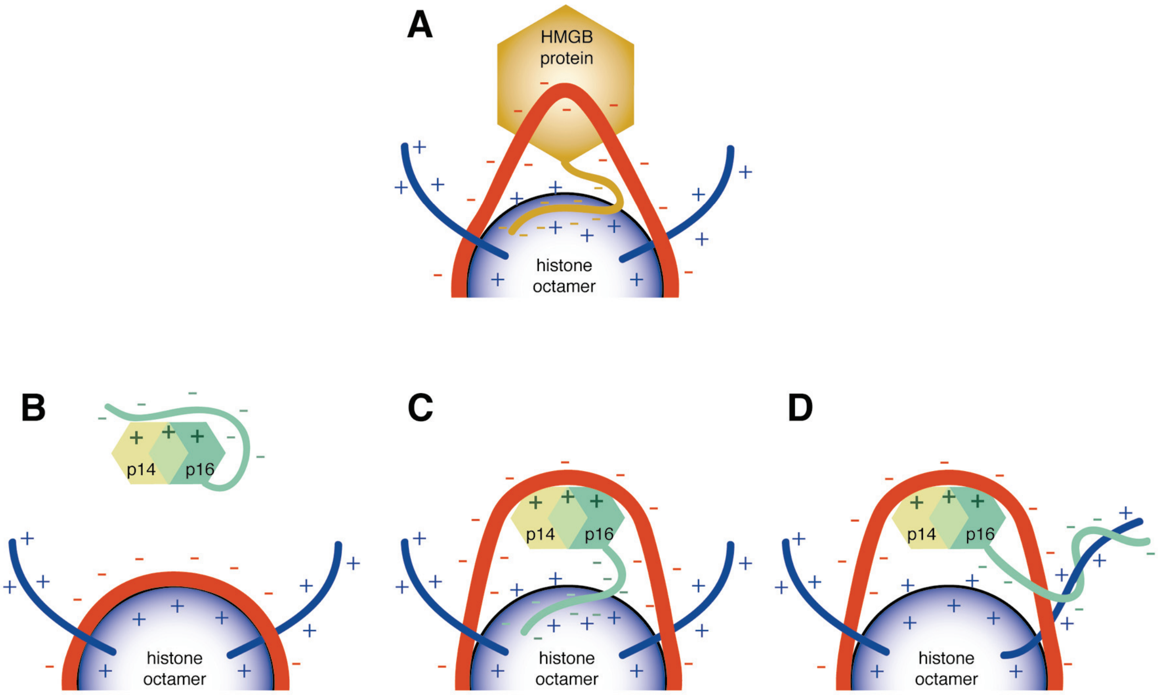

Figure 5.1: Potential interactions of the acidic C-terminal tails of HMGB proteins and CHRAC16 with nucleosomes. A: Interaction of HMGB proteins with DNA (red) and the positively charged histone octamer surface through the acidic C-terminal tail (orange). Adapted from (Travers, 2003). B: The C-terminal tail of CHRAC p16 hampers binding to the nucleosome by both its negative charge and covering the positively charged DNA binding surface C: Interaction of the CHRAC p14-p16 heterodimer with DNA and the histone octamer surface via the p16 C-terminal tail (green). D: Alternative interaction of the p16 C-terminal tail with positively charged N-terminal histone tails (blue)

A main feature of HMG box proteins is their high affinity to bent or distorted DNA, and likewise, HMG box proteins are known to introduce 90° to 100° bents into linear B-form DNA upon binding (Payet and Travers, 1997; Travers, 2003). The binding of proteins to four-way junction DNA has been established as a standard assay for monitoring the affinity to distorted DNA (Bianchi *et al.*, 1989). Here, the ability of the CHRAC14-CHRAC16 heterodimer to bind four-way junction DNA has been examined (Figure 4.23). It turned out that neither full length CHRAC14-CHRAC16 nor the CHRAC14-CHRAC16ΔC deletion mutant show a preference for four-way junction DNA when directly compared to double stranded linear DNA of the same approximate molecular weight. This result argues against a preference for bent DNA structures; however, it does not necessarily rule out the possibility that CHRAC14-CHRAC16 are able to bend DNA.

Importantly, all histone fold heterodimers that show a high structural similarity to CHRAC14-CHRAC16 bind to severely bent DNA: Histones H2A-H2B bind distorted DNA within the nucleosome, NFYB-NFYC at CCAAT boxes and NC-2α/β at the TATA box of promoter regions. Still, neither of these heterodimers distorts the DNA on its own, but only in concert with other protein partners. H2A-H2B interact with histones H3-H4 and form a histone octamer, around which the DNA is wrapped in almost two turns (Luger *et al.*, 1997). NFYB-NFYC bind to the non-histone fold NFYA subunit, and only this heterotrimeric complex is able to bind to DNA and introduce a 60° to 80° inclination (Romier *et al.*, 2003; Ronchi *et al.*, 1995). Finally, NC-2α/β bind to promoters at the opposite side of the TATA binding protein (TBP), a factor which is known to induce a severe DNA distortion at the TATA element (Kamada *et al.*, 2001).

Therefore, it is tempting to speculate that DNA binding by CHRAC14-CHRAC16 also involves DNA bending, as suggested by the model of the heterodimer interacting with DNA (Figure 4.18). Presumably, this bending is not exclusively achieved by CHRAC14-CHRAC16, but might also involve the other CHRAC subunits, ACF1 and/or ISWI. It can thus be hypothesised that DNA distortion is crucial for the enhancement of nucleosome sliding by CHRAC14-CHRAC16.

5.2.2 CHRAC histone fold subunits and nucleosome remodelling

In CHRAC, the p14-p16 heterodimer is tightly associated with the N-terminus of ACF1 (see 4.3.1). In contrast, the heterodimer interacts only weakly with DNA, and its DNA binding properties appear to be rather dynamic and modulated by the C-terminal tails of both subunits (see 4.5.2). Whereas the C-terminus of CHRAC14 contributes to DNA binding and deletion of the tail leads to an almost complete loss of DNA binding ability, the acidic CHRAC16 C-terminus has an opposite effect on the DNA binding properties: Due to its negative charge, it prevents tight DNA binding, and its deletion leads to a strong increase of DNA affinity (see Figure 4.19 and 5.2.1).

The enhancement of ACF nucleosome sliding activity by p14-p16 (Figure 4.24) is both dependent on the association of p14-p16 with ACF1 and with DNA, since a loss of either of these two interactions results in a loss of the observed activating effect (compare Figure 4.25 and 4.26 A, B). Furthermore, the p14-p16ΔC deletion variant inhibits the sliding activity of ACF due to its increased DNA affinity (Figure 4.26 C).

Biochemical studies of human CHRAC17-CHRAC15 by Varga-Weisz and colleagues have led to similar results (Kukimoto *et al.*, 2004). In agreement with the analysis presented here, the human homologues interact with the N-terminus of human ACF1 and facilitate ACF-mediated nucleosome sliding in a manner that is dependent on interaction with both DNA and ACF1. Besides, the authors report a stimulating effect of hCHRAC17-hCHRAC15 on ACF-dependent chromatin assembly reactions. However, this feature does not seem to be specific for the two CHRAC subunits, since other histone fold proteins such as the two small DNA polymerase ε subunits or negative cofactor 2 (NC-2) show the same effect (Kukimoto *et al.*, 2004).

The authors also demonstrate that deletion of any of the hCHRAC17-hCHRAC15 C-terminal tails impairs the stimulation of hACF sliding activity. Like for the *Drosophila* proteins, this effect seems to be caused by altered DNA affinities of the deletion variants. However, in contrast to the results for *Drosophila* p14-p16 presented here, the authors did not detect any significant increase in DNA binding and did not observe any direct sliding inhibition with the human deletion variants. This discrepancy could be species-specific, but it might also be caused by the fact that the C-terminal tail truncations were chosen such that additional flanking sequences to the acidic residues were deleted. Therefore, the authors failed to conclude about the potential mechanism of CHRAC-mediated chromatin remodelling (Kukimoto *et al.*, 2004).

It has been mentioned previously that the effects of p14-p16 on nucleosome remodelling were only detectable in the presence of a high excess of p14-p16 (see 4.6.1). Despite several attempts, this issue could not be solved and satisfactorily explained. One possibility could be suboptimal conditions during the nucleosome mobilisation reaction. Although the *in vitro* sliding assay has been optimised for ACF (Eberharter *et al.*, 2004a), it might be that p14-p16 are not maximally active under the same conditions and the change of one or more parameters such as temperature, ionic strength, buffer conditions, ATP concentration etc. could improve their activity. However, attempts to increase their effect on nucleosome remodelling by optimising the assay conditions were unsuccessful.

Alternatively, the requirement for the large excess of p14-p16 in the nucleosome sliding reactions might be due to the quality of the two recombinantly expressed subunits. Several protein preparations purified from *E. coli* were tested, and all of them had essentially the same activity in the sliding reactions. It cannot be ruled out that p14-p16 produced by a prokaryotic system (*E. coli*) are partially misfolded and therefore less active. However, recombinant p14-p16 produced by an eukaryotic system (Sf9-cells) co-purified a highly active ATP-dependent chromatin remodelling activity (see 4.1.2.2 and Figure 4.4). Heat-inactivation of the contaminating remodelling ATPase (30 to 60 min at 37°C) resulted in p14-p16 that had approximately the same specific activity in nucleosome sliding assays than *E. coli*-expressed p14-p16 (not shown). Therefore, misfolding of the recombinant protein can only partially explain its weak activity.

An accurate way of measuring the influence of p14-p16 on nucleosome sliding would be the direct comparison of reconstituted ACF and CHRAC, purified in parallel from the same source (Sf9 cells). Yet, the co-expression of all four CHRAC subunits by co-infection of Sf9 cells with three different baculoviruses turned out to be very difficult, and it was impossible to get the four proteins expressed at stoichiometric levels. Furthermore, the experience with the contaminating chromatin remodelling activity in the p14-p16 preparations (see 4.1.2.2, Figure 4.4 and above) shows that co-expression of all four CHRAC subunits in Sf9 cells would be problematic as well. Presumably, the protein preparations would also be contaminated by Sf9 cell-specific chromatin remodelling factors, which would be extremely difficult to monitor (see also 5.4).

It should be mentioned here that the nucleosome mobilisation assays with human ACF and human CHRAC17-CHRAC15 were also carried out with an excess of the CHRAC17-CHRAC15 heterodimer over hACF, although this excess was much less pronounced (approximately 25-fold, (Kukimoto *et al.*, 2004). However, the catalytic activity of human ACF itself appeared to be very weak, so that efficient remodelling was achieved only at an equimolar ratio of hACF and mononucleosomes or even an excess of hACF. Therefore, similar concerns about enzyme activity can be raised in that case as well. Besides, the poor activity of hACF might be very efficiently increased even by a weak stimulus of hCHRAC17-hCHRAC15, whereas the activity of *Drosophila* ACF appears to be very high even without CHRAC14-CHRAC16, and a stimulatory effect of these two subunits might be more difficult to observe.

5.2.3 A potential mechanism of CHRAC histone fold subunits

Considering that neither p14-p16 nor p14-p16ΔC influence the ATPase activity of the ACF complex (Figure 4.27), the data collected here suggest that p14-p16 facilitate nucleosome sliding by transient interactions with nucleosomal or linker DNA sequences, thereby stabilising a certain favourable DNA conformation during an intermediate step of the remodelling cycle (Figure 5.2). Fine-tuned and dynamic DNA interactions are the prerequisite for such a 'DNA chaperone' function, since the DNA has to be caught and released quickly. The hypothesis that the DNA double helix might adopt a bent conformation upon interaction with p14-p16 and additional protein sequences within CHRAC (see 5.2.1) is consistent with this model. As the histone fold domains of p14-p16 closely resemble histones H2A-H2B (see Figures 4.16 B and 4.17), the dimer could provide a transient DNA binding surface for stretches of DNA that have been displaced from the nucleosomal surface during remodelling (see below and Figure 5.2 B).

In addition to the transient interactions with DNA, CHRAC14-CHRAC16 could possibly bind histones within the nucleosomes. Histone binding via the PHD fingers of ACF1 is known to be required for the remodelling activity of ACF (Eberharter *et al.*, 2004b), and the ISWI ATPase activity is stimulated by the histone H4 N-terminus, presumably via direct interaction of ISWI with a patch of basic residues within the H4 tail sequence (Clapier *et al.*, 2001; Clapier *et al.*, 2002), see 2.4.5.1). Likewise, CHRAC14-CHRAC16 could establish additional histone contacts, either via the acidic C-terminus of CHRAC16 (see 5.2.1) or via their histone fold domains. The murine orthologue of CHRAC14, YBL1, has been reported to interact with histones H2A and H3 *in vitro* (Bolognese *et al.*, 2000). However, further studies are required to investigate if the interactions with histones are also relevant during chromatin remodelling.

So far, it is not clear which step of the remodelling process is affected by p14-p16, and several scenarios are possible. For instance, the linker DNA could interact with p14-p16 and adopt a conformation that favours remodelling by ACF1 and ISWI (Figure 5.2 A). This mechanism would be similar to the model proposed for the action of HMGB1 during nucleosome remodelling (Bonaldi *et al.*, 2002), although in that case, no direct interaction between ACF and HMGB1 is required. Likewise, p14-p16 could also act at a later stage and might function as acceptor site for DNA bulges created by ISWI during remodelling (see above and Figure 5.2 B).

Moreover, the CHRAC histone fold subunits could also influence nucleosome remodelling by additional qualities. For instance, they could modulate the binding of CHRAC to its chromatin substrate. This idea is supported by the observation that human CHRAC17-

CHRAC15 seem to improve the interactions of hACF with mononucleosomes (Kukimoto *et al.*, 2004).

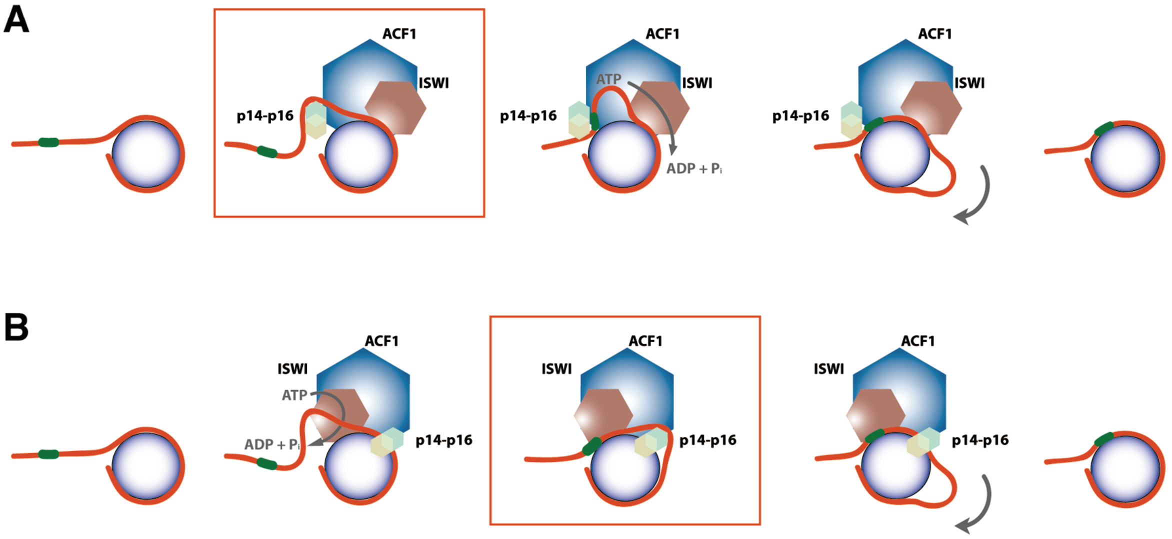

Figure 5.2: Potential mechanisms of histone fold subunit function within CHRAC. A: Transient interaction of p14-p16 with linker DNA facilitates the creation of a DNA bulge by ACF1 and ISWI. B: p14-p16 serve as a transient DNA acceptor after the creation of a DNA bulge by ACF1 and ISWI. Note that the stages of p14-p16-DNA interaction (framed in red) are distinct from the stages of ATP hydrolysis. Moreover, interactions between p14-p16 and the histone octamer are possible (not shown, see Figure 5.1).

The overall structure and charge distribution of CHRAC14-CHRAC16 resemble that of H2A-H2B (Figure 4.17). Several studies have reported a displacement or an exchange of histones H2A-H2B during ATP-dependent chromatin remodelling (Bruno *et al.*, 2003; Kusch *et al.*, 2004; Mizuguchi *et al.*, 2004; Vicent *et al.*, 2004). The intriguing similarity of the two small CHRAC subunits with histones H2A-H2B could be an indication that histone dimer exchange might be a novel feature of CHRAC. However, several reasons argue against this hypothesis. Biochemical studies of YBL1-YCL1, the murine homologues of CHRAC14-CHRAC16, revealed that these proteins are indeed able to interact with core histones, but do not form octamer-like structures with histones (Bolognese *et al.*, 2000). Furthermore, the N- and C-terminal tail extensions are not conserved between H2A-H2B and the CHRAC histone-like subunits, and a careful comparison of the histone fold core structures reveals important differences as well: In the nucleosome structure, the residues following helix αC in histone H2A form a two-stranded β-sheet with the C-terminal end of the neighbouring H4 histone, which is important for the stability of the histone octamer (Luger *et al.*, 1997). In contrast to histone H2A, this region corresponds to helix αC in CHRAC16, packing against the helices α2 and α3 of the histone fold. In a hypothetical nucleosome-like model with CHRAC14-CHRAC16 replacing histones H2A-H2B, this helix would interfere with the histone H4 interaction and destabilise the complex dramatically.

Histone H2A.Bbd (see 2.3.2) is an example for a variant histone which causes a nucleosomal conformation that is more relaxed and organises only approximately 118 base pairs of DNA (Bao *et al.*, 2004). However, it has never been observed that CHRAC-mediated nucleosome remodelling alters or destabilises nucleosomes (Längst *et al.*, 1999; Varga-Weisz *et al.*, 1997). Hence, an exchange reaction of p14-p16 with histones H2A-H2B appears to be unlikely.

5.3 What is the role of CHRAC histone fold subunits *in vivo*?

5.3.1 Are ACF and CHRAC distinct complexes?

The two small CHRAC subunits are conserved throughout eukaryotic species (see 2.5). It should be stressed that Itc1p, the large subunit of the *Saccharomyces cerevisiae* remodelling complexes ISW2 and yCHRAC (see Table 2.II), does not share any sequence homology with ACF1 or other members of the BAZ/WAL family except for the N-terminal WAC motif (Gelbart *et al.*, 2001; Iida and Araki, 2004). This motif has been shown to interact with the CHRAC histone fold subunits in human and *Drosophila* (Kukimoto *et al.*, 2004) and this work, also discussed in 5.3.2.2). Therefore, the two histone fold proteins are the only subunits of ISWI-containing complexes apart from the ISWI ATPases that are highly conserved from yeast to mammals (McConnell *et al.*, 2004), which emphasises their relevance and argues for their functional importance.

Nevertheless, the question whether ACF and CHRAC exist as two distinct complexes has still not been answered conclusively. The two histone fold subunits that distinguish CHRAC from ACF are small in size, whereas the ACF1- and ISWI subunits are relatively large proteins (in *Drosophila* 175 kDa and 110 kDa, respectively). Therefore, the histone-like CHRAC subunits could have been easily overlooked in protein purifications. Furthermore, they are not required for the chromatin remodelling activity of the ACF1-ISWI heteromer (the ACF complex), which has been shown to be a potent remodelling machine *in vitro* (Eberharter *et al.*, 2001).

Some evidence for the existence of both CHRAC and ACF comes from studies in *Saccharomyces cerevisiae* (McConnell *et al.*, 2004). Quantitative immunoprecipitation of tagged versions of either of the two histone fold proteins Dpb4p and Dls1p efficiently co-precipitates Isw2p, and for Dls1p it has also been shown to co-precipitate Itc1p. However, considerable amounts of Isw2p (and Itc1p) remain in the unbound fraction, arguing for the existence of the ISW2 complex, only consisting of Isw2p and Itc1p. However, the authors could not exclude that the precipitated complex had been destabilised by epitope-tagging of the subunits or during precipitation and purification, which would also account for the presence of CHRAC subunits in the unbound fraction (McConnell *et al.*, 2004).

5.3.2 Potential roles of CHRAC histone fold subunits

5.3.2.1 Regulation of chromatin structure and transcription

The CHRAC histone fold subunits stimulate the remodelling activity of ACF, but this effect appears to be rather subtle and only visible with suboptimal ACF concentrations *in vitro* (Kukimoto *et al.*, 2004, and this work). However, the influence of the small subunits could be more pronounced *in vivo*. For instance, hACF is only active at relatively low salt concentrations in the *in vitro* nucleosome sliding assay (50 to 80 mM KCl), but hCHRAC17-hCHRAC15 were reported to allow hACF-mediated nucleosome remodelling at salt concentrations up to 160 mM KCl (Kukimoto *et al.*, 2004). It is therefore conceivable that the histone fold subunits allow efficient chromatin remodelling at physiological salt concentrations *in vivo*.

Likewise, the effect of the CHRAC histone fold subunits on chromatin containing linker histone H1 has not been examined yet. In most eukaryotic cells, linker histones are highly abundant. About 80% of the nucleosomes contain H1, but the total levels and the relative abundance of linker histone isoforms vary significantly between different cell types (Bustin *et al.*, 2005; Rupp and Becker, 2005; Zlatanova *et al.*, 2000). Linker histones are known to be involved in both transcriptional repression and activation (Bouvet *et al.*, 1994; Sandaltzopoulos *et al.*, 1994; Shen and Gorovsky, 1996), and they repress nucleosome fluidity and inhibit or modulate ATP-dependent chromatin remodelling (Hill and Imbalzano, 2000; Ramachandran *et al.*, 2003). Therefore, nucleosome remodelling complexes have to find means to deal with the presence of linker histones *in vivo*.

It remains to be investigated whether the two small CHRAC subunits allow efficient chromatin remodelling in the presence of linker histones. HMGB proteins, which share many similarities with the CHRAC histone fold subunits (see 5.2.1), dynamically compete with histone H1 for chromatin binding sites both *in vitro* and *in vivo* and thereby change the nucleosomal accessibility (Catez *et al.*, 2004; Ner *et al.*, 2001; Ragab and Travers, 2003). The CHRAC histone fold subunits might be able to facilitate the removal of linker histones in a similar manner.

In *Drosophila*, histone H1 is absent during the earliest stages of fly development and is substituted by the HMGB1 orthologue HMG-D (Ner and Travers, 1994). Chromatin lacking H1 is less compacted and rather flexible (Fan *et al.*, 2005; Zlatanova *et al.*, 2000), and this 'open' chromatin state seems to be required during early development. Likewise, histone H1 and other factors involved in chromatin architecture bind to chromatin only loosely and very dynamically in mammalian embryonic stem cells (ES cells), and this dynamic state of chromatin is functionally relevant for stem cell differentiation (Meshorer *et al.*, 2006). It is intriguing that *Drosophila* CHRAC is most abundant during the earliest developmental stages (Corona *et al.*, 2000, and this work), i. e. at stages without or with low levels of histone H1 (Ner and Travers, 1994). CHRAC, HMG-D and further factors might hence be required for global structural maintenance and the regulation of embryonic chromatin during differentiation.

In *Saccharomyces cerevisiae*, the CHRAC histone fold subunits have been shown to have a strong influence on Isw2-dependent regulation of chromatin structure and transcription *in vivo* (McConnell *et al.*, 2004). The yeast ISW2 complex (see 2.3.5.2 and 2.4.5.2) represses transcription of a variety of genes in concert with the Rpd3-Sin3 histone deacetylase complex (Fazzio *et al.*, 2001). Recently, the two histone fold proteins Dpb4p and Dls1p have been shown to be associated with ISW2, thereby forming yeast CHRAC (Iida and Araki, 2004; McConnell *et al.*, 2004, see also Table 2.II and 5.3.2.2). The effect of the yCHRAC histone fold subunits on Isw2p-dependent transcriptional regulation was examined by DNA microarray and Northern blotting analysis of *isw2* and *dls1* mutant strains (McConnell *et al.*, 2004). The majority of genes showed similar changes in expression levels in both mutant strains, however, a small subset of genes was only deregulated by the *isw2* mutation, but not by the *dls1* mutation. Besides, the nucleosomal positioning was changed at several promoters in a similar way in both mutant backgrounds. These results support an important role of the CHRAC histone fold subunits during ISWI-dependent remodelling and demonstrate their direct influence on chromatin structure. Presumably, the Dpb4p-Dls1p heterodimer acts according to the mechanisms suggested above (see 5.2.3).

5.3.2.2 Crosstalk between CHRAC and DNA polymerase epsilon

DNA polymerase ε has functions during DNA replication and repair (see 2.2.2.5). The *Saccharomyces cerevisiae* DNA Pol ε complex consists of the subunits Pol2p and Dpb2p, which are essential for viability (Sugino, 1995), and of two small non-essential histone fold subunits, Dpb3p and Dpb4p (Araki *et al.*, 1991; Ohya *et al.*, 2000). Interestingly, the Dpb4p subunit is shared between DNA Pol ε and yeast CHRAC, in which it interacts with the histone fold protein Dls1p (Iida and Araki, 2004). Also human DNA Pol ε and hCHRAC share the histone fold protein p17, which is either associated with the Pol ε-specific p12 subunit or with the hCHRAC-specific p15 subunit (Li *et al.*, 2000; Poot *et al.*, 2000). As the subunit composition of DNA Pol ε and CHRAC appear to be conserved from yeast to human, it seems likely that histone fold subunits are shared between them also in other species.

Both DNA Pol ε and yCHRAC regulate the epigenetic inheritance of silenced and expressed states at *S. cerevisiae* telomeres (Iida and Araki, 2004). Detailed studies with strains deficient in the histone fold subunits specific for either DNA Pol ε (*dpb3Δ*) or yCHRAC (*dls1Δ*) or the shared subunit (*dpb4Δ*) with a variety of reporter genes at telomere-proximal loci revealed that DNA Pol ε operates for stable inheritance of the silent state, whereas yCHRAC acts for the inheritance of a transcriptionally active state. Since telomere length and Sir protein levels at telomeres are not affected by the deletions of the DNA Pol ε and yCHRAC subunits, these data argue for the two complexes maintaining the telomeric heterochromatin structure (Iida and Araki, 2004). Consistent with these findings, yCHRAC and DNA Pol ε – among further chromatin remodelling and modifying factors – have recently been reported to be located at the boundary elements adjacent to the silent mating type loci HMR and HML on yeast chromosome III, and they seem to be required for maintenance of the chromatin structure at boundaries (Tackett *et al.*, 2005).

At first sight, it seems to be contradictory that yCHRAC counteracts heterochromatic silencing at telomeres and chromatin boundaries on the one hand (Iida and Araki, 2004; Tackett *et al.*, 2005), but represses the transcription of a wide variety of gene loci on the other hand (McConnell *et al.*, 2004, see 5.3.2.1). However, these findings could merely reflect the fact that CHRAC fulfils different functions in distinct chromosomal domains.

In mammalian cells, both DNA Pol ε and a remodelling complex containing ACF1 and SNF2H (i. e. ACF or CHRAC) have been reported to be targeted to heterochromatic foci, and both complexes seem to be involved in the replication of heterochromatin during late S-phase (Collins *et al.*, 2002; Fuss and Linn, 2002). It is tempting to speculate that in mammals, the two complexes co-operate during heterochromatin replication in a way similar to the mechanisms that regulate telomere position effects in yeast (see above). Although it has not been examined whether the SNF2H-containing complex included the p17-p15 subunits characteristic for CHRAC, it seems reasonable that a potential crosstalk between DNA Pol ε and the chromatin remodelling complex might involve the histone-like proteins.

Moreover, the histone fold proteins could also be involved in targeting CHRAC and DNA Pol ε to heterochromatic sites. The N-terminal 350 amino acids of ACF1, which include the WAC motif, have been shown to target a reporter protein to pericentromeric heterochromatin in mouse cells (Tate *et al.*, 1998). The mammalian WICH complex – consisting of SNF2H and the ACF1-related protein WSTF – is also directed to heterochromatin, but it has been demonstrated that the N-terminal 400 amino acids of WSTF are not involved in the targeting process, although the sequence contains a WAC motif as well. This suggests that the ACF and WICH complexes might be targeted to heterochromatin by different mechanisms and that the WAC motif is not directly involved in heterochromatin binding (Bozhenok *et al.*, 2002). Considering that the CHRAC histone fold subunits interact with the ACF1 N-terminus (Kukimoto *et al.*, 2004, and this work), the targeting of ACF1 to heterochromatin might occur indirectly via the histone fold subunits. Likewise, the DNA Pol ε histone fold subunits could direct the polymerase complex to heterochromatin.

The DNA Pol ε and CHRAC histone fold dimers are very similar, as one subunit is identical in both complexes and the other one is highly homologous (see above). For this reason, it has been proposed that the two histone fold subcomplexes have a similar molecular function within DNA Pol ε and CHRAC (McConnell *et al.*, 2004). From what is known of the human and the *Drosophila* CHRAC subunits (Kukimoto *et al.*, 2004, and this work), the histone-like proteins of DNA Pol ε could exert their roles in DNA replication and repair by transient interactions with DNA, bending of the DNA double helix, or by interaction with nucleosomal histones, either via their histone fold domains or their acidic sequence motifs[3] (see 5.2.1 and 5.2.3). It is currently unclear whether sharing of one histone fold subunit has additional functions other than guaranteeing a high functional similarity of the histone-like subcomplex. The shared protein might play a role in targeting CHRAC and DNA Pol ε to heterochromatin (discussed above), and it might also have regulatory functions in both complexes. Even though a direct physical interaction between DNA Pol ε and CHRAC has not been observed (Iida and Araki, 2004), the shared subunit could establish a crosstalk between the two complexes. For instance, DNA Pol ε and CHRAC could compete for the shared histone fold subunit and thereby regulate their levels in a reciprocal manner. This potential mechanism of mutual control might be important for the fine-tuning of their opposing activities at telomeres and heterochromatic boundaries.

5.3.2.3 Potential regulatory roles

Only little information is currently available about the regulatory mechanisms concerning the CHRAC histone fold subunits. Although the yCHRAC subunit Dls1p is required for Isw2p-dependent gene repression (see 5.3.2.1), chromatin immunoprecipitation (ChIP) of Isw2p gave identical results in wild type and *dls1* deletion strains, suggesting that Dls1p does not affect the interaction of the ISW2 complex with chromatin (McConnell *et al.*, 2004).

---

[3] The yeast and human DNA Pol ε histone fold subunits also contain an acidic sequence motif, although in yeast Dpb3p, it is not found at the C-terminus, but more internally, and in human, the acidic C-terminal tail is located at p17, the shared subunit between DNA Pol ε and hCHRAC.

Consequently, the yCHRAC histone fold subunits do not seem to be responsible for targeting the complex to specific genes, but are required for functions subsequent to chromatin binding such as facilitating Isw2p-dependent chromatin remodelling.

In *Drosophila*, CHRAC14-CHRAC16 are developmentally regulated and most abundant in early embryos (Corona *et al.*, 2000, see also 4.2.1, 4.2.3 and 5.4). The relatively high concentrations at this developmental stage suggest a global role in chromatin regulation, but they might be still present at low levels in later embryonic stages and larval, pupal and adult tissues, where CHRAC could fulfil more specific functions.

Recently, it has become evident that *Drosophila* CHRAC is regulated by post-translational modifications. Its ATPase subunit ISWI is acetylated in a cell cycle-dependent manner by the histone acetyltransferase GCN5 at a specific lysine residue within the so-called HAND domain (see 2.4.5.1, R. Ferreira *et al.*, manuscript submitted). Besides, it could be shown here that CHRAC16, but not CHRAC14, is being phosporylated in Sf9 cells (see 4.1.2.1). So far, the function of this modification is not clear, and the phosphorylated and dephosphorylated proteins show identical behaviour in EMSA and nucleosome remodelling assays (not shown). The phosphorylation site has not been mapped yet, but it might be located at the highly accessible acidic C-terminal tail, which contains several serine residues. This modification might regulate CHRAC by an unknown mechanism, but phosphorylation of the acidic C-terminus might simply increase its high negative charge.

5.4 Open questions and future experiments

Recently, a number of studies have contributed to our knowledge about the CHRAC histone fold subunits. The discovery of homologues in different species has proven their ubiquitous conservation (Bolognese *et al.*, 2000; Corona *et al.*, 2000; Poot *et al.*, 2000) (Iida and Araki, 2004; MacCallum *et al.*, 2002), their crystal structure has been solved (Hartlepp *et al.*, 2005), and important functions have been described both *in vitro* (Hartlepp *et al.*, 2005; Kukimoto *et al.*, 2004) and *in vivo* (Iida and Araki, 2004; McConnell *et al.*, 2004). But still there are a lot of open questions to be answered. This paragraph summarises unsolved issues predominantly concerning the p14-p16 subunits of *Drosophila* CHRAC and suggests some future experimental strategies.

The structural and biochemical analysis of CHRAC14-CHRAC16 has provided valuable insights, but a lot of mechanistic details are not fully understood yet (see 5.2). Chromatin remodelling with CHRAC subunits labelled with specific, inducible cross-linkers could trap intermediate states and reveal new aspects of interactions with histones and DNA. A similar approach with nucleosomes labelled with photo-inducible cross-linkers has been used to study histone-DNA contacts before and after nucleosome remodelling by the ISW2 complex (Kassabov *et al.*, 2002). Likewise, fluorescence-based techniques such as fluorescence resonance energy transfer (FRET) and fluorescence cross-correlation spectroscopy (FCCS) have been successfully used to monitor the dynamics of nucleosomal DNA and to determine the stoichiometry of ACF and ISWI bound to nucleosomes (Li *et al.*, 2005; Strohner *et al.*, 2005) and could be used with CHRAC in the future.

Another aspect that remains to be clarified is the potential interaction of CHRAC14-CHRAC16 with histone H1 (see 5.3.2.1). Chromatin remodelling of nucleosomal arrays including histone H1 could reveal stimulating effects of CHRAC14-CHRAC16 in the presence of linker histones and might uncover new important functions of CHRAC.

The prerequisite for most of these studies is a pure, intact and active Chromatin Accessibility Complex, but so far, co-expression and co-purification of all four subunits together do not give satisfying results (see 5.2.2). Therefore, new strategies are required for the expression of recombinant CHRAC. A novel vector has recently been described that allows the expression of multiple proteins from one baculovirus construct (Berger *et al.*, 2004). The use of this vector might significantly facilitate the expression of all four CHRAC subunits at stoichiometric amounts. Alternatively, one or both of the ORFs encoding for the CHRAC histone fold subunits could be N-terminally fused to the ACF1 ORF for CHRAC expression. As the histone fold heterodimer interacts with the N-terminal ACF1 WAC motif (see 4.3.1), the creation of such an N-terminal fusion should not destroy the CHRAC architecture, and the association of the histone fold dimer with ATP-dependent chromatin remodelling complexes from the Sf9 cell expression system (see 4.1.2.2) would be minimised. Yet, it certainly would have to be tested whether the fusion proteins are still active in chromatin remodelling. Another approach to be tried is the *in vitro*-reconstitution and purification of CHRAC using purified ACF1 and ISWI expressed in Sf9 cells and purified p14-p16 expressed in *E. coli*.

To date, very little is known about CHRAC14-CHRAC16 *in vivo*. The two subunits are developmentally regulated and are highly abundant only during the early embryonic stage (Corona *et al.*, 2000). Here, this finding has been supported by the use of new rat monoclonal antibodies raised against recombinant CHRAC14-CHRAC16. In Western blot analysis, both subunits could be detected in *Drosophila* embryo extracts (TRAX and DREX), but the signals in *Drosophila* cell line extracts were much weaker and not reproducible (see 4.2.1). Likewise, immunofluorescence signals were most convincing in early embryos, whereas signals in late embryos, S2 cells and on 3rd instar larvae polytene chromosomes were weak or undetectable (see 4.2.3). These data are difficult to interpret, because the rat monoclonal antibodies seem to have a low affinity to their antigenes, and some of them – in particular the CHRAC14-specific 4F7 and 5C7 antibodies – cross-react with other proteins. The antibody quality is therefore insufficient for the detection of low to moderate levels of p14 and p16 on polytene chromosomes, in cell lines or in other *Drosophila* tissues.

For these reasons, more specific and reliable antibodies are necessary for further *in vivo* analyses of p14-p16, and the generation of new polyclonal or monoclonal antibodies against both subunits should help to solve a variety of problems. For instance, one of the most urging questions is the sub-cellular localisation of p14 and p16. Immunofluorescence studies could provide valuable information about the localisation of CHRAC, ACF and DNA polymerase ε.

Alternatively, fly lines expressing epitope-tagged CHRAC subunits could – at least in part – bypass the requirement of specific antibodies against p14 and p16. It has already been tried to establish fly lines expressing ISWI, ACF1 and CHRAC16 tagged with different fluorescent proteins. However, it has been impossible to obtain homozygous flies with the expression construct for yellow fluorescent protein (YFP)-tagged CHRAC16, and a heterozygous fly line with the expression construct for cyan fluorescent protein (CFP)-tagged ACF1 that is located on the X chromosome leads to male lethality, presumably due to higher expression levels of the dosage compensated male X chromosome Therefore, the overexpression of these CHRAC subunits seems to cause lethality in *Drosophila* (M. Chioda, unpublished observations).

In yeast, the CHRAC histone fold subunits Dpb4p and Dls1p are not essential, but their deletion leads to a variety of phenotypes such as altered chromatin structure at promoters, transcriptional derepression and loss of the maintenance of heterochromatin structure at telomeres and chromatin boundaries (Iida and Araki, 2004; McConnell *et al.*, 2004; Tackett *et al.*, 2005), see 5.3.2). It would be interesting to study the effect of p14-p16 deletions in *Drosophila*. Most *acf1* $^{-/-}$ flies, which lack both CHRAC and ACF, die during the larval-pupal transition, but the phenotype of the surviving animals is rather mild. They show an altered chromatin structure that suggests a repressive role for ACF/CHRAC, but otherwise no obvious severe defects (Fyodorov *et al.*, 2004). Therefore, the phenotypes of the p14-p16 deletions might be subtle and hard to detect. A disruption of the CHRAC14- and CHRAC16 genes would be difficult to perform, since both reside in very gene-dense chromosomal regions. Hence, a knockdown of the subunits by RNA interference (RNAi) might be more appropriate, which can be carried out both in *Drosophila* cell lines by transient transfection and in fly lines carrying constructs for expression of double stranded RNA. In fact, the constructs for a knockdown of both CHRAC14 and CHRAC16 have already been prepared and await analysis (pWIZ11-12 and pWIZ13-14, see Table 3.I, (Lee and Carthew, 2003)). However, a very careful interpretation of the CHRAC14-specific knockdown experiments will be necessary, because this subunit might be shared with *Drosophila* DNA Pol ε and a knockdown might therefore affect the Pol ε complex as well. Furthermore, the CHRAC14 gene locus encodes for a second, non-overlapping open reading frame of an endodesoxyribonuclease with a putative function in nucleotide excision repair (FlyBase, http://flybase.bio.indiana.edu). According to the transcript predictions, it is not clear if the two coding sequences are transcribed separately or as a bicistronic RNA. If the latter case applies, the levels of that protein will be also affected by an RNAi knockdown.

Certainly, the analysis of CHRAC will remain challenging in the future, but will lead to further fascinating insights into the mechanism and regulation of ISWI-dependent chromatin remodelling. Our knowledge about CHRAC will thereby contribute to a deeper understanding of chromatin structure, transcription and epigenetic inheritance.

Appendix

Plasmid maps

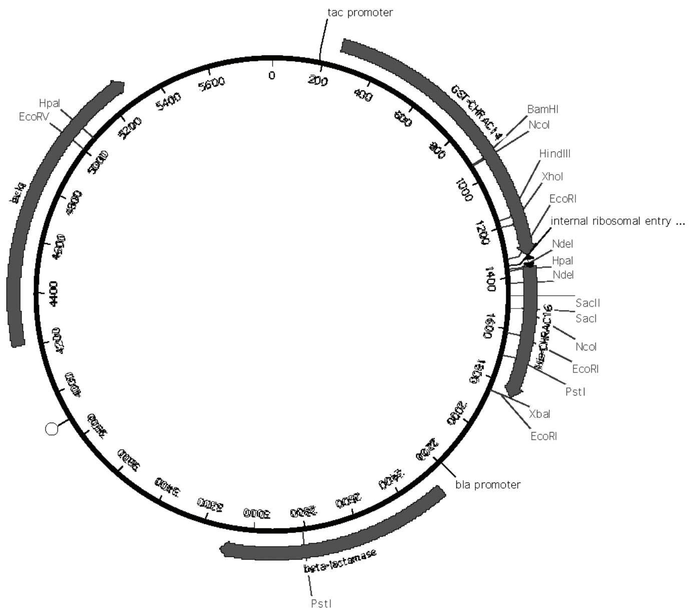
tac promoter
GST-CHRAC14
BamHI
NcoI
HindIII
XhoI
EcoRI
internal ribosomal entry ...
NdeI
HpaI
NdeI
SacII
SacI
His-CHRAC16
NcoI
EcoRI
PstI
XbaI
EcoRI
bla promoter
beta-lactamase
PstI
lacIq
HpaI
EcoRV
0
200
400
600
800
1000
1200
1400
1600
1800
2000
2200
2400
2600
2800
3000
3200
3400
3600
3800
4000
4200
4400
4600
4800
5000
5200
5400
5600

pBCMaJoHIS

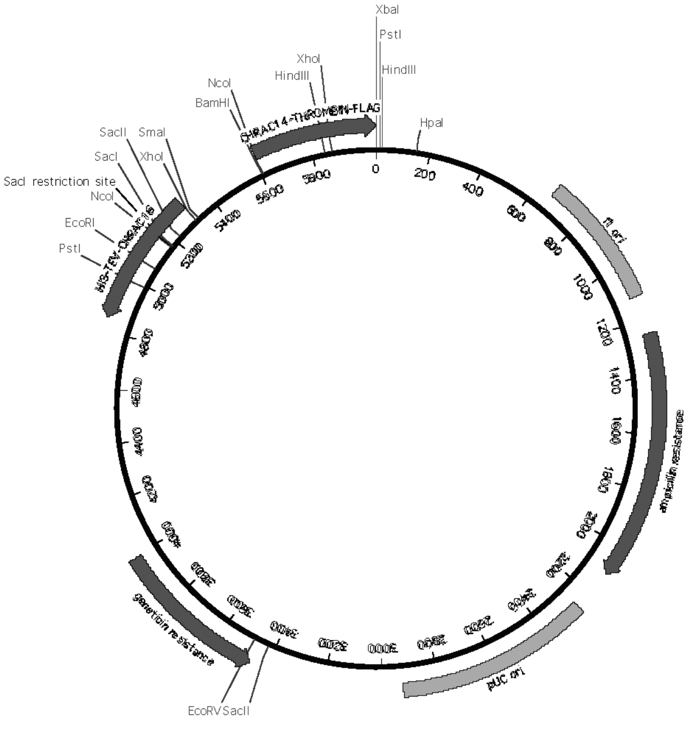
XbaI
PstI
HindIII
HpaI
XhoI
HindIII
NcoI
BamHI
CHRAC14-THROMBIN-FLAG
SacII
SmaI
SacI
XhoI
SacI restriction site
NcoI
EcoRI
PstI
HIS-TEV-CHRAC16
f1 ori
ampicillin resistance
pUC ori
gentamicin resistance
EcoRV
SacII
0
200
400
600
800
1000
1200
1400
1600
1800
2000
2200
2400
2600
2800
3000
3200
3400
3600
3800
4000
4200
4400
4600
4800
5000
5200
5400
5600
5800

pFBDMaJo corrected

List of abbreviations and acronyms

aa	amino acid(s)
ab	antibody
ACF	ATP-utilising chromatin assembly and remodelling factor
AMP	ampicillin
ARP	actin-related protein
ATP	adenosine triphosphate
BAF/BAP	brahma-associated factors/proteins
BAZ/WAL family	bromodomain adjacent to zinc finger/WSTF-ACF1-like family
bp	base pairs
BPTF	bromodomain-PHD finger transcription factor
brd	bromo domain
BRM/brm	brahma
BSA	bovine serum albumine
CAF-1	chromatin assembly factor 1
CBF	CCAAT binding factor
CBP	CREB binding protein
CENP-A	centromere protein A
CFP	cyan fluorescent protein
CHD1	chromatin organisation modifier/helicase/DNA binding domains
ChIP	chromatin immunoprecipitation
CHL	chloramphenicol
CHRAC	Chromatin Accessibility Complex
CIP	calf intestine phosphatase
CK II	casein kinase II
Dls1p	Dbp3p-like subunit
DNA	desoxyribonucleic acid
Dpb2p/Dpb3p/Dpb4p	DNA polymerase B (DNA Pol ε) subunits
DREX	*Drosophila* chromatin assembly extract
DTT	dithiotreithol
EcR	ecdysone receptor
EDTA	ethylene diamine tetraacetic acid
ELISA	enzyme-linked immunosorbent assay

EM	electron microscopy
EMSA	electrophoretic mobility shift assay
ESI-MS	electrospray ionisation mass spectrometry
FCCS	fluorescence cross-correlation spectroscopy
FCS	fetal calf serum
FITC	Fluorescein isothiocyanate
FRET	fluorescence resonance energy transfer
GCN5	general control nonderepressible
GFP	green fluorescent protein
GST	glutathione-S-transferase
HAP	heme activator protein
HAT	histone acetyl transferase
HDAC	histone deacetylase
HEPES	*N*(2-hydroxyethyl)piperazine-*N'*(2-ethanesulphonic acid)
Hir	histone regulation
HMfA/HMfB	histone from *Methanothermus fervidus* A/B
HMGB	high mobility group box
HML/HMR	homothallic mating left/right
HMT	histone methyl transferase
HP-1	heterochromatin protein 1
HRP	horse radish peroxidase
Htz1p	H2A.Z ('histone two A.Z')
INO80	inositol requiring
Ioc2p/Ioc3p/Ioc4p	ISW1 ('ISW one') complex subunits (ISW1a/ISW1b)
IPTG	1-isopropyl-β-D-1-thiogalacto-pyranoside
IRES	internal ribosomal entry site
ISW1/ISW2	imitation SWI (*S. cerevisiae*)
ISWI	imitation SWI (*Drosophila, Xenopus*)
Itc1p	ISW2 ('ISW two') complex subunit
KAN	kanamycin
K_D	dissociation constant
M	molar (mol/L)
MALDI-MS	matrix-associated laser desorption ionisation mass spectrometry
MBD	methylated DNA-binding
MeCP1	methyl-CpG-binding

MOF	males absent on the first
MYST-family	MOZ, Ybf2/Sas3, Sas2, Tip60
Nap-1	nucleosome assembly protein 1
NC-2	negative cofactor 2
NF-Y	nuclear factor Y
NLS	nuclear localisation signal
NoRC	nucleolar remodelling complex
NUMAC	nucleosomal methylation activator complex
NuRD	nucleosome remodelling/deacetylation
NURF	nucleosome remodelling factor
OD_{600}	optical density at $\lambda = 600$ nm
ORF	open reading frame
PAGE	polyacrylamide gel electrophoresis
PBAF/PBAP	Polybromo-associated BAF/BAP
PBS	phosphate buffered saline
PCAF	p300/CBP-associated factor
PCR	polymerase chain reaction
PHD	plant homeo domain
PIC	preinitation complex
PMSF	phenylmethane sulfonyl fluoride
Pol	polymerase
Rad51/Rad54	radiation sensitive
RbAP	retinoblastoma-associated protein
rDNA	ribosomal DNA (= ribosomal RNA gene)
r.m.s.d.	root mean square deviation
RNA	ribonucleic acid
Rpd3p	reduced potassium dependency
RSC	remodels the structure of chromatin
RSF	remodelling and spacing factor
RT	room temperature
RT-PCR	reverse transcription polymerase chain reaction
SAGA	Spt-Ada-Gcn5 acetyltransferase
SANT	SWI/SNF, ADA, N-CoR, TFIIIB
SDS	sodium dodecyl sulfate
SF2	superfamily 2

Sin3p	SWI-independent
Sir2p/Sir3p/Sir4p	silent information regulator proteins
SLIDE	SANT-like ISWI domain
Spt3p/Spt7p	suppressor of ty
SRCAP	SNF2-related CBP activator protein
STAGA	SPT3-TAF$_{II}$31-GCN5-L acetylase
Sth1p	Snf2p ('Snf two')-homologous
SUMO	small ubiquitin-related modifier
SWI/SNF	mating type switch/sucrose non-fermenting
SWIRM	Swi3p/Rsc8p/Moira
SWR1	sick with Rat8 *ts*, also: Swi2p-related
TAF	TBP-associated factor
TBP	TATA binding protein
TFTC	TBP-free TAF containing complex
TOF	time of flight
TPE	telomere position effect
TRAX	*Drosophila* transcription extract
TRRAP	transformation/transcription domain associated protein
WAC	WSTF/ACF1/cbp146
WAKZ	WSTF/ACF1/KIAA0314/ZK783.4
WICH	WSTF-ISWI chromatin remodelling complex
WINAC	WSTF-including nucleosome assembly complex
YBL1	NFYB-like
YCL1	NFYC-like
YFP	yellow fluorescent protein

References

Aasland, R., Gibson, T.J. and Stewart, A.F. (1995) The PHD finger: implications for chromatin-mediated transcriptional regulation. *Trends Biochem Sci*, **20**, 56-59.

Aasland, R. and Stewart, A.F. (1995) The chromo shadow domain, a second chromo domain in heterochromatin-binding protein 1, HP1. *Nucleic Acids Res*, **23**, 3168-3174.

Aasland, R., Stewart, A.F. and Gibson, T. (1996) The SANT domain: a putative DNA-binding domain in the SWI-SNF and ADA complexes, the transcriptional co-repressor N-CoR and TFIIIB. *Trends Biochem Sci*, **21**, 87-88.

Agresti, A., Scaffidi, P., Riva, A., Caiolfa, V.R. and Bianchi, M.E. (2005) GR and HMGB1 interact only within chromatin and influence each other's residence time. *Mol Cell*, **18**, 109-121.

Ahmad, K. and Henikoff, S. (2002) The histone variant H3.3 marks active chromatin by replication-independent nucleosome assembly. *Mol Cell*, **9**, 1191-1200.

Akhtar, A., Zink, D. and Becker, P.B. (2000) Chromodomains are protein-RNA interaction modules. *Nature*, **407**, 405-409.

Andel, F., 3rd, Ladurner, A.G., Inouye, C., Tjian, R. and Nogales, E. (1999) Three-dimensional structure of the human TFIID-IIA-IIB complex. *Science*, **286**, 2153-2156.

Aoyagi, N., Oshige, M., Hirose, F., Kuroda, K., Matsukage, A. and Sakaguchi, K. (1997) DNA polymerase epsilon from Drosophila melanogaster. *Biochem Biophys Res Commun*, **230**, 297-301.

Aoyagi, S. and Hayes, J.J. (2002) hSWI/SNF-catalyzed nucleosome sliding does not occur solely via a twist-diffusion mechanism. *Mol Cell Biol*, **22**, 7484-7490.

Aoyagi, S., Wade, P.A. and Hayes, J.J. (2003) Nucleosome sliding induced by the xMi-2 complex does not occur exclusively via a simple twist-diffusion mechanism. *J Biol Chem*, **278**, 30562-30568.

Araki, H., Hamatake, R.K., Morrison, A., Johnson, A.L., Johnston, L.H. and Sugino, A. (1991) Cloning DPB3, the gene encoding the third subunit of DNA polymerase II of Saccharomyces cerevisiae. *Nucleic Acids Res*, **19**, 4867-4872.

Araki, H., Leem, S.H., Phongdara, A. and Sugino, A. (1995) Dpb11, which interacts with DNA polymerase II(epsilon) in Saccharomyces cerevisiae, has a dual role in S-phase progression and at a cell cycle checkpoint. *Proc Natl Acad Sci U S A*, **92**, 11791-11795.

Arents, G., Burlingame, R.W., Wang, B.-C., Love, W.E. and Moudrianakis, E.N. (1991) The nucleosomal core histone octamer at 3.1 A resolution: A tripartite protein assembly and a left-handed superhelix. Proc. Natl. Acad. Sci. USA, 88, 10148-10152.

Arents, G. and Moudrianakis, E.N. (1993) Topography of the histone octamer surface: repeating structural motifs in the docking of nucleosomal DNA. *Proc. Natl. Acad. Sci. USA*, **90**, 10489-10493.

Arents, G. and Moudrianakis, E.N. (1995) The histone fold: a ubiquitous architectural motif utilized in DNA compaction and protein dimerization. *Proc. Natl. Acad. Sci. USA*, **92**, 11170-11174.

Ashburner, M. (1989) *Drosophila: A laboratory manual.* Cold Spring Harbor Laboratory Press, Cold Spring Harbor, New York.

Asturias, F.J., Chung, W.H., Kornberg, R.D. and Lorch, Y. (2002) Structural analysis of the RSC chromatin-remodeling complex. *Proc Natl Acad Sci U S A*, **99**, 13477-13480.

Badenhorst, P., Voas, M., Rebay, I. and Wu, C. (2002) Biological functions of the ISWI chromatin remodeling complex NURF. *Genes Dev*, **16**, 3186-3198.

Badenhorst, P., Xiao, H., Cherbas, L., Kwon, S.Y., Voas, M., Rebay, I., Cherbas, P. and Wu, C. (2005) The Drosophila nucleosome remodeling factor NURF is required for Ecdysteroid signaling and metamorphosis. *Genes Dev*, **19**, 2540-2545.

Bao, Y., Konesky, K., Park, Y.J., Rosu, S., Dyer, P.N., Rangasamy, D., Tremethick, D.J., Laybourn, P.J. and Luger, K. (2004) Nucleosomes containing the histone variant H2A.Bbd organize only 118 base pairs of DNA. *Embo J*, **23**, 3314-3324.

Barak, O., Lazzaro, M.A., Lane, W.S., Speicher, D.W., Picketts, D.J. and Shiekhattar, R. (2003) Isolation of human NURF: a regulator of Engrailed gene expression. *Embo J*, **22**, 6089-6100.

Baumli, S., Hoeppner, S. and Cramer, P. (2005) A conserved mediator hinge revealed in the structure of the MED7.MED21 (Med7.Srb7) heterodimer. *J Biol Chem*, **280**, 18171-18178.

Becker, P.B. (2002) Nucleosome sliding: facts and fiction. *Embo J*, **21**, 4749-4753.

Becker, P.B. (2005) Nucleosome remodelers on track. *Nat Struct Mol Biol*, **12**, 732-733.

Becker, P.B. and Hörz, W. (2002) ATP-dependent nucleosome remodeling. *Annu Rev Biochem*, **71**, 247-273.

Becker, P.B. and Wu, C. (1992) Cell-free system for assembly of transcriptionally repressed chromatin from *Drosophila* embryos. *Mol. Cell. Biol.*, **12**, 2241-2249.

Berger, I., Fitzgerald, D.J. and Richmond, T.J. (2004) Baculovirus expression system for heterologous multiprotein complexes. *Nat Biotechnol*, **22**, 1583-1587.

Bianchi, M.E., Beltrame, M. and Paonessa, G. (1989) Specific recognition of cruciform DNA by nuclear protein HMG1. *Science*, **243**, 1056-1059.

Birck, C., Poch, O., Romier, C., Ruff, M., Mengus, G., Lavigne, A.C., Davidson, I. and Moras, D. (1998) Human TAF(II)28 and TAF(II)18 interact through a histone fold encoded by atypical evolutionary conserved motifs also found in the SPT3 family. *Cell*, **94**, 239-249.

Bochar, D.A., Savard, J., Wang, W., Lafleur, D.W., Moore, P., Cote, J. and Shiekhattar, R. (2000) A family of chromatin remodeling factors related to Williams syndrome transcription factor. *Proc Natl Acad Sci U S A*, **97**, 1038-1043.

Bolognese, F., Imbriano, C., Caretti, G. and Mantovani, R. (2000) Cloning and characterization of the histone-fold proteins YBL1 and YCL1. *Nucleic Acids Res*, **28**, 3830-3838.

Bonaldi, T., Längst, G., Strohner, R., Becker, P.B. and Bianchi, M.E. (2002) The DNA chaperone HMGB1 facilitates ACF/CHRAC-dependent nucleosome sliding. *Embo J*, **21**, 6865-6873.

Boonyaratanakornkit, V., Melvin, V., Prendergast, P., Altmann, M., Ronfani, L., Bianchi, M.E., Taraseviciene, L., Nordeen, S.K., Allegretto, E.A. and Edwards, D.P. (1998) High-mobility group chromatin proteins 1 and 2 functionally interact with steroid hormone receptors to enhance their DNA binding in vitro and transcriptional activity in mammalian cells. *Mol Cell Biol*, **18**, 4471-4487.

Bouazoune, K., Mitterweger, A., Langst, G., Imhof, A., Akhtar, A., Becker, P.B. and Brehm, A. (2002) The dMi-2 chromodomains are DNA binding modules important for ATP-dependent nucleosome mobilization. *Embo J*, **21**, 2430-2440.

Bouvet, P., Dimitrov, S. and Wolffe, A.P. (1994) Specific regulation of Xenopus chromosomal 5S rRNA gene transcription in vivo by histone H1. *Genes Dev.*, **8**, 1147-1159.

Bowen, N.J., Fujita, N., Kajita, M. and Wade, P.A. (2004) Mi-2/NuRD: multiple complexes for many purposes. *Biochim Biophys Acta*, **1677**, 52-57.

Bozhenok, L., Wade, P.A. and Varga-Weisz, P. (2002) WSTF-ISWI chromatin remodeling complex targets heterochromatic replication foci. *Embo J*, **21**, 2231-2241.

Brand, M., Leurent, C., Mallouh, V., Tora, L. and Schultz, P. (1999a) Three-dimensional structures of the TAFII-containing complexes TFIID and TFTC. *Science*, **286**, 2151-2153.

Brand, M., Yamamoto, K., Staub, A. and Tora, L. (1999b) Identification of TATA-binding protein-free TAFII-containing complex subunits suggests a role in nucleosome acetylation and signal transduction. *J Biol Chem*, **274**, 18285-18289.

Brehm, A., Längst, G., Kehle, J., Clapier, C.R., Imhof, A., Eberharter, A., Muller, J. and Becker, P.B. (2000) dMi-2 and ISWI chromatin remodelling factors have distinct nucleosome binding and mobilization properties]. *EMBO J*, **19**, 4332-4341.

Brunger, A.T., Adams, P.D., Clore, G.M., DeLano, W.L., Gros, P., Grosse-Kunstleve, R.W., Jiang, J.S., Kuszewski, J., Nilges, M., Pannu, N.S., Read, R.J., Rice, L.M., Simonson, T. and Warren, G.L. (1998) Crystallography & NMR system: A new software suite for macromolecular structure determination. *Acta Crystallogr D Biol Crystallogr*, **54 (Pt 5)**, 905-921.

Bruno, M., Flaus, A., Stockdale, C., Rencurel, C., Ferreira, H. and Owen-Hughes, T. (2003) Histone H2A/H2B dimer exchange by ATP-dependent chromatin remodeling activities. *Mol Cell*, **12**, 1599-1606.

Budd, M.E. and Campbell, J.L. (1995) DNA polymerases required for repair of UV-induced damage in Saccharomyces cerevisiae. *Mol Cell Biol*, **15**, 2173-2179.

Bustin, M. (2001) Revised nomenclature for high mobility group (HMG) chromosomal proteins. *Trends Biochem Sci*, **26**, 152-153.

Bustin, M., Catez, F. and Lim, J.H. (2005) The dynamics of histone H1 function in chromatin. *Mol Cell*, **17**, 617-620.

Cai, Y., Jin, J., Florens, L., Swanson, S.K., Kusch, T., Li, B., Workman, J.L., Washburn, M.P., Conaway, R.C. and Conaway, J.W. (2005) The mammalian YL1 protein is a shared subunit of the TRRAP/TIP60 histone acetyltransferase and SRCAP complexes. *J Biol Chem*, **280**, 13665-13670.

Cai, Y., Jin, J., Tomomori-Sato, C., Sato, S., Sorokina, I., Parmely, T.J., Conaway, R.C. and Conaway, J.W. (2003) Identification of new subunits of the multiprotein mammalian TRRAP/TIP60-containing histone acetyltransferase complex. *J Biol Chem*, **278**, 42733-42736.

Cairns, B.R., Kim, Y.J., Sayre, M.H., Laurent, B.C. and Kornberg, R.D. (1994) A multisubunit complex containing the SWI1/ADR6, SWI2/SNF2, SWI3, SNF5, and SNF6 gene products isolated from yeast. *Proc Natl Acad Sci U S A*, **91**, 1950-1954.

Cairns, B.R., Lorch, Y., Li, Y., Zhang, M., Lacomis, L., Erdjument-Bromage, H., Tempst, P., Du, J., Laurent, B. and Kornberg, R.D. (1996) RSC, an essential, abundant chromatin-remodeling complex. *Cell*, **87**, 1249-1260.

Carrozza, M.J., Li, B., Florens, L., Suganuma, T., Swanson, S.K., Lee, K.K., Shia, W.J., Anderson, S., Yates, J., Washburn, M.P. and Workman, J.L. (2005) Histone H3 methylation by Set2 directs deacetylation of coding regions by Rpd3S to suppress spurious intragenic transcription. *Cell*, **123**, 581-592.

Carrozza, M.J., Utley, R.T., Workman, J.L. and Cote, J. (2003) The diverse functions of histone acetyltransferase complexes. *Trends Genet*, **19**, 321-329.

Carson, M. (1991) Ribbons 2.0. *J. Appl. Crystallogr.*, **24**, 958-961.

Caruthers, J.M. and McKay, D.B. (2002) Helicase structure and mechanism. *Curr Opin Struct Biol*, **12**, 123-133.

Catez, F., Yang, H., Tracey, K.J., Reeves, R., Misteli, T. and Bustin, M. (2004) Network of dynamic interactions between histone H1 and high-mobility-group proteins in chromatin. *Mol Cell Biol*, **24**, 4321-4328.

CCP4. (1994) Collaborative Computational Project Number 4. The CCP4 suite: Programs for protein crystallography. *Acta Crystallogr.*, **D 50**, 760-776.

Chi, T.H., Wan, M., Zhao, K., Taniuchi, I., Chen, L., Littman, D.R. and Crabtree, G.R. (2002) Reciprocal regulation of CD4/CD8 expression by SWI/SNF-like BAF complexes. *Nature*, **418**, 195-199.

Clapier, C.R., Langst, G., Corona, D.F., Becker, P.B. and Nightingale, K.P. (2001) Critical role for the histone H4 N terminus in nucleosome remodeling by ISWI. *Mol. Cell. Biol.*, **21**, 875-883.

Clapier, C.R., Nightingale, K.P. and Becker, P.B. (2002) A critical epitope for substrate recognition by the nucleosome remodeling ATPase ISWI. *Nucleic Acids Res*, **30**, 649-655.

Clayton, A.L. and Mahadevan, L.C. (2003) MAP kinase-mediated phosphoacetylation of histone H3 and inducible gene regulation. *FEBS Lett*, **546**, 51-58.

Collins, N., Poot, R.A., Kukimoto, I., Garcia-Jimenez, C., Dellaire, G. and Varga-Weisz, P.D. (2002) An ACF1-ISWI chromatin-remodeling complex is required for DNA replication through heterochromatin. *Nat Genet*, **32**, 627-632.

Corona, D.F., Eberharter, A., Budde, A., Deuring, R., Ferrari, S., Varga-Weisz, P., Wilm, M., Tamkun, J. and Becker, P.B. (2000) Two histone fold proteins, CHRAC-14 and CHRAC-16, are developmentally regulated subunits of chromatin accessibility complex (CHRAC). *Embo J*, **19**, 3049-3059.

Corona, D.F. and Tamkun, J.W. (2004) Multiple roles for ISWI in transcription, chromosome organization and DNA replication. *Biochim Biophys Acta*, **1677**, 113-119.

Corona, D.F.V., Längst, G., Clapier, C.R., Bonte, E.J., Ferrari, S., Tamkun, J.W. and Becker, P.B. (1999) ISWI is an ATP-dependent nucleosome remodeling factor. *Molecular Cell*, **3**, 239-245.

Cuthbert, G.L., Daujat, S., Snowden, A.W., Erdjument-Bromage, H., Hagiwara, T., Yamada, M., Schneider, R., Gregory, P.D., Tempst, P., Bannister, A.J. and Kouzarides, T. (2004) Histone deimination antagonizes arginine methylation. *Cell*, **118**, 545-553.

DeLano, W.L. (2002) The PyMOL Molecular Graphics System. DeLano Scientific, San Carlos, CA, USA.

Deuring, R., Fanti, L., Armstrong, J., Sarte, M., Papoulas, O., Prestel, M., Daubresse, G., Verardo, M., Moseley, S., Berloco, M., Tsukiyama, T., Wu, C., Pimpinelli, S. and Tamkun, J.W. (2000) The ISWI chromatin remodeling protein is required for gene expression and the maintenance of higher order chromaitn structure in vivo. *Mol. Cell*, **5**, 355–365.

Dingwall, A.K., Beek, S.J., McCallum, C.M., Tamkun, J.W., Kalpana, G.V., Goff, S.P. and Scott, M.P. (1995) The Drosophila snr1 and brm proteins are related to yeast SWI/SNF proteins and are components of a large protein complex. *Mol Biol Cell*, **6**, 777-791.

Doerks, T., Copley, R.R. and Bork, P. (2001) DDT - a novel domain in different transcription and chromosome remodeling factors. *Trends Biochem Sci*, **26**, 145-146.

Dorigo, B., Schalch, T., Kulangara, A., Duda, S., Schroeder, R.R. and Richmond, T.J. (2004) Nucleosome arrays reveal the two-start organization of the chromatin fiber. *Science*, **306**, 1571-1573.

Dürr, H., Korner, C., Muller, M., Hickmann, V. and Hopfner, K.P. (2005) X-ray structures of the Sulfolobus solfataricus SWI2/SNF2 ATPase core and its complex with DNA. *Cell*, **121**, 363-373.

Eberharter, A. and Becker, P.B. (2002) Histone acetylation: a switch between repressive and permissive chromatin: Second in review series on chromatin dynamics. *EMBO Rep*, **3**, 224-229.

Eberharter, A. and Becker, P.B. (2004) ATP-dependent nucleosome remodelling: factors and functions. *J Cell Sci*, **117**, 3707-3711.

Eberharter, A., Ferrari, S., Langst, G., Straub, T., Imhof, A., Varga-Weisz, P., Wilm, M. and Becker, P.B. (2001) Acf1, the largest subunit of CHRAC, regulates ISWI-induced nucleosome remodelling. *EMBO J.*, **20**, 3781-3788.

Eberharter, A., Ferreira, R. and Becker, P. (2005) Dynamic chromatin: concerted nucleosome remodelling and acetylation. *Biol Chem*, **386**, 745-751.

Eberharter, A., Längst, G. and Becker, P.B. (2004a) A nucleosome sliding assay for chromatin remodeling factors. *Methods Enzymol*, **377**, 344-353.

Eberharter, A., Vetter, I., Ferreira, R. and Becker, P.B. (2004b) Acf1 improves the effectiveness of nucleosome mobilization by ISWI through PHD-histone contacts. *Embo J*, **in press**.

Eisen, J.A., Sweder, K.S. and Hanawalt, P.C. (1995) Evolution of the SNF2 family of proteins: subfamilies with distinct sequences and functions. *Nucleic Acids Res.*, **14**, 2715-2723.

Elfring, L.K., Deuring, R., McCallum, C.M., Peterson, C.L. and Tamkun, J.W. (1994) Identification and characterization of Drosophila relatives of the yeast transcriptional activator SNF2/SWI2. *Mol Cell Biol*, **14**, 2225-2234.

Fan, Y., Nikitina, T., Zhao, J., Fleury, T.J., Bhattacharyya, R., Bouhassira, E.E., Stein, A., Woodcock, C.L. and Skoultchi, A.I. (2005) Histone h1 depletion in mammals alters global chromatin structure but causes specific changes in gene regulation. *Cell*, **123**, 1199-1212.

Fazzio, T.G., Kooperberg, C., Goldmark, J.P., Neal, C., Basom, R., Delrow, J. and Tsukiyama, T. (2001) Widespread collaboration of isw2 and sin3-rpd3 chromatin remodeling complexes in transcriptional repression. *Mol Cell Biol*, **21**, 6450-6460.

Fazzio, T.G. and Tsukiyama, T. (2003) Chromatin remodeling in vivo: evidence for a nucleosome sliding mechanism. *Mol Cell*, **12**, 1333-1340.

Feng, Q. and Zhang, Y. (2001) The MeCP1 complex represses transcription through preferential binding, remodeling, and deacetylating methylated nucleosomes. *Genes Dev*, **15**, 827-832.

Filipski, J., Leblanc, J., Youdale, T., Sikorska, M. and Walker, P.R. (1990) Periodicity of DNA folding in higher order chromatin structures. *Embo J*, **9**, 1319-1327.

Finch, J.T. and Klug, A. (1976) Solenoidal model for superstructure in chromatin. *Proc. Natl. Acad. Sci. USA*, **73**, 1897-1901.

Fischle, W., Wang, Y. and Allis, C.D. (2003) Binary switches and modification cassettes in histone biology and beyond. *Nature*, **425**, 475-479.

Fitzgerald, D.J., DeLuca, C., Berger, I., Gaillard, H., Sigrist, R., Schimmele, K. and Richmond, T.J. (2004) Reaction cycle of the yeast Isw2 chromatin remodeling complex. *Embo J*, **23**, 3836-3843.

Flaus, A. and Owen-Hughes, T. (2004) Mechanisms for ATP-dependent chromatin remodelling: farewell to the tuna-can octamer? *Curr Opin Genet Dev*, **14**, 165-173.

Fribourg, S., Romier, C., Werten, S., Gangloff, Y.G., Poterszman, A. and Moras, D. (2001) Dissecting the interaction network of multiprotein complexes by pairwise coexpression of subunits in E. coli. *J Mol Biol*, **306**, 363-373.

Frontini, M., Imbriano, C., diSilvio, A., Bell, B., Bogni, A., Romier, C., Moras, D., Tora, L., Davidson, I. and Mantovani, R. (2002) NF-Y recruitment of TFIID, multiple interactions with histone fold TAF(II)s. *J Biol Chem*, **277**, 5841-5848.

Fugmann, S.D., Lee, A.I., Shockett, P.E., Villey, I.J. and Schatz, D.G. (2000) The RAG proteins and V(D)J recombination: complexes, ends, and transposition. *Annu Rev Immunol*, **18**, 495-527.

Fuss, J. and Linn, S. (2002) Human DNA polymerase epsilon colocalizes with proliferating cell nuclear antigen and DNA replication late, but not early, in S phase. *J Biol Chem*, **277**, 8658-8666.

Fyodorov, D.V., Blower, M.D., Karpen, G.H. and Kadonaga, J.T. (2004) Acf1 confers unique activities to ACF/CHRAC and promotes the formation rather than disruption of chromatin in vivo. *Genes Dev*, **18**, 170-183.

Fyodorov, D.V. and Kadonaga, J.T. (2002) Binding of Acf1 to DNA involves a WAC motif and is important for ACF-mediated chromatin assembly. *Mol Cell Biol*, **22**, 6344-6353.

Gangloff, Y.G., Sanders, S.L., Romier, C., Kirschner, D., Weil, P.A., Tora, L. and Davidson, I. (2001) Histone folds mediate selective heterodimerization of yeast TAF(II)25 with TFIID components yTAF(II)47 and yTAF(II)65 and with SAGA component ySPT7. *Mol Cell Biol*, **21**, 1841-1853.

Gangloff, Y.G., Werten, S., Romier, C., Carre, L., Poch, O., Moras, D. and Davidson, I. (2000) The human TFIID components TAF(II)135 and TAF(II)20 and the yeast SAGA components ADA1 and TAF(II)68 heterodimerize to form histone-like pairs. *Mol Cell Biol*, **20**, 340-351.

Gdula, D.A., Sandaltzopoulos, R., Tsukiyama, T., Ossipow, V. and Wu, C. (1998) Inorganic pyrophosphatase is a component of the Drosophila nucleosome remodeling factor complex. *Genes Dev*, **12**, 3206-3216.

Gelbart, M.E., Rechsteiner, T., Richmond, T.J. and Tsukiyama, T. (2001) Interactions of Isw2 chromatin remodeling complex with nucleosomal arrays: analyses using recombinant yeast histones and immobilized templates. *Mol Cell Biol*, **21**, 2098-2106.

Gilfillan, S., Stelzer, G., Piaia, E., Hofmann, M.G. and Meisterernst, M. (2005) Efficient binding of NC2.TATA-binding protein to DNA in the absence of TATA. *J Biol Chem*, **280**, 6222-6230.

Goldmark, J.P., Fazzio, T.G., Estep, P.W., Church, G.M. and Tsukiyama, T. (2000) The Isw2 chromatin remodeling complex represses early meiotic genes upon recruitment by Ume6p. *Cell*, **103**, 423-433.

Goppelt, A., Stelzer, G., Lottspeich, F. and Meisterernst, M. (1996) A mechanism for repression of class II gene transcription through specific binding of NC2 to TBP-promoter complexes via heterodimeric histone fold domains. *Embo J*, **15**, 3105-3116.

Grant, P.A., Schieltz, D., Pray-Grant, M.G., Steger, D.J., Reese, J.C., Yates, J.R., 3rd and Workman, J.L. (1998) A subset of TAF(II)s are integral components of the SAGA complex required for nucleosome acetylation and transcriptional stimulation [see comments]. *Cell*, **94**, 45-53.

Grayling, R.A., Bailey, K.A. and Reeve, J.N. (1997) DNA binding and nuclease protection by the HMf histones from the hyperthermophilic archaeon Methanothermus fervidus. *Extremophiles*, **1**, 79-88.

Grayling, R.A., Sandman, K. and Reeve, J.N. (1996) Histones and chromatin structure in hyperthermophilic Archaea. *FEMS Microbiol Rev*, **18**, 203-213.

Greil, F., van der Kraan, I., Delrow, J., Smothers, J.F., de Wit, E., Bussemaker, H.J., van Driel, R., Henikoff, S. and van Steensel, B. (2003) Distinct HP1 and Su(var)3-9 complexes bind to sets of developmentally coexpressed genes depending on chromosomal location. *Genes Dev*, **17**, 2825-2838.

Grüne, T., Brzeski, J., Eberharter, A., Clapier, C.R., Corona, D.F., Becker, P.B. and Müller, C.W. (2003) Crystal structure and functional analysis of a nucleosome recognition module of the remodeling factor ISWI. *Mol Cell*, **12**, 449-460.

Guschin, D., Geiman, T.M., Kikyo, N., Tremethick, D.J., Wolffe, A.P. and Wade, P.A. (2000a) Multiple ISWI ATPase complexes from xenopus laevis. Functional conservation of an ACF/CHRAC homolog. *J Biol Chem*, **275**, 35248-35255.

Guschin, D., Wade, P.A., Kikyo, N. and Wolffe, A.P. (2000b) ATP-Dependent histone octamer mobilization and histone deacetylation mediated by the Mi-2 chromatin remodeling complex. *Biochemistry*, **39**, 5238-5245.

Hagemeier, C., Cook, A. and Kouzarides, T. (1993) The retinoblastoma protein binds E2F residues required for activation in vivo and TBP binding in vitro. *Nucleic Acids Res*, **21**, 4998-5004.

Hamatake, R.K., Hasegawa, H., Clark, A.B., Bebenek, K., Kunkel, T.A. and Sugino, A. (1990) Purification and characterization of DNA polymerase II from the yeast Saccharomyces cerevisiae. Identification of the catalytic core and a possible holoenzyme form of the enzyme. *J Biol Chem*, **265**, 4072-4083.

Hartlepp, K.F., Fernández-Tornero, C., Eberharter, A., Grüne, T., Müller, C.W. and Becker, P.B. (2005) The Histone Fold Subunits of Drosophila CHRAC Facilitate Nucleosome Sliding through Dynamic DNA Interactions. *Mol Cell Biol*, **25**, 9886-9896.

Havas, K., Flaus, A., Phelan, M., Kingston, R., Wade, P.A., Lilley, D.M. and Owen-Hughes, T. (2000) Generation of superhelical torsion by ATP-dependent chromatin remodeling activities. *Cell*, **103**, 1133-1142.

Hill, D.A. and Imbalzano, A.N. (2000) Human SWI/SNF nucleosome remodeling activity is partially inhibited by linker histone H1. *Biochemistry*, **39**, 11649-11656.

Hiraga, S., Hagihara-Hayashi, A., Ohya, T. and Sugino, A. (2005) DNA polymerases alpha, delta, and epsilon localize and function together at replication forks in Saccharomyces cerevisiae. *Genes Cells*, **10**, 297-309.

Hoffmann, A., Chiang, C.M., Oelgeschlager, T., Xie, X., Burley, S.K., Nakatani, Y. and Roeder, R.G. (1996) A histone octamer-like structure within TFIID. *Nature*, **380**, 356-359.

Horn, P.J., Carruthers, L.M., Logie, C., Hill, D.A., Solomon, M.J., Wade, P.A., Imbalzano, A.N., Hansen, J.C. and Peterson, C.L. (2002) Phosphorylation of linker histones regulates ATP-dependent chromatin remodeling enzymes. *Nat Struct Biol*, **9**, 263-267.

Huynh, V.A., Robinson, P.J. and Rhodes, D. (2005) A method for the in vitro reconstitution of a defined "30 nm" chromatin fibre containing stoichiometric amounts of the linker histone. *J Mol Biol*, **345**, 957-968.

Igo-Kemenes, T. and Zachau, H.G. (1978) Domains in chromatin structure. *Cold Spring Harb Symp Quant Biol*, **42 Pt 1**, 109-118.

Iida, T. and Araki, H. (2004) Noncompetitive counteractions of DNA polymerase epsilon and ISW2/yCHRAC for epigenetic inheritance of telomere position effect in Saccharomyces cerevisiae. *Mol Cell Biol*, **24**, 217-227.

Imbriano, C., Gurtner, A., Cocchiarella, F., Di Agostino, S., Basile, V., Gostissa, M., Dobbelstein, M., Del Sal, G., Piaggio, G. and Mantovani, R. (2005) Direct p53 transcriptional repression: in vivo analysis of CCAAT-containing G2/M promoters. *Mol Cell Biol*, **25**, 3737-3751.

Iratni, R., Yan, Y.T., Chen, C., Ding, J., Zhang, Y., Price, S.M., Reinberg, D. and Shen, M.M. (2002) Inhibition of excess nodal signaling during mouse gastrulation by the transcriptional corepressor DRAP1. *Science*, **298**, 1996-1999.

Ito, T., Bulger, M., Pazin, M.J., Kobayashi, R. and Kadonaga, J.T. (1997) ACF, an ISWI-containing and ATP-utilizing chromatin assembly and remodeling factor. *Cell*, **90**, 145-155.

Ito, T., Levenstein, M.E., Fyodorov, D.V., Kutach, A.K., Kobayashi, R. and Kadonaga, J.T. (1999) ACF consists of two subunits, Acf1 and ISWI, that function cooperatively in the ATP-dependent catalysis of chromatin assembly. *Genes Dev*, **13**, 1529-1539.

Izumi, H., Molander, C., Penn, L.Z., Ishisaki, A., Kohno, K. and Funa, K. (2001) Mechanism for the transcriptional repression by c-Myc on PDGF beta-receptor. *J Cell Sci*, **114**, 1533-1544.

Jaskelioff, M., Gavin, I.M., Peterson, C.L. and Logie, C. (2000) SWI-SNF-mediated nucleosome remodeling: role of histone octamer mobility in the persistence of the remodeled state. *Mol Cell Biol*, **20**, 3058-3068.

Jaskelioff, M., Van Komen, S., Krebs, J.E., Sung, P. and Peterson, C.L. (2003) Rad54p is a chromatin remodeling enzyme required for heteroduplex DNA joint formation with chromatin. *J Biol Chem*, **278**, 9212-9218.

Jayaraman, L., Moorthy, N.C., Murthy, K.G., Manley, J.L., Bustin, M. and Prives, C. (1998) High mobility group protein-1 (HMG-1) is a unique activator of p53. *Genes Dev*, **12**, 462-472.

Jenuwein, T. and Allis, C.D. (2001) Translating the histone code. *Science*, **293**, 1074-1080.

Jin, J., Cai, Y., Li, B., Conaway, R.C., Workman, J.L., Conaway, J.W. and Kusch, T. (2005a) In and out: histone variant exchange in chromatin. *Trends Biochem Sci.*

Jin, J., Cai, Y., Yao, T., Gottschalk, A.J., Florens, L., Swanson, S.K., Gutierrez, J.L., Coleman, M.K., Workman, J.L., Mushegian, A., Washburn, M.P., Conaway, R.C. and Conaway, J.W. (2005b) A mammalian chromatin remodeling complex with similarities to the yeast INO80 complex. *J Biol Chem*.

Jones, M.H., Hamana, N., Nezu, J. and Shimane, M. (2000) A novel family of bromodomain genes. *Genomics*, **63**, 40-45.

Jones, T., Zhou, J., Cowan, S. and Kjeldgaard, M. (1991) Improved methods for building protein models in electron density maps and the location of errors in these models. *Acta Crystallogr.*, **A47**, 110-119.

Kagalwala, M.N., Glaus, B.J., Dang, W., Zofall, M. and Bartholomew, B. (2004) Topography of the ISW2-nucleosome complex: insights into nucleosome spacing and chromatin remodeling. *Embo J*, **23**, 2092-2104.

Kamada, K., Shu, F., Chen, H., Malik, S., Stelzer, G., Roeder, R.G., Meisterernst, M. and Burley, S.K. (2001) Crystal structure of negative cofactor 2 recognizing the TBP-DNA transcription complex. *Cell*, **106**, 71-81.

Kamakaka, R.T. and Biggins, S. (2005) Histone variants: deviants? *Genes Dev*, **19**, 295-310.

Kassabov, S.R., Henry, N.M., Zofall, M., Tsukiyama, T. and Bartholomew, B. (2002) High-resolution mapping of changes in histone-DNA contacts of nucleosomes remodeled by ISW2. *Mol Cell Biol*, **22**, 7524-7534.

Kassabov, S.R., Zhang, B., Persinger, J. and Bartholomew, B. (2003) SWI/SNF unwraps, slides, and rewraps the nucleosome. *Mol Cell*, **11**, 391-403.

Kelley, D.E., Stokes, D.G. and Perry, R.P. (1999) CHD1 interacts with SSRP1 and depends on both its chromodomain and its ATPase/helicase-like domain for proper association with chromatin. *Chromosoma*, **108**, 10-25.

Keogh, M.C., Kurdistani, S.K., Morris, S.A., Ahn, S.H., Podolny, V., Collins, S.R., Schuldiner, M., Chin, K., Punna, T., Thompson, N.J., Boone, C., Emili, A., Weissman, J.S., Hughes, T.R., Strahl, B.D., Grunstein, M., Greenblatt, J.F., Buratowski, S. and Krogan, N.J. (2005) Cotranscriptional set2 methylation of histone H3 lysine 36 recruits a repressive Rpd3 complex. *Cell*, **123**, 593-605.

Kim, S., Na, J.G., Hampsey, M. and Reinberg, D. (1997) The Dr1/DRAP1 heterodimer is a global repressor of transcription in vivo. *Proc Natl Acad Sci U S A*, **94**, 820-825.

Kingston, R.E. and Narlikar, G.J. (1999) ATP-dependent remodeling and acetylation as regulators of chromatin fluidity. *Genes Dev*, **13**, 2339-2352.

Kitagawa, H., Fujiki, R., Yoshimura, K., Mezaki, Y., Uematsu, Y., Matsui, D., Ogawa, S., Unno, K., Okubo, M., Tokita, A., Nakagawa, T., Ito, T., Ishimi, Y., Nagasawa, H., Matsumoto, T., Yanagisawa, J. and Kato, S. (2003) The chromatin-remodeling complex WINAC targets a nuclear receptor to promoters and is impaired in Williams syndrome. *Cell*, **113**, 905-917.

Knapp, S., Muller, S., Digilio, G., Bonaldi, T., Bianchi, M.E. and Musco, G. (2004) The long acidic tail of high mobility group box 1 (HMGB1) protein forms an extended and flexible structure that interacts with specific residues within and between the HMG boxes. *Biochemistry*, **43**, 11992-11997.

Kobor, M.S., Venkatasubrahmanyam, S., Meneghini, M.D., Gin, J.W., Jennings, J.L., Link, A.J., Madhani, H.D. and Rine, J. (2004) A protein complex containing the conserved Swi2/Snf2-related ATPase Swr1p deposits histone variant H2A.Z into euchromatin. *PLoS Biol*, **2**, E131.

Kokubo, T., Gong, D.W., Wootton, J.C., Horikoshi, M., Roeder, R.G. and Nakatani, Y. (1994) Molecular cloning of Drosophila TFIID subunits. *Nature*, **367**, 484-487.

Krebs, J.E., Fry, C.J., Samuels, M.L. and Peterson, C.L. (2000) Global role for chromatin remodeling enzymes in mitotic gene expression. *Cell*, **102**, 587-598.

Krogan, N.J., Keogh, M.C., Datta, N., Sawa, C., Ryan, O.W., Ding, H., Haw, R.A., Pootoolal, J., Tong, A., Canadien, V., Richards, D.P., Wu, X., Emili, A., Hughes, T.R., Buratowski, S. and Greenblatt, J.F. (2003) A Snf2 family ATPase complex required for recruitment of the histone H2A variant Htz1. *Mol Cell*, **12**, 1565-1576.

Kukimoto, I., Elderkin, S., Grimaldi, M., Oelgeschlager, T. and Varga-Weisz, P.D. (2004) The histone-fold protein complex CHRAC-15/17 enhances nucleosome sliding and assembly mediated by ACF. *Mol Cell*, **13**, 265-277.

Kusch, T., Florens, L., Macdonald, W.H., Swanson, S.K., Glaser, R.L., Yates, J.R., 3rd, Abmayr, S.M., Washburn, M.P. and Workman, J.L. (2004) Acetylation by Tip60 is required for selective histone variant exchange at DNA lesions. *Science*, **306**, 2084-2087.

Lachner, M., O'Carroll, D., Rea, S., Mechtler, K. and Jenuwein, T. (2001) Methylation of histone H3 lysine 9 creates a binding site for HP1 proteins. *Nature*, **410**, 116-120.

Laemmli, U.K. (1970) Cleavage of structural proteins during the assembly of the head of bacteriophage T4. *Nature*, **227**, 680-685.

Längst, G. and Becker, P.B. (2001a) ISWI induces nucleosome sliding on nicked DNA. *Mol Cell*, **8**, 1085-1092.

Längst, G. and Becker, P.B. (2001b) Nucleosome mobilization and positioning by ISWI-containing chromatin remodeling factors. *J. Cell Science*, **114**, 2561-2568.

Längst, G. and Becker, P.B. (2004) Nucleosome remodeling: one mechanism, many phenomena? *Biochim Biophys Acta*, **1677**, 58-63.

Längst, G., Bonte, E.J., Corona, D.F.V. and Becker, P.B. (1999) Nucleosome movement by CHRAC and ISWI without disruption or trans-displacement of the histone octamer. *Cell*, **97**, 843-852.

Lee, Y.S. and Carthew, R.W. (2003) Making a better RNAi vector for Drosophila: use of intron spacers. *Methods*, **30**, 322-329.

LeRoy, G., Loyola, A., Lane, W.S. and Reinberg, D. (2000) Purification and characterization of a human factor that assembles and remodels chromatin. *J Biol Chem*, **275**, 14787-14790.

LeRoy, G., Orphanides, G., Lane, W.S. and Reinberg, D. (1998) Requirement of RSF and FACT for transcription of chromatin templates in vitro [see comments]. *Science*, **282**, 1900-1904.

Leurent, C., Sanders, S., Ruhlmann, C., Mallouh, V., Weil, P.A., Kirschner, D.B., Tora, L. and Schultz, P. (2002) Mapping histone fold TAFs within yeast TFIID. *Embo J*, **21**, 3424-3433.

Leurent, C., Sanders, S.L., Demeny, M.A., Garbett, K.A., Ruhlmann, C., Weil, P.A., Tora, L. and Schultz, P. (2004) Mapping key functional sites within yeast TFIID. *Embo J*, **23**, 719-727.

Li, G., Levitus, M., Bustamante, C. and Widom, J. (2005) Rapid spontaneous accessibility of nucleosomal DNA. *Nat Struct Mol Biol*, **12**, 46-53.

Li, Y., Pursell, Z.F. and Linn, S. (2000) Identification and cloning of two histone fold motif-containing subunits of HeLa DNA polymerase epsilon. *J Biol Chem*, **275**, 31554.

Liang, S.G. and Maity, S.N. (1998) Pathway of complex formation between DNA and three subunits of CBF/NF-Y. Photocross-linking analysis of DNA-protein interaction and characterization of equilibrium steps of subunit interaction and dna binding. *J Biol Chem*, **273**, 31590-31598.

Lorch, Y., Davis, B. and Kornberg, R.D. (2005) Chromatin remodeling by DNA bending, not twisting. *Proc Natl Acad Sci U S A*, **102**, 1329-1332.

Lorch, Y., Zhang, M. and Kornberg, R.D. (2001) RSC unravels the nucleosome. *Mol Cell*, **7**, 89-95.

Loyola, A. and Almouzni, G. (2004) Histone chaperones, a supporting role in the limelight. *Biochim Biophys Acta*, **1677**, 3-11.

Loyola, A., Huang, J.Y., LeRoy, G., Hu, S., Wang, Y.H., Donnelly, R.J., Lane, W.S., Lee, S.C. and Reinberg, D. (2003) Functional analysis of the subunits of the chromatin assembly factor RSF. *Mol Cell Biol*, **23**, 6759-6768.

Luger, K., Mäder, A.W., Richmond, R.K., Sargent, D.F. and Richmond, T.J. (1997) Crystal structure of the nucleosome core particle at 2.8 A resolution. *Nature*, **389**, 251-260.

Luger, K., Rechsteiner, T.J. and Richmond, T.J. (1999) Preparation of nucleosome core particle from recombinant histones. *Methods Enzymol*, **304**, 3-19.

Luger, K. and Richmond, T.J. (1998) DNA binding within the nucleosome core. *Curr Opin Struct Biol*, **8**, 33-40.

Lusser, A., Urwin, D.L. and Kadonaga, J.T. (2005) Distinct activities of CHD1 and ACF in ATP-dependent chromatin assembly. *Nat Struct Mol Biol*, **12**, 160-166.

Lutzmann, M., Kunze, R., Buerer, A., Aebi, U. and Hurt, E. (2002) Modular self-assembly of a Y-shaped multiprotein complex from seven nucleoporins. *Embo J*, **21**, 387-397.

MacCallum, D.E., Losada, A., Kobayashi, R. and Hirano, T. (2002) ISWI remodeling complexes in Xenopus egg extracts: identification as major chromosomal components that are regulated by INCENP-aurora B. *Mol Biol Cell*, **13**, 25-39.

Maity, S.N. and de Crombrugghe, B. (1998) Role of the CCAAT-binding protein CBF/NF-Y in transcription. *Trends Biochem Sci*, **23**, 174-178.

Martinez-Balbas, M.A., Tsukiyama, T., Gdula, D. and Wu, C. (1998) Drosophila NURF-55, a WD repeat protein involved in histone metabolism. *Proc Natl Acad Sci U S A*, **95**, 132-137.

Mateescu, B., England, P., Halgand, F., Yaniv, M. and Muchardt, C. (2004) Tethering of HP1 proteins to chromatin is relieved by phosphoacetylation of histone H3. *EMBO Rep*, **5**, 490-496.

McConnell, A.D., Gelbart, M.E. and Tsukiyama, T. (2004) Histone fold protein Dls1p is required for Isw2-dependent chromatin remodeling in vivo. *Mol Cell Biol*, **24**, 2605-2613.

McNabb, D.S., Xing, Y. and Guarente, L. (1995) Cloning of yeast HAP5: a novel subunit of a heterotrimeric complex required for CCAAT binding. *Genes Dev*, **9**, 47-58.

Medina, P.P., Carretero, J., Fraga, M.F., Esteller, M., Sidransky, D. and Sanchez-Cespedes, M. (2004) Genetic and epigenetic screening for gene alterations of the chromatin-remodeling factor, SMARCA4/BRG1, in lung tumors. *Genes Chromosomes Cancer*, **41**, 170-177.

Meeks-Wagner, D. and Hartwell, L.H. (1986) Normal stoichiometry of histone dimer sets is necessary for high fidelity of mitotic chromosome transmission. *Cell*, **44**, 43– 52.

Meisterernst, M. and Roeder, R.G. (1991) Family of proteins that interact with TFIID and regulate promoter activity. *Cell*, **67**, 557-567.

Mellor, J. and Morillon, A. (2004) ISWI complexes in Saccharomyces cerevisiae. *Biochim Biophys Acta*, **1677**, 100-112.

Meshorer, E., Yellajoshula, D., George, E., Scambler, P.J., Brown, D.T. and Misteli, T. (2006) Hyperdynamic plasticity of chromatin proteins in pluripotent embryonic stem cells. *Dev Cell*, **10**, 105-116.

Mizuguchi, G., Shen, X., Landry, J., Wu, W.H., Sen, S. and Wu, C. (2004) ATP-driven exchange of histone H2AZ variant catalyzed by SWR1 chromatin remodeling complex. *Science*, **303**, 343-348.

Mizzen, C.A., Yang, X.J., Kokubo, T., Brownell, J.E., Bannister, A.J., Owen-Hughes, T., Workman, J., Wang, L., Berger, S.L., Kouzarides, T., Nakatani, Y. and Allis, C.D. (1996) The TAF(II)250 subunit of TFIID has histone acetyltransferase activity. *Cell*, **87**, 1261-1270.

Mohrmann, L., Langenberg, K., Krijgsveld, J., Kal, A.J., Heck, A.J. and Verrijzer, C.P. (2004) Differential targeting of two distinct SWI/SNF-related Drosophila chromatin-remodeling complexes. *Mol Cell Biol*, **24**, 3077-3088.

Mohrmann, L. and Verrijzer, C.P. (2005) Composition and functional specificity of SWI2/SNF2 class chromatin remodeling complexes. *Biochim Biophys Acta*, **1681**, 59-73.

Morrison, A., Araki, H., Clark, A.B., Hamatake, R.K. and Sugino, A. (1990) A third essential DNA polymerase in S. cerevisiae. *Cell*, **62**, 1143-1151.

Müller, F. and Tora, L. (2004) The multicoloured world of promoter recognition complexes. *Embo J*, **23**, 2-8.

Muller, S., Bianchi, M.E. and Knapp, S. (2001) Thermodynamics of HMGB1 interaction with duplex DNA. *Biochemistry*, **40**, 10254-10261.

Navas, T.A., Zhou, Z. and Elledge, S.J. (1995) DNA polymerase epsilon links the DNA replication machinery to the S phase checkpoint. *Cell*, **80**, 29-39.

Neigeborn, L. and Carlson, M. (1984) Genes affecting the regulation of SUC2 gene expression by glucose repression in Saccharomyces cerevisiae. *Genetics*, **108**, 845-858.

Ner, S.S., Blank, T., Perez-Paralle, M.L., Grigliatti, T.A., Becker, P.B. and Travers, A.A. (2001) HMG-D and histone H1 interplay during chromatin assembly and early embryogenesis. *J. Biol. Chem.*, **276**, 37569-37576.

Ner, S.S. and Travers, A.A. (1994) HMG-D, the *Drosophila melanogaster* homologue of HMG 1 protein, is associated with early embryonic chromatin in the absence of histone H1. *EMBO J.*, **13**, 1817-1822.

Nicholls, A., Bharadwaj, R. and Honig, B. (1993) GRASP - graphical representation and analysis of surface properties. *Biophysics Journal*, **64**, A166-A166.

Nightingale, K., Dimitrov, S., Reeves, R. and Wolffe, A.P. (1996) Evidence for a shared structural role for HMG1 and linker histones B4 and H1 in organizing chromatin. *Embo J*, **15**, 548-561.

Nightingale, K.P., Wellinger, R.E., Sogo, J.M. and Becker, P.B. (1998) Histone acetylation facilitates RNA polymerase II transcription of the Drosophila hsp26 gene in chromatin. *Embo J*, **17**, 2865-2876.

Nowak, S.J. and Corces, V.G. (2004) Phosphorylation of histone H3: a balancing act between chromosome condensation and transcriptional activation. *Trends Genet*, **20**, 214-220.

Ogata, K., Morikawa, S., Nakamura, H., Sekikawa, A., Inoue, T., Kanai, H., Sarai, A., Ishii, S. and Nishimura, Y. (1994) Solution structure of a specific DNA complex of the Myb DNA-binding domain with cooperative recognition helices. *Cell*, **79**, 639-648.

Ohya, T., Maki, S., Kawasaki, Y. and Sugino, A. (2000) Structure and function of the fourth subunit (Dpb4p) of DNA polymerase epsilon in Saccharomyces cerevisiae. *Nucleic Acids Res*, **28**, 3846-3852.

Oshige, M., Yoshida, H., Hirose, F., Takata, K.I., Inoue, Y., Aoyagi, N., Yamaguchi, M., Koiwai, O., Matsukage, A. and Sakaguchi, K. (2000) Molecular cloning and expression during development of the Drosophila gene for the catalytic subunit of DNA polymerase epsilon. *Gene*, **256**, 93-100.

Papoulas, O., Beek, S.J., Moseley, S.L., McCallum, C.M., Sarte, M., Shearn, A. and Tamkun, J.W. (1998) The Drosophila trithorax group proteins BRM, ASH1 and ASH2 are subunits of distinct protein complexes. *Development*, **125**, 3955-3966.

Papoulas, O., Daubresse, G., Armstrong, J.A., Jin, J., Scott, M.P. and Tamkun, J.W. (2001) The HMG-domain protein BAP111 is important for the function of the BRM chromatin-remodeling complex in vivo. *Proc Natl Acad Sci U S A*, **98**, 5728-5733.

Payet, D. and Travers, A. (1997) The acidic tail of the high mobility group protein HMG-D modulates the structural selectivity of DNA binding. *J Mol Biol*, **266**, 66-75.

Pennings, S., Meersseman, G. and Bradbury, E.M. (1994) Linker histones H1 and H5 prevent the mobility of positioned nucleosomes. *Proc. Natl. Acad. Sci. USA*, **91**.

Pereira, S.L. and Reeve, J.N. (1998) Histones and nucleosomes in Archaea and Eukarya: a comparative analysis. *Extremophiles*, **2**, 141-148.

Peterson, C.L. and Cote, J. (2004) Cellular machineries for chromosomal DNA repair. *Genes Dev*, **18**, 602-616.

Peterson, C.L., Dingwall, A. and Scott, M.P. (1994) Five SWI/SNF gene products are components of a large multisubunit complex required for transcriptional enhancement [see comments]. *Proc Natl Acad Sci U S A*, **91**, 2905-2908.

Phelan, M.L., Schnitzler, G.R. and Kingston, R.E. (2000) Octamer transfer and creation of stably remodeled nucleosomes by human SWI-SNF and its isolated ATPases. *Mol Cell Biol*, **20**, 6380-6389.

Phelan, M.L., Sif, S., Narlikar, G.J. and Kingston, R.E. (1999) Reconstitution of a core chromatin remodeling complex from SWI/SNF subunits. *Mol Cell*, **3**, 247-253.

Poot, R.A., Dellaire, G., Hulsmann, B.B., Grimaldi, M.A., Corona, D.F., Becker, P.B., Bickmore, W.A. and Varga-Weisz, P.D. (2000) HuCHRAC, a human ISWI chromatin remodelling complex contains hACF1 and two novel histone-fold proteins. *Embo J*, **19**, 3377-3387.

Qian, C., Zhang, Q., Li, S., Zeng, L., Walsh, M.J. and Zhou, M.M. (2005) Structure and chromosomal DNA binding of the SWIRM domain. *Nat Struct Mol Biol*, **12**, 1078-1085.

Ragab, A. and Travers, A. (2003) HMG-D and histone H1 alter the local accessibility of nucleosomal DNA. *Nucleic Acids Res*, **31**, 7083-7089.

Ramachandran, A., Omar, M., Cheslock, P. and Schnitzler, G.R. (2003) Linker histone H1 modulates nucleosome remodeling by human SWI/SNF. *J Biol Chem*, **278**, 48590-48601.

Ramstein, J., Locker, D., Bianchi, M.E. and Leng, M. (1999) Domain-domain interactions in high mobility group 1 protein (HMG1). *Eur J Biochem*, **260**, 692-700.

Rangasamy, D., Berven, L., Ridgway, P. and Tremethick, D.J. (2003) Pericentric heterochromatin becomes enriched with H2A.Z during early mammalian development. *Embo J*, **22**, 1599-1607.

Rangasamy, D., Greaves, I. and Tremethick, D.J. (2004) RNA interference demonstrates a novel role for H2A.Z in chromosome segregation. *Nat Struct Mol Biol*, **11**, 650-655.

Redon, C., Pilch, D., Rogakou, E., Sedelnikova, O., Newrock, K. and Bonner, W. (2002) Histone H2A variants H2AX and H2AZ. *Curr Opin Genet Dev*, **12**, 162-169.

Reese, J.C., Zhang, Z. and Kurpad, H. (2000) Identification of a yeast transcription factor IID subunit, TSG2/TAF48. *J Biol Chem*, **275**, 17391-17398.

Reeve, J.N., Bailey, K.A., Li, W.T., Marc, F., Sandman, K. and Soares, D.J. (2004) Archaeal histones: structures, stability and DNA binding. *Biochem Soc Trans*, **32**, 227-230.

Richmond, T.J. and Davey, C.A. (2003) The structure of DNA in the nucleosome core. *Nature*, **423**, 145-150.

Romier, C., Cocchiarella, F., Mantovani, R. and Moras, D. (2003) The NF-YB/NF-YC structure gives insight into DNA binding and transcription regulation by CCAAT factor NF-Y. *J Biol Chem*, **278**, 1336-1345.

Ronchi, A., Bellorini, M., Mongelli, N. and Mantovani, R. (1995) CCAAT-box binding protein NF-Y (CBF, CP1) recognizes the minor groove and distorts DNA. *Nucleic Acids Res*, **23**, 4565-4572.

Rost, B. (1996) PHD: predicting one-dimensional protein structure by profile-based neural networks. *Methods Enzymol*, **266**, 525-539.

Rost, B. and Sander, C. (1994) Combining evolutionary information and neural networks to predict protein secondary structure. *Proteins*, **19**, 55-72.

Rupp, R.A. and Becker, P.B. (2005) Gene regulation by histone h1: new links to DNA methylation. *Cell*, **123**, 1178-1179.

Saha, A., Wittmeyer, J. and Cairns, B.R. (2005) Chromatin remodeling through directional DNA translocation from an internal nucleosomal site. *Nat Struct Mol Biol*, **12**, 747-755.

Sambrook, J. and Russell, D.W. (2001) *Molecular Cloning - A Laboratory Manual.* Cold Spring Harbor Laboratory Press, Cold Spring Harbor, New York.

Sandaltzopoulos, R., Blank, T. and Becker, P.B. (1994) Transcriptional repression by nucleosomes but not H1 in reconstituted preblastoderm Drosophila chromatin. *EMBO J.*, **13**, 373-379.

Sanders, S.L. and Weil, P.A. (2000) Identification of two novel TAF subunits of the yeast Saccharomyces cerevisiae TFIID complex. *J Biol Chem*, **275**, 13895-13900.

Sandman, K., Grayling, R.A., Dobrinski, B., Lurz, R. and Reeve, J.N. (1994) Growth-phase-dependent synthesis of histones in the archaeon Methanothermus fervidus. *Proc Natl Acad Sci U S A*, **91**, 12624-12628.

Santos-Rosa, H., Schneider, R., Bannister, A.J., Sherriff, J., Bernstein, B.E., Emre, N.C., Schreiber, S.L., Mellor, J. and Kouzarides, T. (2002) Active genes are tri-methylated at K4 of histone H3. *Nature*, **419**, 407-411.

Sarma, K. and Reinberg, D. (2005) Histone variants meet their match. *Nat Rev Mol Cell Biol*, **6**, 139-149.

Schalch, T., Duda, S., Sargent, D.F. and Richmond, T.J. (2005) X-ray structure of a tetranucleosome and its implications for the chromatin fibre. *Nature*, **436**, 138-141.

Schnitzler, G.R., Cheung, C.L., Hafner, J.H., Saurin, A.J., Kingston, R.E. and Lieber, C.M. (2001) Direct imaging of human SWI/SNF-remodeled mono- and polynucleosomes by atomic force microscopy employing carbon nanotube tips. *Mol Cell Biol*, **21**, 8504-8511.

Schwanbeck, R., Xiao, H. and Wu, C. (2004) Spatial contacts and nucleosome step movements induced by the NURF chromatin remodeling complex. *J Biol Chem*, **279**, 39933-39941.

Selleck, W., Howley, R., Fang, Q., Podolny, V., Fried, M.G., Buratowski, S. and Tan, S. (2001) A histone fold TAF octamer within the yeast TFIID transcriptional coactivator. *Nat Struct Biol*, **8**, 695-700.

Shahbazian, M.D., Zhang, K. and Grunstein, M. (2005) Histone H2B ubiquitylation controls processive methylation but not monomethylation by Dot1 and Set1. *Mol Cell*, **19**, 271-277.

Shen, X. and Gorovsky, M.A. (1996) Linker histone H1 regulates specific gene expression but not global transcription in vivo. *Cell*, **86**, 475-483.

Shen, X., Mizuguchi, G., Hamiche, A. and Wu, C. (2000) A chromatin remodelling complex involved in transcription and DNA processing. *Nature*, **406**, 541-544.

Shi, Y., Lan, F., Matson, C., Mulligan, P., Whetstine, J.R., Cole, P.A. and Casero, R.A. (2004) Histone demethylation mediated by the nuclear amine oxidase homolog LSD1. *Cell*, **119**, 941-953.

Sinha, S., Maity, S.N., Lu, J. and de Crombrugghe, B. (1995) Recombinant rat CBF-C, the third subunit of CBF/NFY, allows formation of a protein-DNA complex with CBF-A and CBF-B and with yeast HAP2 and HAP3. *Proc Natl Acad Sci U S A*, **92**, 1624-1628.

Smith, C.L., Horowitz-Scherer, R., Flanagan, J.F., Woodcock, C.L. and Peterson, C.L. (2003) Structural analysis of the yeast SWI/SNF chromatin remodeling complex. *Nat Struct Biol*, **10**, 141-145.

Smith, C.L. and Peterson, C.L. (2005) A conserved Swi2/Snf2 ATPase motif couples ATP hydrolysis to chromatin remodeling. *Mol Cell Biol*, **25**, 5880-5892.

Smith, E.R., Pannuti, A., Gu, W., Steurnagel, A., Cook, R.G., Allis, C.D. and Lucchesi, J.C. (2000) The drosophila MSL complex acetylates histone H4 at lysine 16, a chromatin modification linked to dosage compensation. *Mol Cell Biol*, **20**, 312-318.

Soutoglou, E., Demeny, M.A., Scheer, E., Fienga, G., Sassone-Corsi, P. and Tora, L. (2005) The nuclear import of TAF10 is regulated by one of its three histone fold domain-containing interaction partners. *Mol Cell Biol*, **25**, 4092-4104.

Stern, M., Jensen, R. and Herskowitz, I. (1984) Five SWI genes are required for expression of the HO gene in yeast. *J Mol Biol*, **178**, 853-868.

Stokes, D.G. and Perry, R.P. (1995) DNA-binding and chromatin localization properties of CHD1. *Mol Cell Biol*, **15**, 2745-2753.

Strohner, R., Nemeth, A., Jansa, P., Hofmann-Rohrer, U., Santoro, R., Langst, G. and Grummt, I. (2001) NoRC, a novel member of mammalian ISWI-containing chromatin remodeling machines. *Embo J*, **20**, 4892-4900.

Strohner, R., Wachsmuth, M., Dachauer, K., Mazurkiewicz, J., Hochstatter, J., Rippe, K. and Langst, G. (2005) A 'loop recapture' mechanism for ACF-dependent nucleosome remodeling. *Nat Struct Mol Biol*, **12**, 683-690.

Sugino, A. (1995) Yeast DNA polymerases and their role at the replication fork. *Trends Biochem Sci*, **20**, 319-323.

Szerlong, H., Saha, A. and Cairns, B.R. (2003) The nuclear actin-related proteins Arp7 and Arp9: a dimeric module that cooperates with architectural proteins for chromatin remodeling. *Embo J*, **22**, 3175-3187.

Tackett, A.J., Dilworth, D.J., Davey, M.J., O'Donnell, M., Aitchison, J.D., Rout, M.P. and Chait, B.T. (2005) Proteomic and genomic characterization of chromatin complexes at a boundary. *J Cell Biol*, **169**, 35-47.

Tamkun, J.W., Deuring, R., Scott, M.-P., Kissinger, M., Pattatucci, A.M., Kaufmann, T.C. and Kennison, J.A. (1992) *brahma*: A regulator of *Drosophila* homeotic genes structurally related to the yeast transcriptional activator SNF2/SWI2. *Cell*, **68**, 561-572.

Tate, P., Lee, M., Tweedie, S., Skarnes, W.C. and Bickmore, W.A. (1998) Capturing novel mouse genes encoding chromosomal and other nuclear proteins. *J Cell Sci*, **111 (Pt 17)**, 2575-2585.

Terwilliger, T.C. (2000) Maximum-likelihood density modification. *Acta Crystallogr.*, **D56**, 965-972.

Terwilliger, T.C. and Berendzen, J. (1999) Automated MAD and MIR structure solution. *Acta Crystallogr. D*, **D55**, 849-861.

Testa, A., Donati, G., Yan, P., Romani, F., Huang, T.H., Vigano, M.A. and Mantovani, R. (2005) Chromatin immunoprecipitation (ChIP) on chip experiments uncover a widespread distribution of NF-Y binding CCAAT sites outside of core promoters. *J Biol Chem*, **280**, 13606-13615.

Thomä, N.H., Czyzewski, B.K., Alexeev, A.A., Mazin, A.V., Kowalczykowski, S.C. and Pavletich, N.P. (2005) Structure of the SWI2/SNF2 chromatin-remodeling domain of eukaryotic Rad54. *Nat Struct Mol Biol*, **12**, 350-356.

Thomas, J.O. and Travers, A.A. (2001) HMG1 and 2, and related 'architectural' DNA-binding proteins. *Trends Biochem Sci*, **26**, 167-174.

Tong, J.K., Hassig, C.A., Schnitzler, G.R., Kingston, R.E. and Schreiber, S.L. (1998) Chromatin deacetylation by an ATP-dependent nucleosome remodelling complex. *Nature*, **395**, 917-921.

Tora, L. (2002) A unified nomenclature for TATA box binding protein (TBP)-associated factors (TAFs) involved in RNA polymerase II transcription. *Genes Dev*, **16**, 673-675.

Tran, H.G., Steger, D.J., Iyer, V.R. and Johnson, A.D. (2000) The chromo domain protein chd1p from budding yeast is an ATP-dependent chromatin-modifying factor. *EMBO J.*, **19**, 2323-2331.

Travers, A.A. (2003) Priming the nucleosome: a role for HMGB proteins? *EMBO Rep*, **4**, 131-136.

Tsukada, Y.I., Fang, J., Erdjument-Bromage, H., Warren, M.E., Borchers, C.H., Tempst, P. and Zhang, Y. (2005) Histone demethylation by a family of JmjC domain-containing proteins. *Nature*.

Tsukiyama, T., Daniel, C., Tamkun, J. and Wu, C. (1995) ISWI, a member of the SWI2/SNF2 ATPase family, encodes the 140 kD subunit of the Nucleosome Remodeling Factor. *Cell*, **83**, 1021-1026.

Tsukiyama, T., Palmer, J., Landel, C.C., Shiloach, J. and Wu, C. (1999) Characterization of the Imitation Switch subfamily of ATP-dependent chromatin-remodeling factors in Saccharomyces cerevisiae. *Genes Dev.*, **13**, 686-697.

Tsukiyama, T. and Wu, C. (1995) Purification and properties of an ATP-dependent nucleosome remodeling factor. *Cell*, **83**, 1011-1020.

Turner, B.M. (2002) Cellular Memory and the histone code. *Cell*, **111**, 285-291.

Turner, B.M. (2005) Reading signals on the nucleosome with a new nomenclature for modified histones. *Nat Struct Mol Biol*, **12**, 110-112.

Van Holde, K.E. and Yager, T.D. (1985) Nucleosome motion: Evidence and Models. In Nicolini, C. and Ts´o, P.O.P. (eds.), *Structure and function of the genetic apparatus*. Plenum Press, New York, pp. 35-53.

Varga-Weisz, P.D. and Becker, P.B. (1998) Chromatin-remodeling factors: machines that regulate? *Curr Opin Cell Biol*, **10**, 346-353.

Varga-Weisz, P.D., Wilm, M., Bonte, E., Dumas, K., Mann, M. and Becker, P.B. (1997) Chromatin-remodelling factor CHRAC contains the ATPases ISWI and topoisomerase II [published erratum appears in Nature 1997 Oct 30;389(6654):1003]. *Nature*, **388**, 598-602.

Vary, J.C., Jr., Gangaraju, V.K., Qin, J., Landel, C.C., Kooperberg, C., Bartholomew, B. and Tsukiyama, T. (2003) Yeast Isw1p forms two separable complexes in vivo. *Mol Cell Biol*, **23**, 80-91.

Vicent, G.P., Nacht, A.S., Smith, C.L., Peterson, C.L., Dimitrov, S. and Beato, M. (2004) DNA instructed displacement of histones H2A and H2B at an inducible promoter. *Mol Cell*, **16**, 439-452.

Vignali, M., Hassan, A.H., Neely, K.E. and Workman, J.L. (2000a) ATP-dependent chromatin-remodeling complexes. *Mol Cell Biol*, **20**, 1899-1910.

Vignali, M., Steger, D.J., Neely, K.E. and Workman, J.L. (2000b) Distribution of acetylated histones resulting from Gal4-VP16 recruitment of SAGA and NuA4 complexes. *Embo J*, **19**, 2629-2640.

Wang, W., Chi, T., Xue, Y., Zhou, S., Kuo, A. and Crabtree, G.R. (1998) Architectural DNA binding by a high-mobility-group/kinesin-like subunit in mammalian SWI/SNF-related complexes. *Proc Natl Acad Sci U S A*, **95**, 492-498.

Werten, S., Mitschler, A., Romier, C., Gangloff, Y.G., Thuault, S., Davidson, I. and Moras, D. (2002) Crystal structure of a subcomplex of human transcription factor TFIID formed by TATA binding protein-associated factors hTAF4 (hTAF(II)135) and hTAF12 (hTAF(II)20). *J Biol Chem*, **277**, 45502-45509.

Whitehouse, I., Flaus, A., Cairns, B.R., White, M.F., Workman, J.L. and Owen-Hughes, T. (1999) Nucleosome mobilization catalysed by the yeast SWI/SNF complex. *Nature*, **400**, 784-787.

Whitehouse, I., Stockdale, C., Flaus, A., Szczelkun, M.D. and Owen-Hughes, T. (2003) Evidence for DNA translocation by the ISWI chromatin-remodeling enzyme. *Mol Cell Biol*, **23**, 1935-1945.

Wolff, A., de Nechaud, B., Chillet, D., Mazarguil, H., Desbruyeres, E., Audebert, S., Edde, B., Gros, F. and Denoulet, P. (1992) Distribution of glutamylated alpha and beta-tubulin in mouse tissues using a specific monoclonal antibody, GT335. *Eur J Cell Biol*, **59**, 425-432.

Wong, A.K., Shanahan, F., Chen, Y., Lian, L., Ha, P., Hendricks, K., Ghaffari, S., Iliev, D., Penn, B., Woodland, A.M., Smith, R., Salada, G., Carillo, A., Laity, K., Gupte, J., Swedlund, B., Tavtigian, S.V., Teng, D.H. and Lees, E. (2000) BRG1, a component of the SWI-SNF complex, is mutated in multiple human tumor cell lines. *Cancer Res*, **60**, 6171-6177.

Woodcock, C.L. and Dimitrov, S. (2001) Higher-order structure of chromatin and chromosomes. *Curr Opin Genet Dev*, **11**, 130-135.

Wu, P.Y., Ruhlmann, C., Winston, F. and Schultz, P. (2004) Molecular architecture of the S. cerevisiae SAGA complex. *Mol Cell*, **15**, 199-208.

Xiao, H., Sandaltzopoulos, R., Wang, H., Hamiche, A., Ranallo, R., Lee, K., Fu, D. and Wu, C. (2001) Dual functions of the largest NURF subunit NURF301 in nucleosome sliding and transcription factor interactions. *Mol. Cell*, **8**, 531-543.

Xie, X., Kokubo, T., Cohen, S.L., Mirza, U.A., Hoffmann, A., Chait, B.T., Roeder, R.G., Nakatani, Y. and Burley, S.K. (1996) Structural similarity between TAFs and the heterotetrameric core of the histone octamer [see comments]. *Nature*, **380**, 316-322.

Xu, W., Cho, H., Kadam, S., Banayo, E.M., Anderson, S., Yates, J.R., 3rd, Emerson, B.M. and Evans, R.M. (2004) A methylation-mediator complex in hormone signaling. *Genes Dev*, **18**, 144-156.

Xue, Y., Wong, J., Moreno, G.T., Young, M.K., Cote, J. and Wang, W. (1998) NURD, a novel complex with both ATP-dependent chromatin-remodeling and histone deacetylase activities. *Mol Cell*, **2**, 851-861.

Yang, X.J. and Gregoire, S. (2005) Class II histone deacetylases: from sequence to function, regulation, and clinical implication. *Mol Cell Biol*, **25**, 2873-2884.

Zeitlin, S.G., Barber, C.M., Allis, C.D., Sullivan, K.F. and Sullivan, K. (2001) Differential regulation of CENP-A and histone H3 phosphorylation in G2/M. *J Cell Sci*, **114**, 653-661.

Zeng, L. and Zhou, M.M. (2002) Bromodomain: an acetyl-lysine binding domain. *FEBS Lett*, **513**, 124-128.

Zhang, H., Roberts, D.N. and Cairns, B.R. (2005) Genome-wide dynamics of Htz1, a histone H2A variant that poises repressed/basal promoters for activation through histone loss. *Cell*, **123**, 219-231.

Zhang, Y., LeRoy, G., Seelig, H., Lane, W.S. and Reinberg, D. (1998) The Dermatosis-specific autoantigen Mi2 is a component of a protein complex containing deacetylase and nucleosome remodeling activities. *Cell*, **95**, 279-289.

Zhang, Y., Ng, H.H., Erdjument-Bromage, H., Tempst, P., Bird, A. and Reinberg, D. (1999) Analysis of the NuRD subunits reveals a histone deacetylase core complex and a connection with DNA methylation. *Genes Dev*, **13**, 1924-1935.

Zlatanova, J., Caiafa, P. and Van Holde, K. (2000) Linker histone binding and displacement: versatile mechanism for transcriptional regulation. *Faseb J*, **14**, 1697-1704.

Curriculum Vitae

Name	Klaus Felix Hartlepp
Date of birth	21st May 1976
Place of birth	Augsburg
Marital status	unmarried

Education

09/1982 - 07/1986	Grundschule Friedberg
09/1986 - 06/1995	Wernher-von-Braun-Gymnasium Friedberg; school-leaving examination 1995 (Abitur)

Civilian service

09/1995 - 10/1996	Civilian service at the Sozialstation Friedberg

Course of studies

11/1996 - 12/2001	Biochemistry studies at the Universität Regensburg
10/1998	Intermediate examination (Vordiplom)
08/1999 - 06/2000	Stay abroad at the University of Colorado at Boulder (USA)
03/2001	Oral diploma exams
03/2001 - 12/2001	Diploma thesis at the chair of plant physiology and cellular biology (Prof. Dr. Widmar Tanner) Supervisor: PD Dr. Sabine Strahl Title: "Charakterisierung von *SUP30*, einem multi-copy-Suppressor des *ts*-Phänotyps der *S. cerevisiae pmt1pmt4*-Doppelmutante"
12/2001	Diploma degree in biochemistry

Dissertation

03/2002 – 03/2006	Dissertation at the Adolf Butenant Institute, chair of molecular biology (Prof. Dr. Peter Becker), Ludwigs-Maximilans-Universität München
07/2003	Stay abroad at the European Molecular Biology Laboratory (EMBL) Outstation, Grenoble (France)